NASA TECHNICAL REPORT

NASA TR R-171

NASA TR R-171

THE CORRELATION OF OBLIQUE SHOCK PARAMETERS FOR RATIOS OF SPECIFIC HEATS FROM 1 TO 5/3 WITH APPLICATION TO REAL GAS FLOWS

by Mitchel H. Bertram and Barbara S. Cook

Langley Research Center
Langley Station, Hampton, Va.

NATIONAL AERONAUTICS AND SPACE ADMINISTRATION • WASHINGTON, D. C. • DECEMBER 1963

24

THE CORRELATION OF OBLIQUE SHOCK PARAMETERS FOR RATIOS OF SPECIFIC HEATS FROM 1 TO 5/3 WITH APPLICATION TO REAL GAS FLOWS

By Mitchel H. Bertram and Barbara S. Cook

Langley Research Center
Langley Station, Hampton, Va.

NATIONAL AERONAUTICS AND SPACE ADMINISTRATION

For sale by the Office of Technical Services, Department of Commerce,
Washington, D.C. 20230 -- Price $1.75

THE CORRELATION OF OBLIQUE SHOCK PARAMETERS FOR RATIOS OF SPECIFIC HEATS FROM 1 TO 5/3 WITH APPLICATION TO REAL GAS FLOWS

By Mitchel H. Bertram and Barbara S. Cook

SUMMARY

An analytic investigation was made to show the extent of correlation of the exact oblique shock parameters that may be accomplished by means of similarity parameters suggested by approximate theory. The exact theory for the inviscid flow of a perfect gas was calculated for Mach numbers of 1.1 to 40, ratios of specific heats from 1 to 5/3, and angles of attack from 0° to shock detachment. From consideration of the approximate theory and the concept of effective ratio of specific heats, the oblique shock correlations were found to be useful for the rapid calculation of many flow parameters for an equilibrium real gas. Some useful correlations are also given for the case of isentropic expansion around a sharp corner.

INTRODUCTION

Two-dimensional oblique shock theory is one of the basic tools in aerodynamic work. Tables and charts are now available for results from two-dimensional oblique shock theory for the two gases most widely used in wind-tunnel work, air and helium, over extensive ranges of Mach number. (See refs. 1 to 8, for example.) In reference 9, the desire for air-helium transformations prompted an examination of the oblique shock similarity laws. This examination was for the first-order case with Mach number approaching infinity and some higher order approximations with the air-helium comparison paramount. There are cases where oblique shock parameters are desired for gases other than air or helium or where existing tables for a gas are inadequate. In these cases, the possibility of using existing tables or charts for gases other than the one of interest to obtain the desired information is suggested by similarity considerations.

This analytic investigation was undertaken to determine the correlating powers of certain similarity parameters suggested by approximate theory. Some comparisons with approximate theories were also made. In order to have as wide a comparison as possible, Mach numbers from the low supersonic to the hypersonic range have been included, deflection angles from 0° to shock detachment, and ratios of specific heats from unity to 5/3 in inviscid flow. From consideration of the approximate theory and the effective ratio of specific heats concept, the oblique shock correlations were found useful for the rapid calculation of many flow parameters for an equilibrium real gas.

SYMBOLS

C_p pressure coefficient

h static enthalpy

K flow deflection similarity parameter (see eq. (5))

$K_p \equiv \frac{\gamma + 1}{\gamma}\left(\frac{p_2}{p_\infty} - 1\right)$

$K_\theta \equiv M_\infty \sin \theta = M_N$

$K_\rho \equiv (\gamma + 1)\left(1 - \frac{\rho_\infty}{\rho_2}\right)$

$K_{\rho u} \equiv (\gamma + 1)\left(1 - \frac{\rho_\infty u_\infty}{\rho_2 u_2}\right)$

$K_\delta \equiv (\gamma + 1)\left(\frac{M_\infty^2}{\beta} \sin \delta\right)$

M Mach number

p pressure

T temperature

u velocity

$\beta \equiv \sqrt{M_\infty^2 - 1}$

γ isentropic exponent $\left[\frac{d(\log p)}{d(\log \rho)}\right]_s$; equal to ratio of specific heats for a perfect gas

γ_e effective value of γ for flow across shock waves (eq. (16))

δ flow deflection angle

θ angle between free-stream flow direction and shock wave

ρ density

Subscripts:

2 condition behind shock wave

∞ free-stream conditions

N normal to shock wave

s at constant entropy

t total pressure

Superscripts in parentheses refer to the order of an equation developed in series.

PRESENTATION OF THEORY

First let us examine some sample results from exact two-dimensional oblique shock theory for a perfect gas with a constant value for the ratio of specific heats. (See ref. 2, for example.) Two Mach numbers have been chosen; one is $M_\infty = \sqrt{2}$, which is intended to be representative of the lower supersonic regime, and the other is $M_\infty = 20$, a Mach number high enough to be considered truly hypersonic. The results from the calculations are given in figure 1 for static pressure, density, temperature, mass flow ratio, and shock angle as a function of deflection angle for values of the ratio of specific heats ranging from 1 to 5/3. The first-order effect of γ, the ratio of specific heats, is evident except for the case of density ratio where there is little effect of changing the value of γ at small values of the deflection angle δ. This comment applies also to mass flow ratio, although over a lesser range of angle of attack. Qualitatively, the effect of γ on a given parameter changes little between Mach number $\sqrt{2}$ and 20.

A first-order insight into the effect of γ may be obtained from the following equations which are the first-order small-perturbation theory for a wedge flow:

$$\left(\frac{p_2}{p_\infty} - 1\right)^{(1)} = \gamma \frac{M_\infty^2}{\beta} \delta \tag{1}$$

$$\left(\frac{\rho_2}{\rho_\infty} - 1\right)^{(1)} = \frac{M_\infty^2}{\beta} \delta \tag{2}$$

$$\left(\frac{T_2}{T_\infty} - 1\right)^{(1)} = (\gamma - 1)\frac{M_\infty^2}{\beta} \delta \tag{3}$$

$$(M_\infty \sin \theta)^{(1)} = 1 + \frac{\gamma + 1}{4} \frac{M_\infty^2}{\beta} \delta \tag{4}$$

Equations (1), (2), and (3) are given in reference 2 and equation (4) is obtained by substituting equation (1) into the exact relation between M_N and p_2/p_∞. From this theory, which is exact for the variation of the initial slope of these parameters with wedge deflection angle, the initial influence of γ is clear. Temperature ratio is most sensitive to γ, pressure ratio is less sensitive but γ still has an important effect and density ratio is not a function of γ to first order.

First-order small-perturbation theory would not be expected to be adequate over an extensive range of angle of attack especially in the hypersonic Mach

number regime. For hypersonic flow over a wedge, Linnell (ref. 10) developed the following relation:

$$\frac{p_2}{p_\infty} - 1 = \frac{\gamma(\gamma + 1)}{4} K^2 + \gamma K\sqrt{1 + \left(\frac{\gamma + 1}{4} K\right)^2} \tag{5}$$

in which K is the parameter correlating Mach number and deflection angle effects. In its original form, this parameter was given by the hypersonic result $K = M_\infty\delta$. Ivey and Cline (ref. 11) modified K so as to connect the linearized theory (in this case, eqs. (1) to (4)) with the hypersonic result of Linnell, and they proposed $K = M_\infty^2\delta/\beta$. Equation (5) may also be derived to give the hypersonic result $K = M_\infty \sin\delta$ if the exact oblique shock relations are reduced with the assumption $\sin\delta = \tan\delta$. Following the lead of reference 11 a value of K is proposed to extend the usefulness of equation (5) over a large range of deflection angle and Mach number:

$$K = \frac{M_\infty^2}{\beta} \sin\delta \tag{6}$$

In a form showing the correlation parameters which are obtained, equation (5) with the introduction of equation (6) may be written as

$$\frac{\gamma + 1}{4\gamma}\left(\frac{p_2}{p_\infty} - 1\right) = \left(\frac{\gamma + 1}{4}\frac{M_\infty^2}{\beta}\sin\delta\right)^2 + \frac{\gamma + 1}{4}\frac{M_\infty^2}{\beta}\sin\delta\sqrt{1 + \left(\frac{\gamma + 1}{4}\frac{M_\infty^2}{\beta}\sin\delta\right)^2} \tag{7}$$

or

$$\frac{\gamma + 1}{\gamma}\left(\frac{p_2}{p_\infty} - 1\right) = f\left[(\gamma + 1)\frac{M_\infty^2}{\beta}\sin\delta\right]$$

With the small-perturbation assumption, the first-order solution of equation (7) is equation (1).

If the following exact relation between shock angle parameters and pressure ratio parameter is utilized

$$\frac{\gamma + 1}{4\gamma}\left(\frac{p_2}{p_\infty} - 1\right) = \frac{K_\theta^2 - 1}{2} \tag{8}$$

with equation (7), the relation between shock angle and deflection angle is

$$M_\infty \sin\theta = \frac{\gamma + 1}{4}\frac{M_\infty^2}{\beta}\sin\delta + \sqrt{1 + \left(\frac{\gamma + 1}{4}\frac{M_\infty^2}{\beta}\sin\delta\right)^2} \tag{9}$$

This relation is compatible with equation (4).

In correlation form the density ratio is

$$(\gamma + 1)\left(1 - \frac{\rho_\infty}{\rho_2}\right) = 2\,\frac{(M_\infty \sin\theta)^2 - 1}{(M_\infty \sin\theta)^2} \tag{10}$$

This relation is exact for a perfect gas with constant γ but, where $M_\infty \sin\theta$ is given by equation (9), the limitations inherent in equation (9) apply.

Busemann's small-perturbation theory (ref. 12) for the generally applicable relation between pressure ratio and deflection angle for a shock-wave compression up to the third-order term is (when δ is replaced by $\sin\delta$)

$$\left(\frac{p_2}{p_\infty} - 1\right)^{(3)} = \gamma\,\frac{M_\infty^2}{\beta}\sin\delta + \frac{\gamma}{\beta}\left(\frac{M_\infty^2}{\beta}\right)\left[\frac{\gamma+1}{4}\left(\frac{M_\infty^2}{\beta}\right)^2 - 1\right]\sin^2\delta + \frac{\gamma}{2}\,\frac{M_\infty^2}{\beta^7}\left[\left(\frac{\gamma+1}{4}\right)^4 M_\infty^8 + \frac{3\gamma^2 - 12\gamma - 7}{12}\,M_\infty^6 + \frac{3(\gamma+1)}{2}\,M_\infty^4 - 2M_\infty^2 + \frac{4}{3}\right]\sin^3\delta \tag{11}$$

Still higher order terms in this relation have been considered by Laitone in reference 13. Equation (11) may be compared term by term with equation (7) expanded in series with the assumption of small deflection angles where

$$\frac{p_2}{p_\infty} - 1 = \gamma\,\frac{M_\infty^2}{\beta}\sin\delta + \frac{\gamma(\gamma+1)}{4}\left(\frac{M_\infty^2}{\beta}\sin\delta\right)^2 + \frac{\gamma}{2}\left(\frac{\gamma+1}{4}\right)^2\left(\frac{M_\infty^2}{\beta}\sin\delta\right)^3 \tag{12}$$

Beyond first order, it is clear that the coefficients are not the same.

PRESENTATION OF CORRELATED RESULTS

In order to test the correlation accuracy of the similarity parameters suggested by approximate theories, exact computations have been done to cover the Mach number range from the low supersonic to high hypersonic. The symbols in figure 2 represent the pressure ratio across an oblique shock given by exact two-dimensional theory in the similarity form suggested by equation (7). The value of the ratio of specific heats γ is constant but results have been computed for values of γ from 1 to 5/3 as designated by the different symbols in figure 2.

The end point to these calculations is the angle where shock detachment occurs. For reference purposes and to provide accurate determinations of the values of the various parameters at shock detachment, table I has been prepared.

At all Mach numbers, the pressure-deflection results for the various values of γ at a given Mach number can be seen to correlate in the similarity form (K_p, K_δ) much better than given by the uncorrelated form examples in figures 1(a) and 1(b). Correlation is generally excellent at the relatively low values of K_δ and is poorer at the largest values of K_δ where shock detachment is approached. The correlation is best for those values of γ approaching unity;

one can readily note that at a given Mach number the first set of computations to deviate from correlation is that for $\gamma = 5/3$, the next, the $\gamma = 1.4$ results, and so on.

One finds by comparing the results between the various parts of figure 2 that for $M_\infty \geqq \sqrt{2}$ the correlation of the results for the different free-stream Mach numbers and a fixed value of γ is generally good at the lower values of K_δ for each Mach number. However, the range of good correlation increases with a decrease in the value of γ. This is illustrated in figure 3 for $\gamma = 1$ and $\gamma = 5/3$.

Comparison with approximate theories is also of interest. The solid line in figures 2 and 3 designated "extended hypersonic oblique-shock similarity theory" is a plot of equation (7). As presented, this curve is not a function of Mach number. The prediction of the pressure parameter K_p given by equation (7) is always good at very low values of K_δ and the range of good agreement increases with Mach number. For $\gamma = 1$ and Mach numbers greater than 3, equation (7) gives good predictions of the pressure over almost the entire range from $K_\delta = 0$ to the value of K_δ for shock detachment. The accurate range of applicability of equation (7) decreases as γ increases.

Third-order small-disturbance theory (eq. (11)) for $\gamma = 1$ and $\gamma = 5/3$ is represented by the dashed lines in figure 2. At the lower Mach numbers (fig. 2(a)), this theory represents an improvement over equation (7) in predicting both Mach number effects and the effect of γ. As Mach number increases, the effect of γ in figure 2 tends to diminish and equation (11) approaches equation (12) (which is the third-order form of equation (7)). (For Mach numbers 2 and 3 (fig. 2(b)), the third-order small-disturbance curve for $\gamma = 5/3$ coincides with the extended hypersonic theory curve.)

The correlation parameter for shock angle K_θ is shown as a function of the deflection parameter K_δ in figures 4 and 5. Actually, since the pressure correlation is dependent on the shock correlation, comments on correlation of the exact theory designated by the symbols are generally common to both and the reader is referred to the preceding discussion of the pressure correlation. Equation (9) is shown in figures 4 and 5 and is designated as "extended hypersonic oblique-shock similarity theory."

The correlation of the exact values of static density ratio suggested by equations (9) and (10) is shown in figures 6 and 7. Note that the density correlation parameter K_ρ utilizes density ratio in the form ρ_∞/ρ_2. Some caution should be exercised in trying to judge the success of correlation at high Mach numbers and large K_δ. In this case, the values of ρ_∞/ρ_2 approach $(\gamma - 1)/(\gamma + 1)$ and thus the correlating parameter K_ρ is insensitive to appreciable variations in ρ_∞/ρ_2 as γ approaches 1. The extended hypersonic theory determined from equations (9) and (10) is also shown in figure 4 as the solid line.

The same form of correlation parameters for mass flow ratio was assumed as for the density ratio in the previous section. This correlation for various γ is shown in figure 8 and is considered as good as the density ratio correlation at the low Mach numbers, but at the high values of K_δ and Mach number, there is a considerable deviation from correlation. However, this result still represents a large improvement over the effect of γ exhibited by the uncorrelated results in figures 1(g) and 1(h).

No simple parameter such as K_δ has been found for correlating the higher order effects of γ on static temperature ratio across the oblique shock. Therefore, the first-order prediction of small-perturbation theory was resorted to (eq. (3)) and these results are shown in figure 9. The correlation cannot be considered as successful as the previous ones based on higher order theory as evidenced by the low values of the deflection parameter at which significant deviations from correlation take place. However, a comparison with the uncorrelated results shown in figure 1(i) indicates a major improvement in minimizing the effects of a change in γ and this allows accurate interpolation.

Figure 10 was prepared to show the correlation of static temperature difference ratios for fixed values of γ over a wide range of free-stream Mach numbers. The correlation of Mach number variation effects in figure 10 is obviously better than the correlation of γ variation effects presented in figure 9.

An often desired parameter is the total-pressure ratio across the oblique shock. This ratio can be written as (see ref. 2)

$$\frac{p_{t,2}}{p_{t,\infty}} = \frac{\rho_{t,2}}{\rho_{t,\infty}} = \left[\left(\frac{\rho_2}{\rho_\infty}\right)^\gamma \frac{p_\infty}{p_2}\right]^{\frac{1}{\gamma-1}} = \left[\frac{(\gamma+1)K_\theta{}^2}{(\gamma-1)K_\theta{}^2+2}\right]^{\frac{\gamma}{\gamma-1}} \left[\frac{\gamma+1}{2\gamma K_\theta{}^2-(\gamma-1)}\right]^{\frac{1}{\gamma-1}} \tag{13}$$

Equation (13) is indeterminate for $\gamma = 1$ but, by taking the limit as γ approaches 1, the following form is obtained which is valid for $\gamma = 1$

$$\frac{p_{t,2}}{p_{t,\infty}} = K_\theta{}^2 e^{-\frac{1}{2}\left(K_\theta{}^2 - \frac{1}{K_\theta{}^2}\right)} \tag{14}$$

Only equation (13) was set up on the automatic computing machine, by which most of the computing in this paper was done; therefore, the total-pressure ratio which is plotted in figure 11 does not contain the values for $\gamma = 1$. This ratio is plotted in figure 11 as a function of the wedge deflection correlation parameter. Mach numbers from 1.1 to 40 are shown for a constant value of γ. One finds that for values of the deflection parameter below roughly 2, the ratio of total pressures is virtually independent of the value of γ assumed. However, for values of the deflection parameter greater than about 2, the total-pressure ratio becomes a strong function of the value of γ assumed.

APPLICATION TO A REAL GAS

In a relatively simple manner, a method can be derived which allows the preceding correlations to be used for evaluation of many of the oblique shock parameters in a real gas.

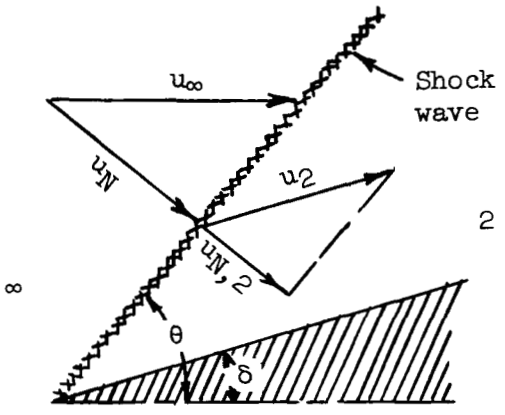

From mass flow and geometrical considerations

$$\frac{u_N}{u_{N,2}} = \frac{\rho_2}{\rho_\infty} = \frac{\tan\theta}{\tan(\theta - \delta)} \tag{15}$$

As given by Trimpi and Jones (ref. 8), an effective value of the isentropic exponent γ_e is used to describe the density change across the oblique shock wave so that the computations may be applied to a real gas in equilibrium. By definition

$$\gamma_e \equiv 2 \frac{\left(\frac{1}{M_N}\right)^2 - 1}{\frac{\rho_\infty}{\rho_2} - 1} - 1 \tag{16}$$

Consider the case where the shock wave angle θ and the deflection angle δ are small enough so that the tangent and sine of these angles may be replaced by the angle in radians. Solving for the density ratio in equation (16), substituting this relation into equation (15), and solving the resulting quadratic gives the following similarity relation between shock angle and deflection angle:

$$M_\infty\theta = \frac{\gamma_e + 1}{4} M_\infty\delta + \sqrt{1 + \left(\frac{\gamma_e + 1}{4} M_\infty\delta\right)^2} \tag{17}$$

When the momentum and continuity equations are combined, the static-pressure ratio across the shock is

$$\frac{p_2}{p_\infty} = 1 + \left(1 - \frac{\rho_\infty}{\rho_2}\right)\frac{\rho_\infty u_N^2}{p_\infty} \tag{18}$$

Substituting for the static density ratio according to equation (16) and further manipulation yields the relation between static-pressure ratio and shock angle

$$\frac{p_2}{p_\infty} = 1 + \frac{2\gamma_\infty}{\gamma_e + 1}\left[(M_\infty\theta)^2 - 1\right] \tag{19}$$

Combining equations (17) and (19) results in relation between pressure ratio and deflection angle which in similarity form is

$$\frac{\gamma_e + 1}{4\gamma_\infty}\left(\frac{p_2}{p_\infty} - 1\right) = \left(\frac{\gamma_e + 1}{4} M_\infty\delta\right)^2 + \frac{\gamma_e + 1}{4} M_\infty\delta\sqrt{1 + \left(\frac{\gamma_e + 1}{4} M_\infty\delta\right)^2} \tag{20}$$

By utilizing the same reasoning as for equation (7), equations (20) and (17) can be written in extended hypersonic similarity form as

$$\frac{\gamma_e + 1}{4\gamma_\infty}\left(\frac{p_2}{p_\infty} - 1\right) = \left(\frac{\gamma_e + 1}{4}\frac{M_\infty^2}{\beta}\sin\delta\right)^2 + \frac{\gamma_e + 1}{4}\frac{M_\infty^2}{\beta}\sin\delta\sqrt{1 + \left(\frac{\gamma_e + 1}{4}\frac{M_\infty^2}{\beta}\sin\delta\right)^2} \tag{21}$$

$$M_\infty^2\sin^2\theta = M_N = \frac{\gamma_e + 1}{4}\frac{M_\infty^2}{\beta}\sin\delta + \sqrt{1 + \left(\frac{\gamma_e + 1}{4}\frac{M_\infty^2}{\beta}\sin\delta\right)^2} \tag{22}$$

By rewriting equation (16) the density ratio in correlation form is

$$\left(\gamma_e + 1\right)\left(1 - \frac{\rho_\infty}{\rho_2}\right) = 2\,\frac{K_\theta^2 - 1}{K_\theta^2} \tag{23}$$

The energy equation with the mass flow equation (15) gives the static enthalpy ratio across the shock

$$\frac{h_2}{h_\infty} - 1 = \frac{u_\infty^2\sin^2\theta}{2h_\infty}\left[1 - \left(\frac{\rho_\infty}{\rho_2}\right)^2\right] = \frac{\gamma_\infty - 1}{2} M_\infty^2\sin^2\theta\left[1 - \left(\frac{\rho_\infty}{\rho_2}\right)^2\right] \tag{24a}$$

or with equation (23) the enthalpy ratio can be written in terms of the shock angle as

$$\frac{h_2}{h_\infty} - 1 = 2\,\frac{\gamma_\infty - 1}{\gamma_e + 1}\left(K_\theta^2 - 1\right)\left[1 - \frac{1}{\gamma_e + 1}\left(1 - \frac{1}{K_\theta^2}\right)\right] \tag{24b}$$

The ratio of the resultant velocity behind the oblique shock to the free-stream velocity is given in appendix B of reference 8 and in the present nomenclature is

$$\frac{u_2}{u_\infty} = \frac{1}{\cos \delta}\left[1 - \left(1 - \frac{\rho_\infty}{\rho_2}\right)\sin^2\theta\right] \tag{25a}$$

or with equation (23)

$$\frac{u_2}{u_\infty} = \frac{1}{\cos \delta}\left[1 - \frac{2}{\gamma_e + 1}\left(1 - \frac{1}{K_\theta{}^2}\right)\sin^2\theta\right] \tag{25b}$$

Equations (21) and (22) are approximate equations corresponding to equations (7) and (9) for a perfect gas. Equations (23), (24), and (25) are exact but, when equation (22) is used to solve those equations, the limitations inherent in equation (22) apply.

If the equations are to be used to solve for the desired conditions of the gas, it may be easier to use equation (22) in the form

$$\left(\gamma_e + 1\right)\frac{M_\infty{}^2}{\beta}\sin \delta = 2\left(M_N - \frac{1}{M_N}\right) \tag{26}$$

since the values of γ_e are usually given as a function of M_N. Such values of γ_e are shown in figure 12 for atmospheric air at various attitudes adapted by Trimpi in unpublished work from the equilibrium normal shock calculations of Huber in reference 14 which uses the ARDC 1959 model atmosphere (ref. 15). A similar plot is shown as figure 2 of reference 8 based essentially on the ARDC 1956 model atmosphere (ref. 16).

To utilize the correlation plots presented earlier, the following procedure can be followed. In figures 2, 4, and 6 (also figs. 3, 5, and 7 with caution since only γ-values of 1 and 5/3 are given) read the $\gamma + 1$ value in the deflection parameter of the abscissa as $\gamma_e + 1$. In figure 2 read the γ-function in the pressure parameter of the ordinate as $(\gamma_e + 1)/\gamma_\infty$. No function of γ is contained in the ordinate (shock angle parameter) of figure 4 and this parameter is read unchanged. In figure 6, the γ-function of the density parameter in the ordinate is read as $\gamma_e + 1$.

The charts given previously are not too useful for obtaining enthalpy ratio because of the more limited range over which correlation was obtained. But K_θ (which is equivalent to M_N) is readily obtained as outlined previously and thus, from K_θ and the known value of γ_∞ and γ_e (fig. 12 for air), the enthalpy ratio is calculated from equation (24). Temperature ratio is then obtained from available tables and charts of thermodynamic properties (for example, refs. 17 and 18 or other appropriate tables or Mollier diagrams for air). An example of the flow-parameter variation with flow-deflection angle in an equilibrium real gas from the correlations in this paper is shown in

figure 13. The Mach number chosen was 20 at an altitude of 120,300 feet. For comparison purposes the equivalent flow parameters for a perfect gas with $\gamma = 1.4$ at the same Mach number are also shown. The real gas calculations were carried out only to a value of $K_\delta = 30$ since above this point the maximum deviations of the exact theory values of the shock angle parameter K_θ from correlation for $\gamma = 1.4$ exceed 1.5 percent (fig. 4(d)). Even with this limitation on K_δ, the real gas computations for this case extend out to a deflection angle of about 40°. Comparison with the more exact formulations given in reference 8 shows that, for the parameters given in figure 13, the error in the value of δ is only $1/4^\circ$ at $\delta = 43^\circ$, 0.1° at $\delta = 35^\circ$, and is reduced to the negligible value of 0.03° at $\delta = 27^\circ$.

PRESSURE RATIO ACROSS SUDDEN EXPANSION

Although this paper primarily considers the oblique shock case, some useful correlations are available for the case of isentropic expansion around a sharp corner. Here, only pressure will be considered. For the expansion case, Linnell (ref. 10) developed the approximate relation

$$\frac{p_2}{p_\infty} = \left(1 + \frac{\gamma - 1}{2} K\right)^{\frac{2\gamma}{\gamma-1}} \tag{27}$$

In this development there is a limitation imposed by certain series approximations used that $M_\infty > \sqrt{\frac{2\gamma}{\gamma - 1}}$; also, equation (27) has no meaning unless $(\gamma - 1)K > -2$. The similarity parameter K was given by Linnell as the hypersonic small angle result $K = M_\infty\delta$. Expanding equation (27) in series gives the result

$$\frac{p_2}{p_\infty} - 1 = \gamma K + \frac{\gamma(\gamma + 1)}{4} K^2 + \frac{\gamma(\gamma + 1)}{12} K^3 + \frac{\gamma(\gamma + 1)(3 - \gamma)}{96} K^4 + \cdots \tag{28}$$

Consistent with Busemann's observation in reference 12, the expansion relation equation (28) is the same up to the second-order term as the shock relation (eq. (5)) expanded in series. (For example, see eq. (12).) This relationship suggests that K be taken as $M_\infty^2 \sin \delta/\beta$ as in the oblique shock case where equation (7) was obtained. Thus equation (27) is written as

$$\frac{p_2}{p_\infty} = \left(1 + \frac{\gamma - 1}{2} \frac{M_\infty^2}{\beta} \sin \delta\right)^{\frac{2\gamma}{\gamma-1}} \tag{29}$$

The second-order equality of the shock and expansion equations further suggests the K_δ, K_p type of presentation to minimize effects of changing the value of γ as was done for the oblique shock case. Such a presentation is given in figure 14. The calculations were based on tables given in references 2, 6, 19, and 20. (It may be noted that ref. 20 used for the lowest values of γ is tabulated only up to a local Mach number of 8.) The best correlation of exact theory (Prandtl-Meyer) for various values of free-stream Mach number at a constant value of γ is obtained at the highest value of specific heat ratio, $\gamma = 5/3$, with a decreasing extent of correlation as γ decreases. Approximate equation (29) given by the solid line in figure 14 is a good fit to the Prandtl-Meyer results at the higher Mach numbers. Correlation of the effect of changing the value of γ is found to be good for values of K_δ approaching 2 if one compares the various parts of figure 14.

CONCLUDING REMARKS

An analytic investigation was done to show the extent of correlation of the exact oblique shock parameters that may be accomplished by means of similarity parameters suggested by approximate theory. The exact theory for the inviscid flow of a perfect gas was calculated for Mach numbers of 1.1 to 40, ratios of specific heats from 1 to 5/3, and angles of attack from 0° to shock detachment.

At all Mach numbers, pressure, density, mass flow ratios, and shock angle can be correlated with excellent accuracy over a significant range of deflection angle; however, this correlation becomes progressively poorer as the angle of attack for shock detachment is approached. However, even at the higher deflection angles, improvements in reducing the effect of γ are found so that accurate interpolation of the results can be made. The same similarity parameters also correlate the effect of Mach number, in the same range where the correlation of the effect of γ is good, for Mach numbers greater than about $\sqrt{2}$.

No simple parameter was found for correlating the higher order effects of γ on static temperature ratio across the oblique shock. However, first-order correlations, although not as successful as those previously referred to, gave a major improvement in reducing the effect of a change in γ so that accurate interpolations of the results are possible. The correlation of the effect of Mach number on temperature ratio was, however, apparently as good as that for the previously described flow parameters.

From consideration of the approximate theory and the concept of effective ratio of specific heats, the oblique shock correlations have been found to be useful for the rapid calculation of many flow parameters for an equilibrium real gas.

Some useful correlations are also given for the case of isentropic expansion around a sharp corner.

Langley Research Center,
National Aeronautics and Space Administration,
Langley Station, Hampton, Va., March 22, 1963.

REFERENCES

1. Neice, Mary M.: Tables and Charts of Flow Parameters Across Oblique Shocks. NACA TN 1673, 1948.

2. Ames Research Staff: Equations, Tables, and Charts for Compressible Flow. NACA Rep. 1135, 1953. (Supersedes NACA TN 1428.)

3. Dailey, C. L., and Wood, F. C.: Computation Curves for Compressible Fluid Problems. John Wiley & Sons, Inc., c.1949.

4. Anon.: Handbook of Supersonic Aerodynamics. NAVORD Rep. 1488 (vol. 2), Bur. Ordnance, Oct. 1, 1950.

5. Staff of the Gas Dynamics Lab., Princeton Univ.: Charts for Flow Parameters of Helium at Hypersonic Speeds - Mach Number 10 to 20. WADC Tech. Note 57-377, ASTIA Doc. No. AD 142310, U.S. Air Force, Nov. 1957.

6. Mueller, James N.: Equations, Tables, and Figures for Use in the Analysis of Helium Flow at Supersonic and Hypersonic Speeds. NACA TN 4063, 1957.

7. Henderson, Arthur, Jr., and Braswell, Dorothy O.: Charts for Conical and Two-Dimensional Oblique-Shock Flow Parameters in Helium at Mach Numbers From About 1 to 100. NASA TN D-819, 1961.

8. Trimpi, Robert L., and Jones, Robert A.: A Method of Solution With Tabulated Results for the Attached Oblique Shock-Wave System for Surfaces at Various Angles of Attack, Sweep, and Dihedral in an Equilibrium Real Gas Including the Atmosphere. NASA TR R-63, 1960.

9. Love, Eugene S., Henderson, Arthur, Jr., and Bertram, Mitchel H.: Some Aspects of Air-Helium Simulation and Hypersonic Approximations. NASA TN D-49, 1959.

10. Linnell, Richard D.: Two-Dimensional Airfoils in Hypersonic Flows. Jour. Aero. Sci., vol. 16, no. 1, Jan. 1949, pp. 22-30.

11. Ivey, H. Reese, and Cline, Charles W.: Effect of Heat-Capacity Lag on the Flow Through Oblique Shock Waves. NACA TN 2196, 1950.

12. Busemann, A.: Aerodynamic Lift at Supersonic Speeds. Ae. Techl. 1201, Rep. No. 2844, British A.R.C., Feb. 3, 1937. (From Luftfahrtforschung, Bd. 12, Nr. 6, Oct. 3, 1935, pp. 210-220.) (Also available as Translation No. 196, Douglas Aircraft Co., Inc.)

13. Laitone, Edmund V.: Exact and Approximate Solutions of Two-Dimensional Oblique Shock Flow. Jour. Aero. Sci., vol. 14, no. 1, Jan. 1947, pp. 25-41.

14. Huber, Paul W.: Hypersonic Shock-Heated Flow Parameters for Velocities to 46,000 Feet Per Second and Altitudes to 323,000 Feet. NASA TR R-163, 1963.

15. Minzner, R. A., Champion, K. S. W., and Pond, H. L.: The ARDC Model Atmosphere, 1959. Air Force Surveys in Geophysics No. 115 (AFCRC-TR-59-267), Air Force Cambridge Res. Center, Aug. 1959.

16. Minzner, R. A., and Ripley, W. S.: The ARDC Model Atmosphere, 1956. Air Force Surveys in Geophysics No. 86 (AFCRC TN-56-204, ASTIA Doc. 110233), Air Force Cambridge Res. Center, Dec. 1956.

17. Hilsenrath, Joseph, Beckett, Charles W., et al.: Tables of Thermal Properties of Gases. NBS Cir. 564, U.S. Dept. Commerce, 1955.

18. Anon.: Thermodynamic Properties of High Temperature Air. Rep. No. RE-1R-14, Chance Vought Res. Center, June 28, 1961.

19. Mueller, Janes N.: Ideal-Gas Tables for Helium Flow in the Mach Number Range From 40 to 100. NASA TN D-1252, 1962.

20. Tempelmeyer, K. E., and Sheraden, G. H.: Compressible Flow Tables for Gases With Specific Heat Ratios From 1.10 to 1.28. AEDC-TN-58-9, ASTIA Doc. No. AD-152041, Arnold Eng. Dev. Center, Mar. 1958.

TABLE I

VALUES OF OBLIQUE SHOCK PARAMETERS AT SHOCK DETACHMENT

[+n or -n, number after tabulated value, indicates that the decimal point should be n places to the right or left, respectively, of the first digit.]

M_∞	γ	δ, deg	$\frac{p_2}{p_\infty}$	$\frac{T_2}{T_\infty}$	$\frac{\rho_2}{\rho_\infty}$	$\frac{p_{t,2}}{p_{t,\infty}}$	$\frac{u_2}{u_\infty}$	$\frac{\rho_2 u_2}{\rho_\infty u_\infty}$	M_2	θ, deg	C_p	$\frac{C_p}{\sin^2\delta}$	$M_\infty \sin\theta$
1.1	1.0	.185848 +1	.114319 +1	.100000 +1	.114319 +1	.999603	.882126	.100844 +1	.970339	.764095 +2	.236663	.225028 +3	.106920 +1
	1.1	.175882 +1	.114968 +1	.101280 +1	.113515 +1	.999607	.887964	.100797 +1	.970570	.763768 +2	.224954	.238751 +3	.106905 +1
	1.2	.166932 +1	.115555 +1	.102445 +1	.112797 +1	.999615	.893251	.100756 +1	.970778	.763474 +2	.214175	.252478 +3	.106892 +1
	1.3	.158850 +1	.116089 +1	.103512 +1	.112151 +1	.999624	.898060	.100718 +1	.970964	.763207 +2	.204698	.266208 +3	.106880 +1
	1.4	.151516 +1	.116578 +1	.104491 +1	.111567 +1	.999632	.902454	.100684 +1	.971133	.762965 +2	.195681	.279942 +3	.106869 +1
	5/3	.134911 +1	.117695 +1	.106749 +1	.110254 +1	.999654	.912509	.100608 +1	.971513	.762416 +2	.175458	.316574 +3	.106844 +1
1.2	1.0	.494016 +1	.130695 +1	.100000 +1	.130695 +1	.996791	.789776	.103220 +1	.947732	.723038 +2	.426287	.574871 +2	.114322 +1
	1.1	.464650 +1	.132010 +1	.102586 +1	.128682 +1	.996901	.800551	.103017 +1	.948477	.722077 +2	.404083	.615886 +2	.114260 +1
	1.2	.438600 +1	.133196 +1	.104946 +1	.126918 +1	.997005	.810269	.102838 +1	.949135	.721222 +2	.384209	.656936 +2	.114206 +1
	1.3	.415331 +1	.134271 +1	.107109 +1	.125359 +1	.997105	.819080	.102679 +1	.949719	.720456 +2	.366088	.698019 +2	.114156 +1
	1.4	.394419 +1	.135250 +1	.109098 +1	.123972 +1	.997201	.827106	.102538 +1	.950243	.719765 +2	.349672	.739126 +2	.114112 +1
	5/3	.347766 +1	.137481 +1	.113696 +1	.120920 +1	.997435	.845385	.102224 +1	.951403	.718218 +2	.312403	.848857 +2	.114011 +1
$\sqrt{2}$	1.0	.127939 +2	.173205 +1	.100000 +1	.173205 +1	.972340	.650115	.112603 +1	.919402	.685293 +2	.732057	.149282 +2	.131607 +1
	1.1	.118887 +2	.175933 +1	.105522 +1	.166727 +1	.974070	.669205	.111574 +1	.921305	.682267 +2	.690336	.162651 +2	.131332 +1
	1.2	.111052 +2	.178377 +1	.110580 +1	.161309 +1	.975596	.686282	.110704 +1	.922950	.679634 +2	.653117	.176053 +2	.131090 +1
	1.3	.104201 +2	.180579 +1	.115230 +1	.156711 +1	.976956	.701653	.109957 +1	.924387	.677321 +2	.619824	.189483 +2	.130874 +1
	1.4	.981578 +1	.182574 +1	.119519 +1	.152758 +1	.978174	.715567	.109309 +1	.925652	.675272 +2	.589842	.202939 +2	.130682 +1
	5/3	.850428 +1	.187083 +1	.129470 +1	.144499 +1	.980877	.746964	.107936 +1	.928391	.670799 +2	.522464	.238916 +2	.130256 +1
2	1.0	.322565 +2	.344949 +1	.100000 +1	.344949 +1	.710650	.458369	.158114 +1	.916738	.682238 +2	.122474 +1	.429966 +1	.185728 +1
	1.1	.292544 +2	.350713 +1	.115137 +1	.304604 +1	.744002	.493086	.150196 +1	.919062	.670769 +2	.113958 +1	.477190 +1	.184206 +1
	1.2	.267918 +2	.355841 +1	.129052 +1	.275734 +1	.770307	.523159	.144253 +1	.921045	.661342 +2	.106602 +1	.524673 +1	.182899 +1
	1.3	.247294 +2	.360434 +1	.141879 +1	.254044 +1	.791620	.549563	.139613 +1	.922760	.653433 +2	.100164 +1	.572376 +1	.181765 +1
	1.4	.229735 +2	.364575 +1	.153734 +1	.237146 +1	.809259	.572991	.135883 +1	.924256	.646690 +2	.944948	.620270 +1	.180770 +1
	5/3	.193449 +2	.373861 +1	.181339 +1	.206167 +1	.844270	.624464	.128744 +1	.927453	.632722 +2	.821589	.748735 +1	.178631 +1
3	1.0	.513286 +2	.821699 +1	.100000 +1	.821699 +1	.143506	.317054	.260523 +1	.951162	.728449 +2	.160379 +1	.263104 +1	.286653 +1
	1.1	.452950 +2	.829707 +1	.138714 +1	.598143 +1	.226782	.373757	.223560 +1	.952030	.701808 +2	.147416 +1	.291826 +1	.282230 +1
	1.2	.407151 +2	.836873 +1	.174187 +1	.480445 +1	.299614	.419163	.201385 +1	.952788	.681621 +2	.136457 +1	.320706 +1	.278472 +1
	1.3	.370685 +2	.843325 +1	.206800 +1	.407797 +1	.361914	.457040	.186380 +1	.953455	.665573 +2	.127061 +1	.349719 +1	.275237 +1
	1.4	.340734 +2	.849166 +1	.236878 +1	.358482 +1	.415100	.489453	.175460 +1	.954046	.652408 +2	.118913 +1	.378849 +1	.272423 +1
	5/3	.281397 +2	.862348 +1	.306696 +1	.281174 +1	.523496	.557687	.156807 +1	.955340	.626377 +2	.101648 +1	.456984 +1	.266435 +1
5	1.0	.669455 +2	.240797 +2	.100000 +1	.240797 +2	.144478 -3	.196141	.472303 +1	.980706	.789387 +2	.184639 +1	.218082 +1	.490711 +1
	1.1	.567850 +2	.241703 +2	.214674 +1	.112591 +2	.541648 -2	.287422	.323611 +1	.980845	.740714 +2	.168511 +1	.240753 +1	.480802 +1
	1.2	.500866 +2	.242520 +2	.319276 +1	.759594 +1	.228955 -1	.350566	.266287 +1	.980971	.708671 +2	.155015 +1	.263489 +1	.472381 +1
	1.3	.450811 +2	.243262 +2	.415072 +1	.586071 +1	.509961 -1	.399759	.234287 +1	.981083	.684757 +2	.143545 +1	.286281 +1	.465131 +1
	1.4	.411177 +2	.243938 +2	.503126 +1	.484845 +1	.853909 -1	.440169	.213414 +1	.981185	.665843 +2	.133681 +1	.309121 +1	.458823 +1
	5/3	.335415 +2	.245480 +2	.706505 +1	.347457 +1	.185024	.521723	.181276 +1	.981414	.629747 +2	.113033 +1	.370225 +1	.445403 +1

TABLE I

VALUES OF OBLIQUE SHOCK PARAMETERS AT SHOCK DETACHMENT - Concluded

M_∞	γ	δ, deg	$\frac{p_2}{p_\infty}$	$\frac{T_2}{T_\infty}$	$\frac{\rho_2}{\rho_\infty}$	$\frac{p_{t,2}}{p_{t,\infty}}$	$\frac{u_2}{u_\infty}$	$\frac{\rho_2 u_2}{\rho_\infty u_\infty}$	M_2	θ, deg	C_p	$\frac{C_p}{\sin^2\delta}$	$M_\infty \sin\theta$
7	1.0	.735771 +2	.480408 +2	.100000 +1	.480408 +2	.181387 -8	.141424	.679411 +1	.989967	.819571 +2	.192003 +1	.208684 +1	.693115 +1
	1.1	.606962 +2	.481337 +2	.328883 +1	.146355 +2	.988542 -4	.256484	.375377 +1	.990005	.756530 +2	.174893 +1	.229987 +1	.678169 +1
	1.2	.530725 +2	.482180 +2	.537332 +1	.897359 +1	.200333 -2	.327850	.294199 +1	.990039	.719250 +2	.160603 +1	.251325 +1	.665456 +1
	1.3	.475554 +2	.482946 +2	.727963 +1	.663421 +1	.887341 -2	.381612	.253170 +1	.990070	.692290 +2	.148485 +1	.272692 +1	.654504 +1
	1.4	.432546 +2	.483646 +2	.902966 +1	.535620 +1	.218614 -1	.425026	.227653 +1	.990098	.671289 +2	.138091 +1	.294085 +1	.644967 +1
	5/3	.351447 +2	.485250 +2	.130639 +2	.371442 +1	.786647 -1	.511264	.189905 +1	.990163	.631727 +2	.116389 +1	.351237 +1	.624660 +1
10	1.0	.785223 +2	.990200 +2	.100000 +1	.990200 +2	.31478 -19	.995038 -1	.985286 +1	.995037	.843187 +2	.196040 +1	.204122 +1	.995088 +1
	1.1	.629890 +2	.991142 +2	.571697 +1	.173368 +2	.464843 -6	.237918	.412474 +1	.995049	.766320 +2	.178389 +1	.224746 +1	.972905 +1
	1.2	.547542 +2	.991996 +2	.100090 +2	.991107 +1	.986671 -4	.314806	.312006 +1	.995057	.725587 +2	.163665 +1	.245387 +1	.954025 +1
	1.3	.489265 +2	.992775 +2	.139309 +2	.712641 +1	.109548 -2	.371400	.264674 +1	.995065	.696773 +2	.151198 +1	.266042 +1	.937751 +1
	1.4	.444290 +2	.993488 +2	.175287 +2	.566777 +1	.440592 -2	.416610	.236125 +1	.995072	.674544 +2	.140498 +1	.286711 +1	.923574 +1
	5/3	.360174 +2	.995124 +2	.258132 +2	.385509 +1	.293948 -1	.505572	.194902 +1	.995088	.632990 +2	.118213 +1	.341878 +1	.893364 +1
15	1.0	.823549 +2	.224009 +3	.100000 +1	.224009 +3	.51046 -46	.665192 -1	.149009 +2	.997785	.861945 +2	.198230 +1	.201802 +1	.149669 +2
	1.1	.642914 +2	.224104 +3	.116691 +2	.192048 +2	.410231 -9	.227230	.436392 +1	.997787	.772038 +2	.180285 +1	.222075 +1	.146275 +2
	1.2	.556828 +2	.224190 +3	.213722 +2	.104898 +2	.235244 -5	.307519	.322581 +1	.997789	.729200 +2	.165327 +1	.242357 +1	.143384 +2
	1.3	.496760 +2	.224268 +3	.302348 +2	.741755 +1	.861464 -4	.365765	.271308 +1	.997790	.699314 +2	.152662 +1	.262645 +1	.140892 +2
	1.4	.450677 +2	.224340 +3	.383615 +2	.584805 +1	.641610 -3	.412000	.240939 +1	.997792	.676390 +2	.141805 +1	.282938 +1	.138721 +2
	5/3	.364893 +2	.224506 +3	.570628 +2	.393436 +1	.912733 -2	.502489	.197697 +1	.997795	.633727 +2	.119201 +1	.337078 +1	.134091 +2
20	1.0	.842680 +2	.399005 +3	.100000 +1	.399005 +3	.54269 -84	.499380 -1	.199255 +2	.998752	.871412 +2	.199002 +1	.201008 +1	.199751 +2
	1.1	.647622 +2	.399100 +3	.200024 +2	.199526 +2	.19462 -11	.223341	.445624 +1	.998753	.774132 +2	.180954 +1	.221161 +1	.195193 +2
	1.2	.560133 +2	.399186 +3	.372812 +2	.107074 +2	.148675 -6	.304911	.326482 +1	.998754	.730504 +2	.165910 +1	.241318 +1	.191312 +2
	1.3	.499413 +2	.399265 +3	.530607 +2	.752468 +1	.134043 -4	.363760	.273718 +1	.998754	.700229 +2	.153177 +1	.261480 +1	.187966 +2
	1.4	.452932 +2	.399337 +3	.675280 +2	.591365 +1	.157814 -3	.410365	.242676 +1	.998754	.677054 +2	.142262 +1	.281644 +1	.185049 +2
	5/3	.366555 +2	.399503 +3	.100813 +3	.396283 +1	.391501 -2	.501403	.198697 +1	.998755	.633996 +2	.119548 +1	.335430 +1	.178830 +2
30	1.0	.861795 +2	.899002 +3	.100000 +1	.899002 +3	.5452 -192	.333152 -1	.299504 +2	.999442	.880919 +2	.199570 +1	.200446 +1	.299834 +2
	1.1	.651037 +2	.899097 +3	.438118 +2	.205218 +2	.78759 -15	.220513	.452531 +1	.999445	.775659 +2	.181435 +1	.220514 +1	.292963 +2
	1.2	.562512 +2	.899184 +3	.827356 +2	.108682 +2	.280345 -8	.303029	.329337 +1	.999445	.731449 +2	.166329 +1	.240584 +1	.287112 +2
	1.3	.501318 +2	.899263 +3	.118278 +3	.760296 +1	.936059 -6	.362318	.275469 +1	.999445	.700890 +2	.153550 +1	.260655 +1	.282067 +2
	1.4	.454549 +2	.899335 +3	.150861 +3	.596134 +1	.213255 -4	.409192	.243933 +1	.999445	.677535 +2	.142593 +1	.280728 +1	.277669 +2
	5/3	.367745 +2	.899501 +3	.225813 +3	.398340 +1	.117390 -2	.500624	.199419 +1	.999445	.634191 +2	.119801 +1	.334262 +1	.268291 +2
40	1.0	.871348 +2	.159900 +4	.100000 +1	.159900 +4	.9568 -347	.249940 -1	.399654 +2	.999765	.885684 +2	.199750 +1	.200250 +1	.399875 +2
	1.1	.652242 +2	.159910 +4	.771452 +2	.207284 +2	.27764 -17	.219512	.455014 +1	.999687	.776200 +2	.181601 +1	.220289 +1	.390699 +2
	1.2	.563349 +2	.159918 +4	.146372 +3	.109255 +2	.162611 -9	.302366	.330350 +1	.999688	.731783 +2	.166478 +1	.240328 +1	.382884 +2
	1.3	.501987 +2	.159926 +4	.209582 +3	.763071 +1	.139546 -6	.361811	.276088 +1	.999688	.701123 +2	.153680 +1	.260368 +1	.376145 +2
	1.4	.455116 +2	.159933 +4	.267528 +3	.597820 +1	.510679 -5	.408779	.244376 +1	.999688	.677705 +2	.142710 +1	.280409 +1	.370270 +2
	5/3	.368162 +2	.159950 +4	.400813 +3	.399065 +1	.497315 -3	.500351.	.199672 +1	.999688	.634260 +2	.119886 +1	.333855 +1	.357743 +2

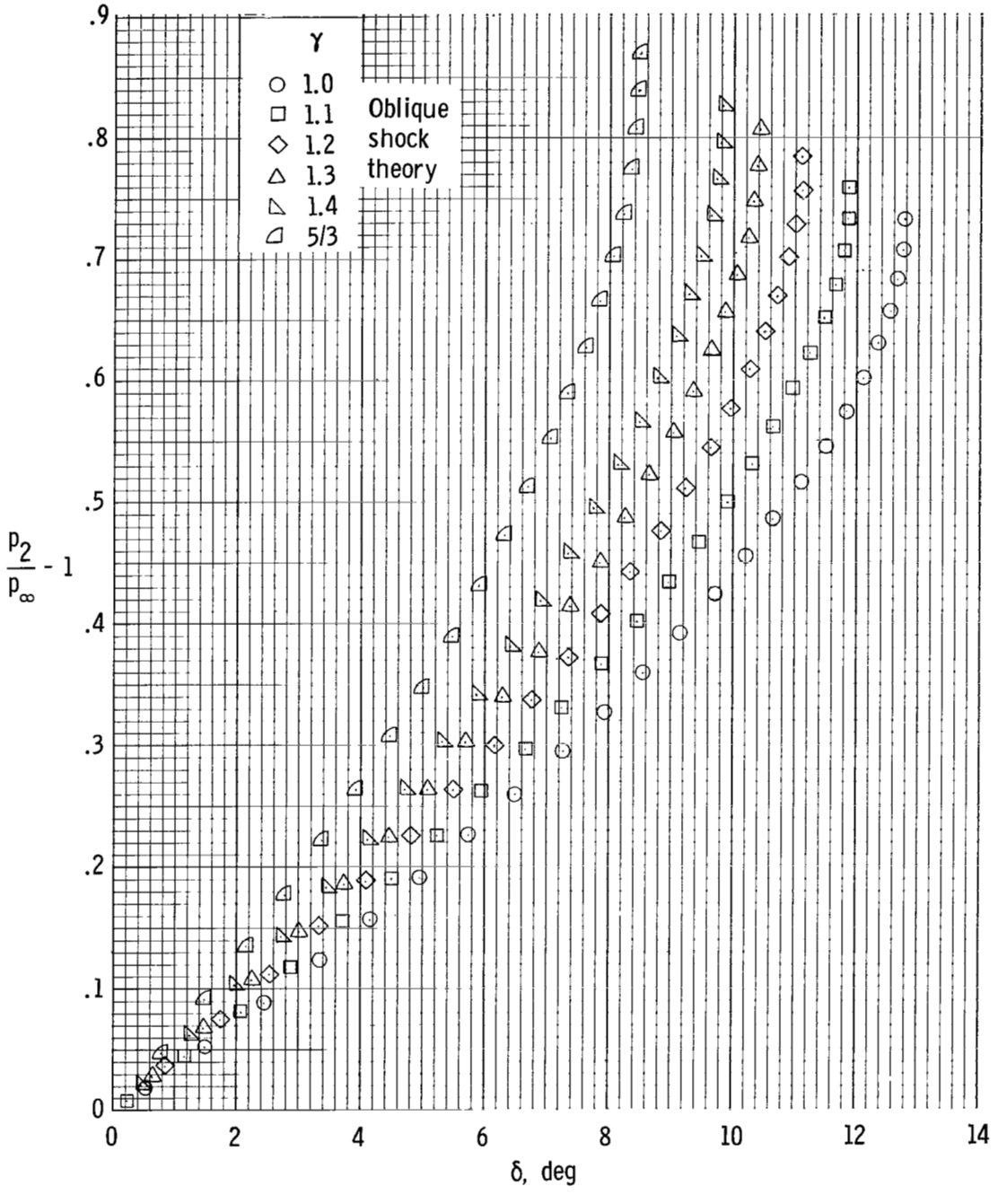

(a) $M_\infty = \sqrt{2}$; pressure difference ratio.

Figure 1.- Flow parameters across an oblique shock as a function of flow-deflection angle.

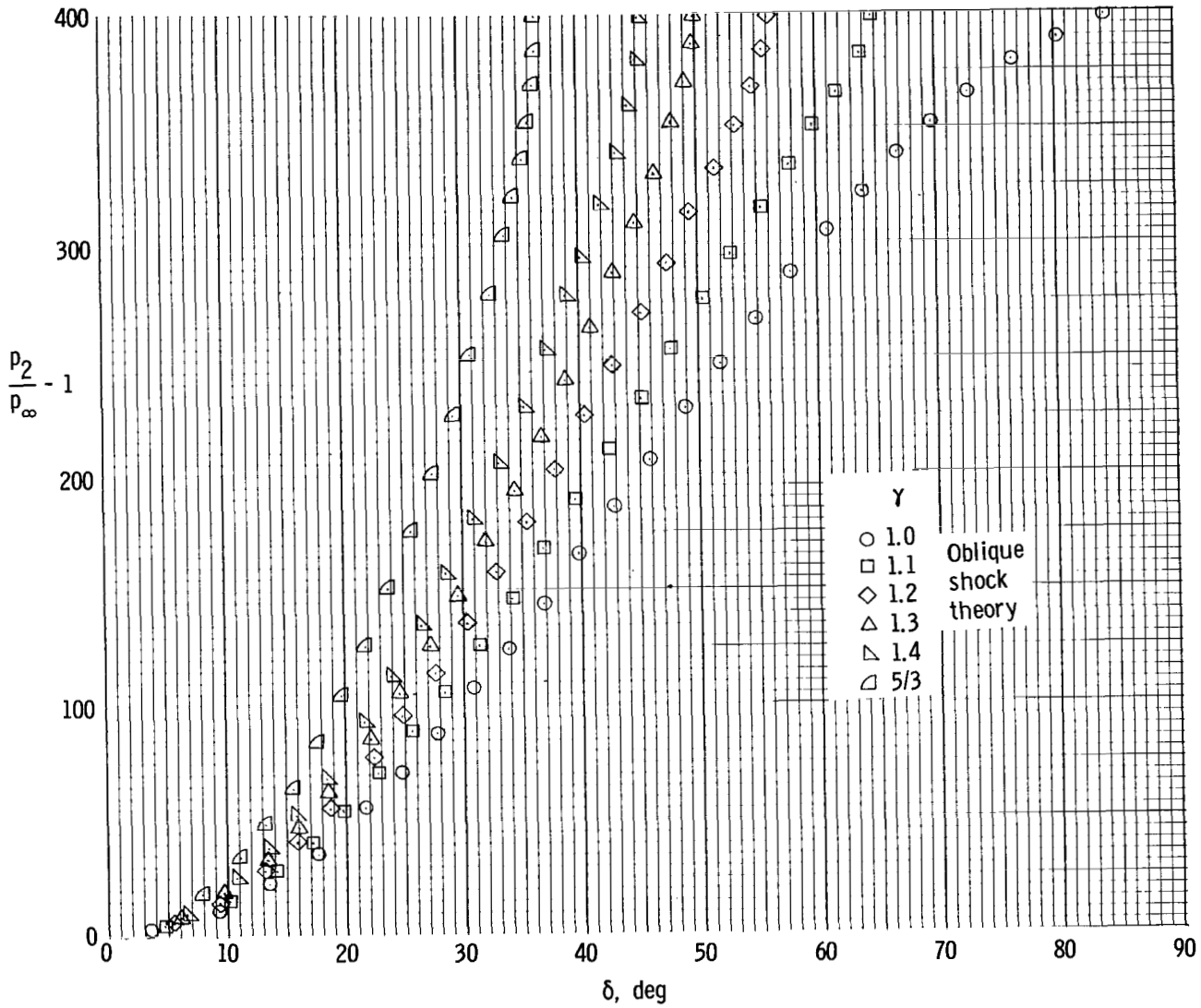

(b) $M_\infty = 20$; pressure difference ratio.

Figure 1.- Continued.

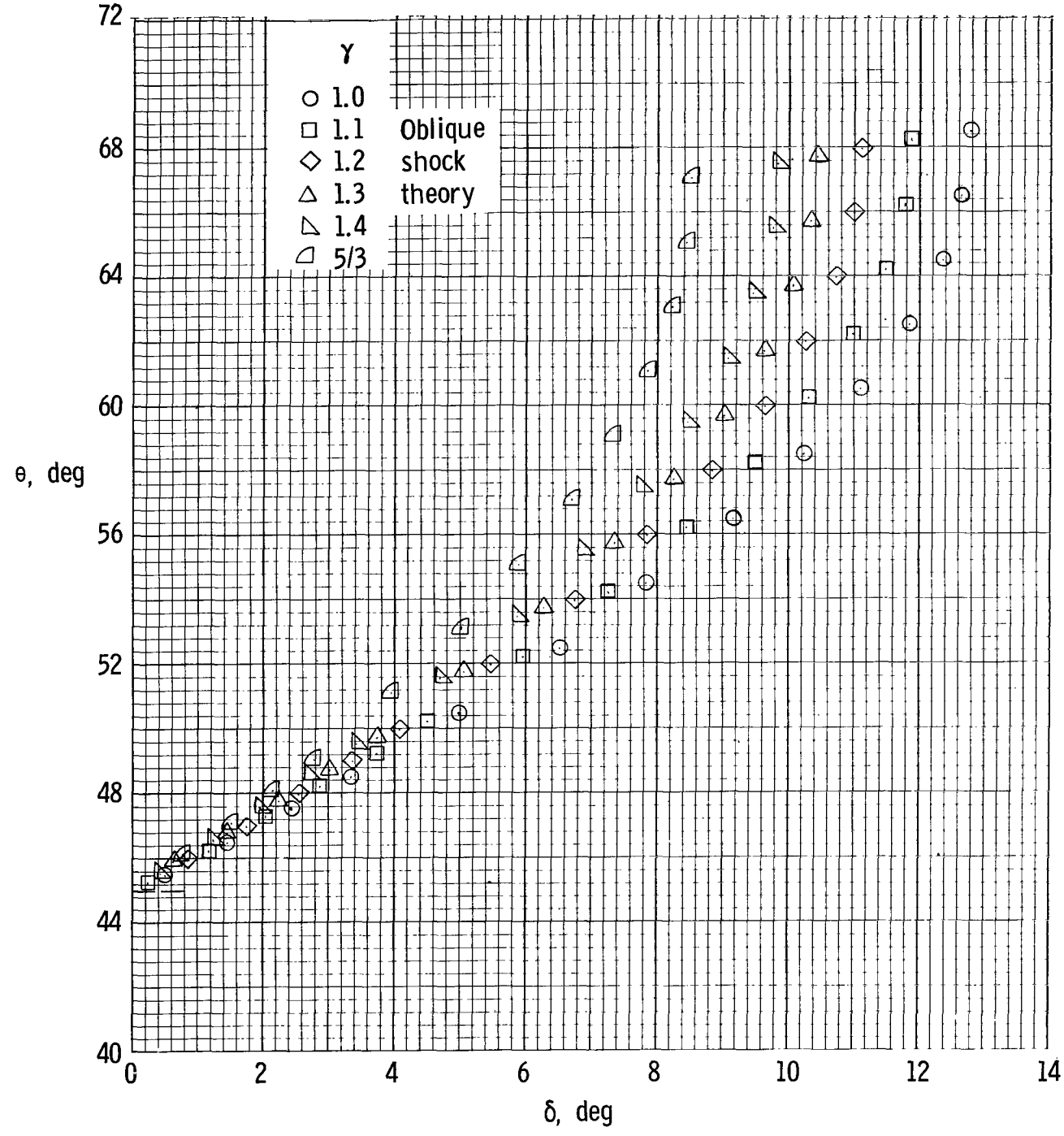

(c) $M_\infty = \sqrt{2}$; shock angle.

Figure 1.- Continued.

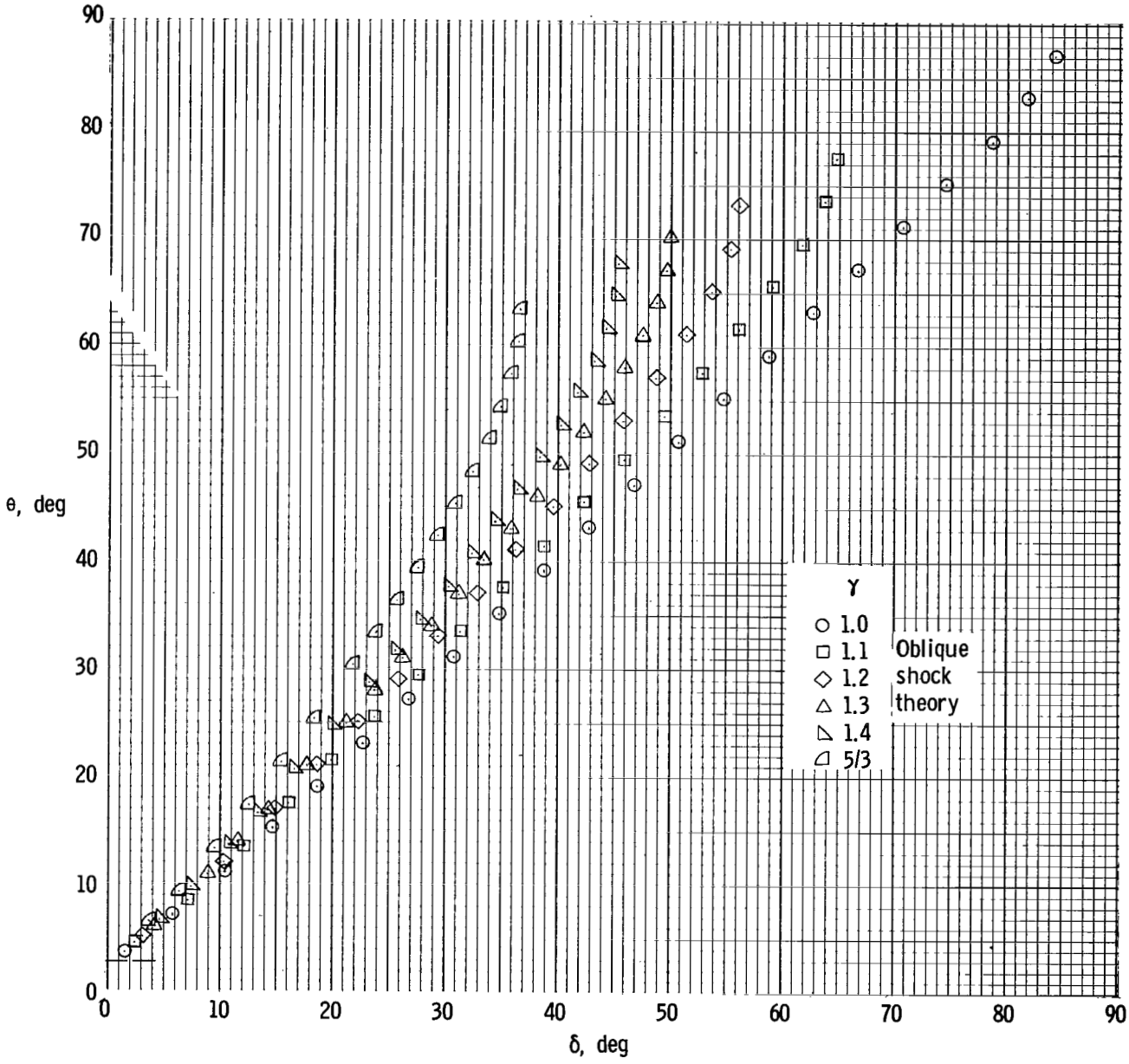

(d) $M_\infty = 20$; shock angle.

Figure 1.- Continued.

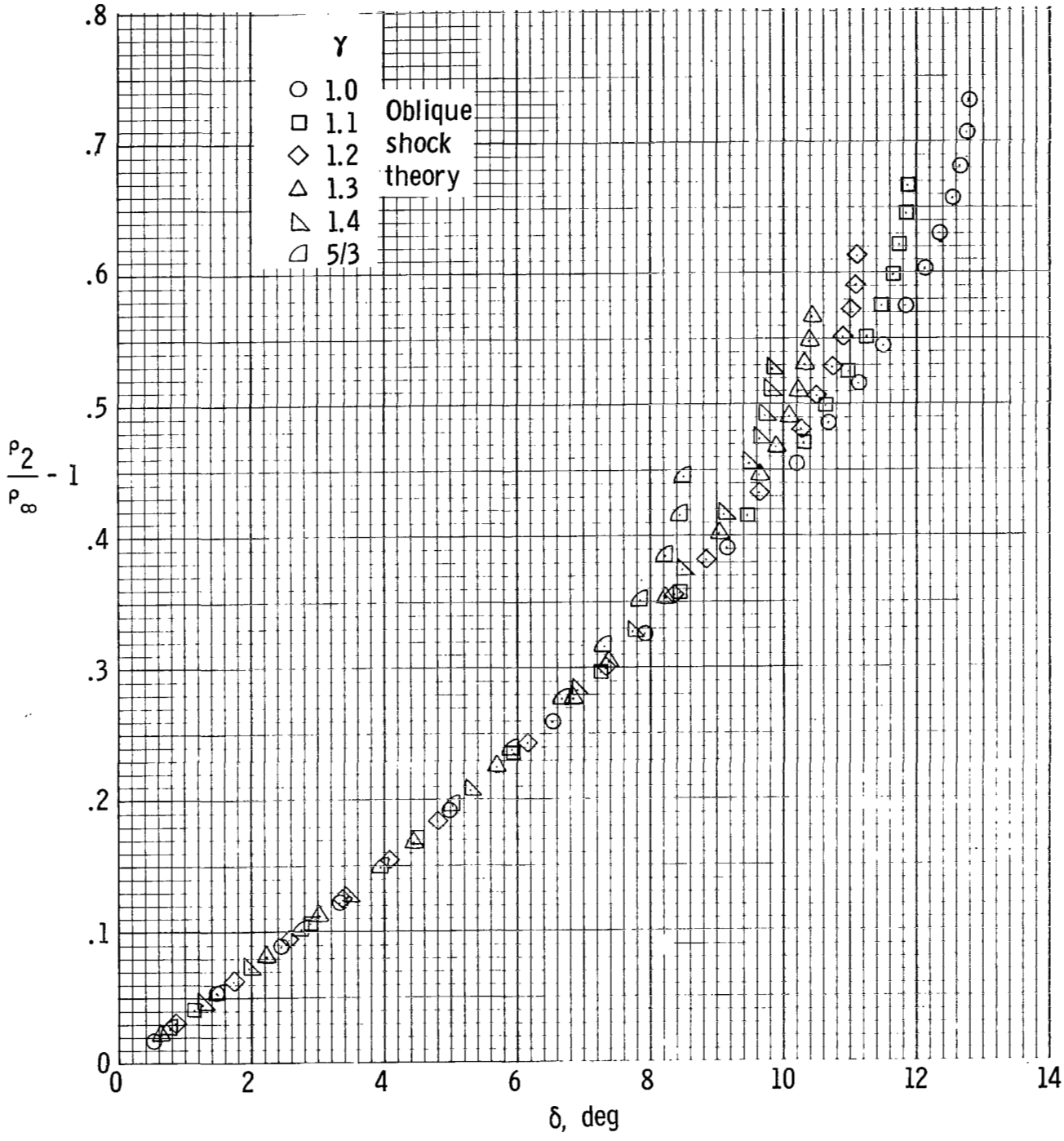

(e) $M_\infty = \sqrt{2}$; density difference ratio.

Figure 1.- Continued.

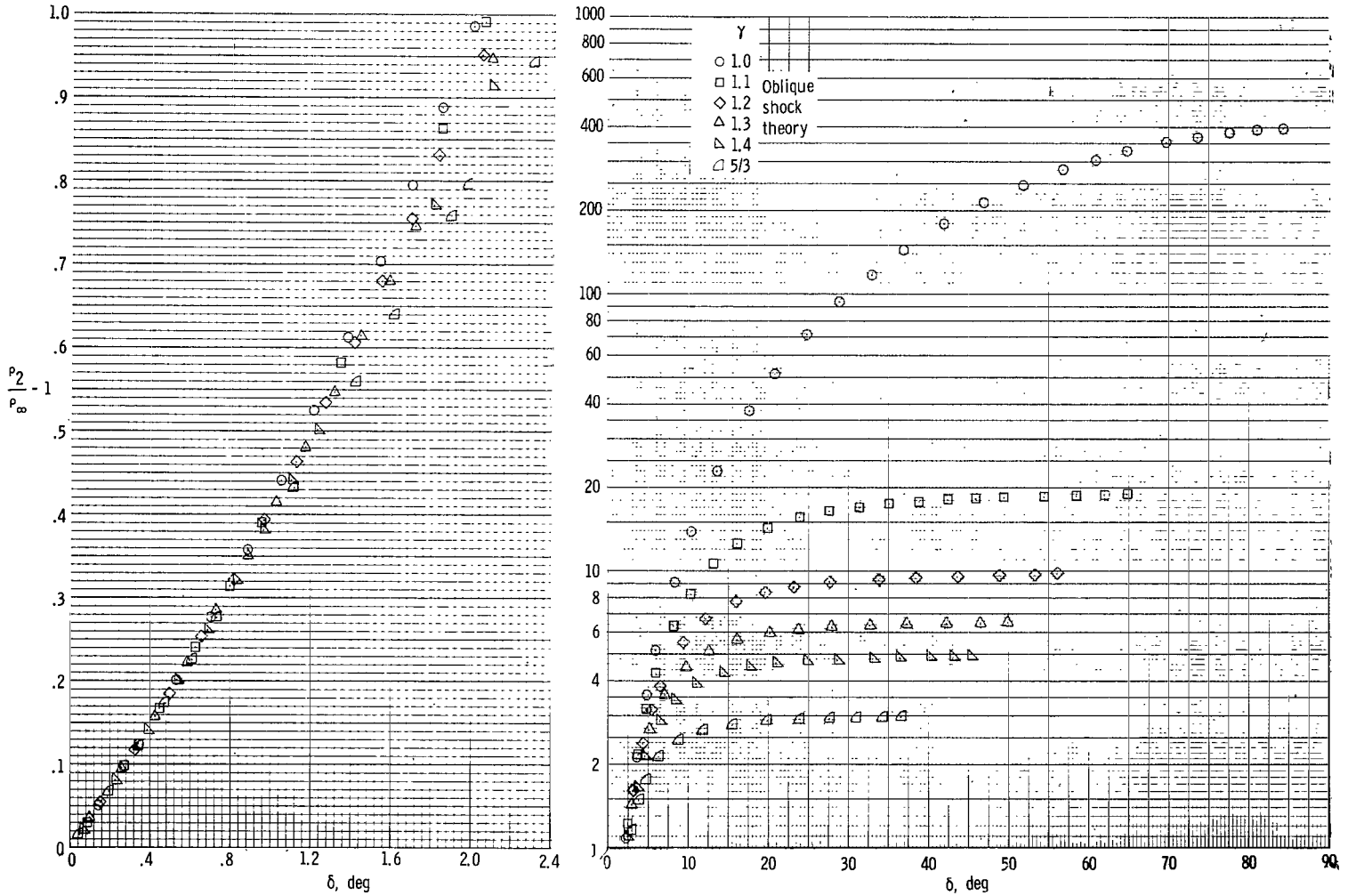

(f) $M_\infty = 20$; density difference ratio.

Figure 1.- Continued.

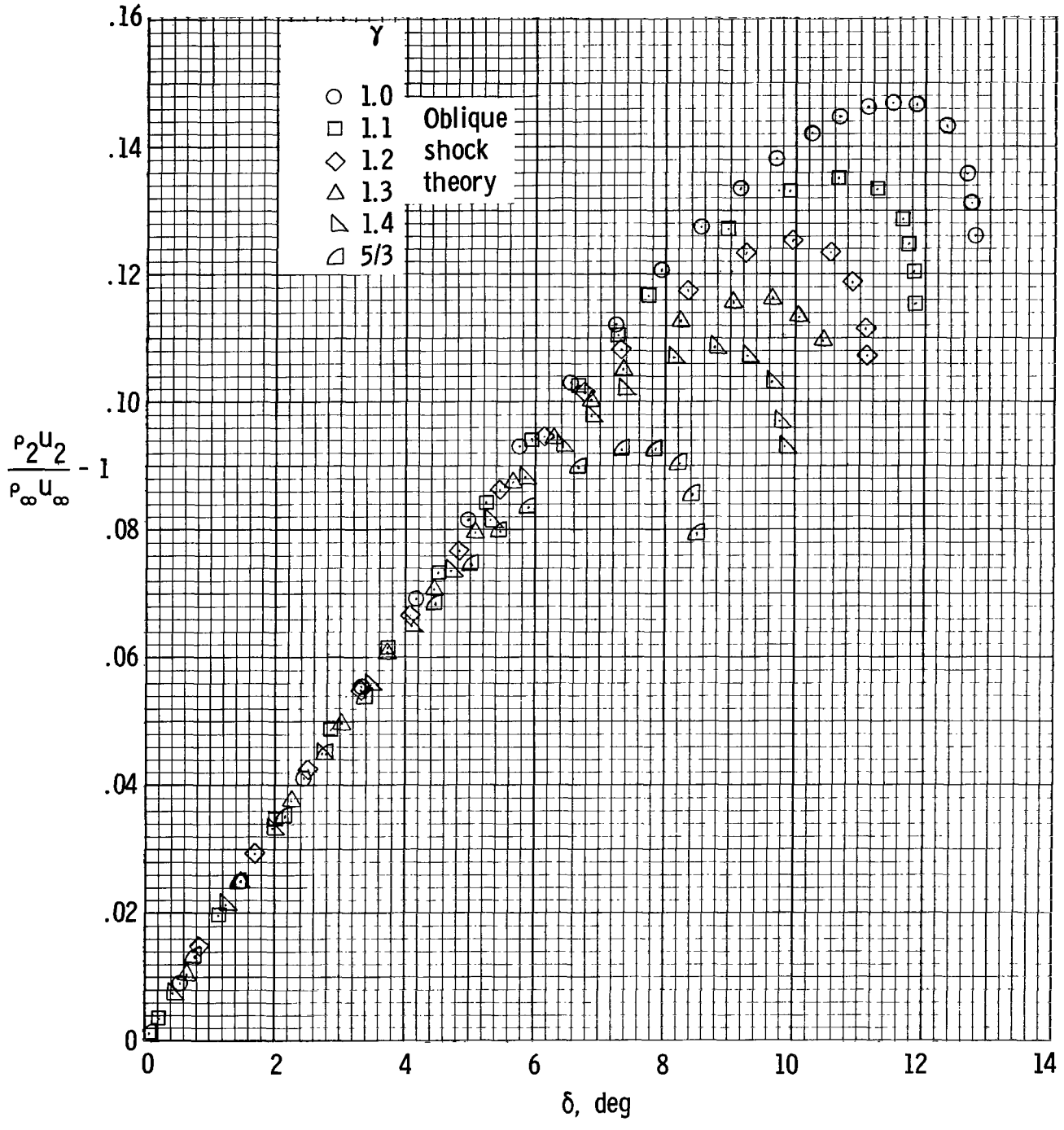

(g) $M_\infty = \sqrt{2}$; mass flow difference ratio.

Figure 1.- Continued.

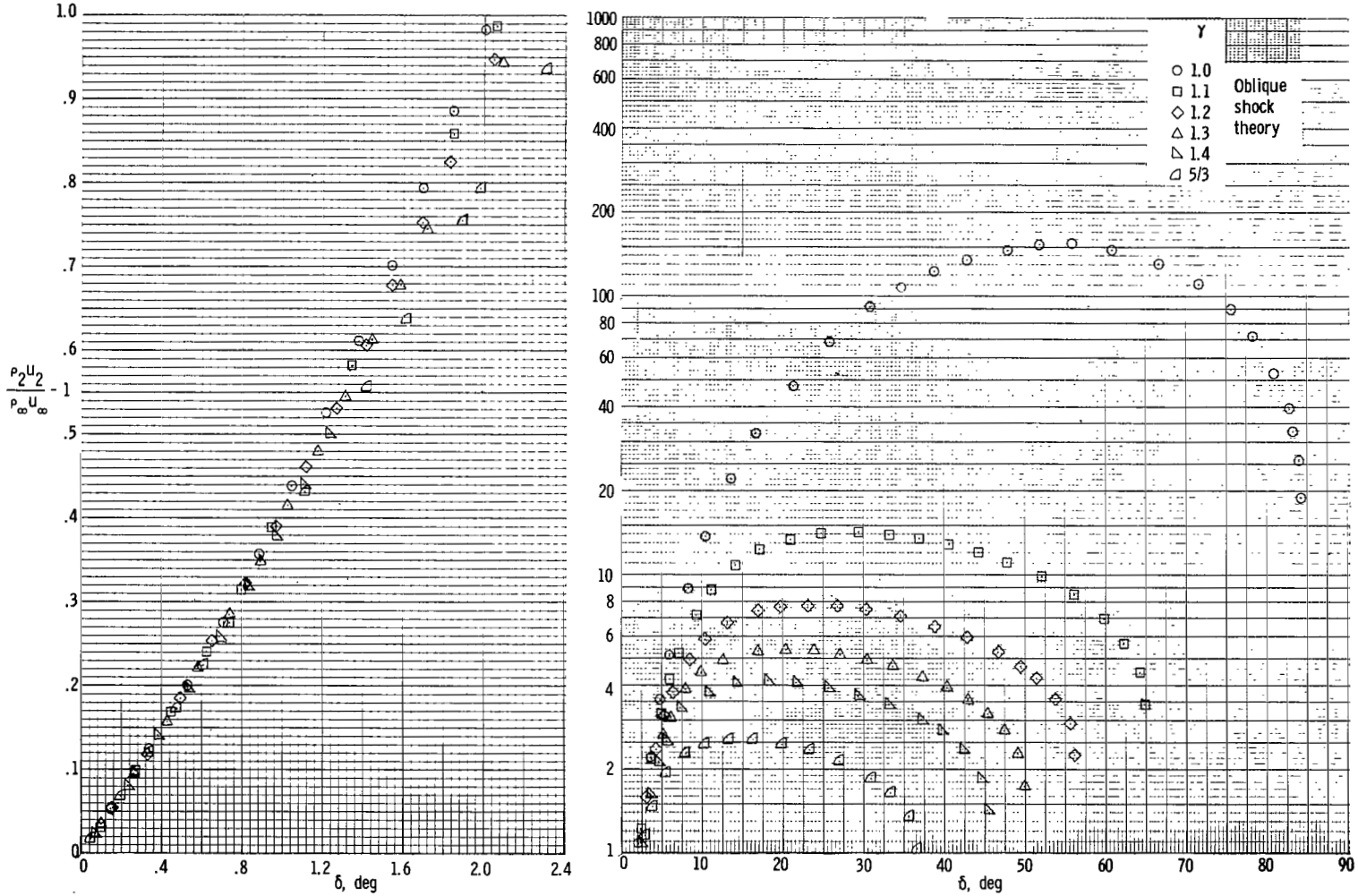

(h) $M_\infty = 20$; mass flow difference ratio.

Figure 1.- Continued.

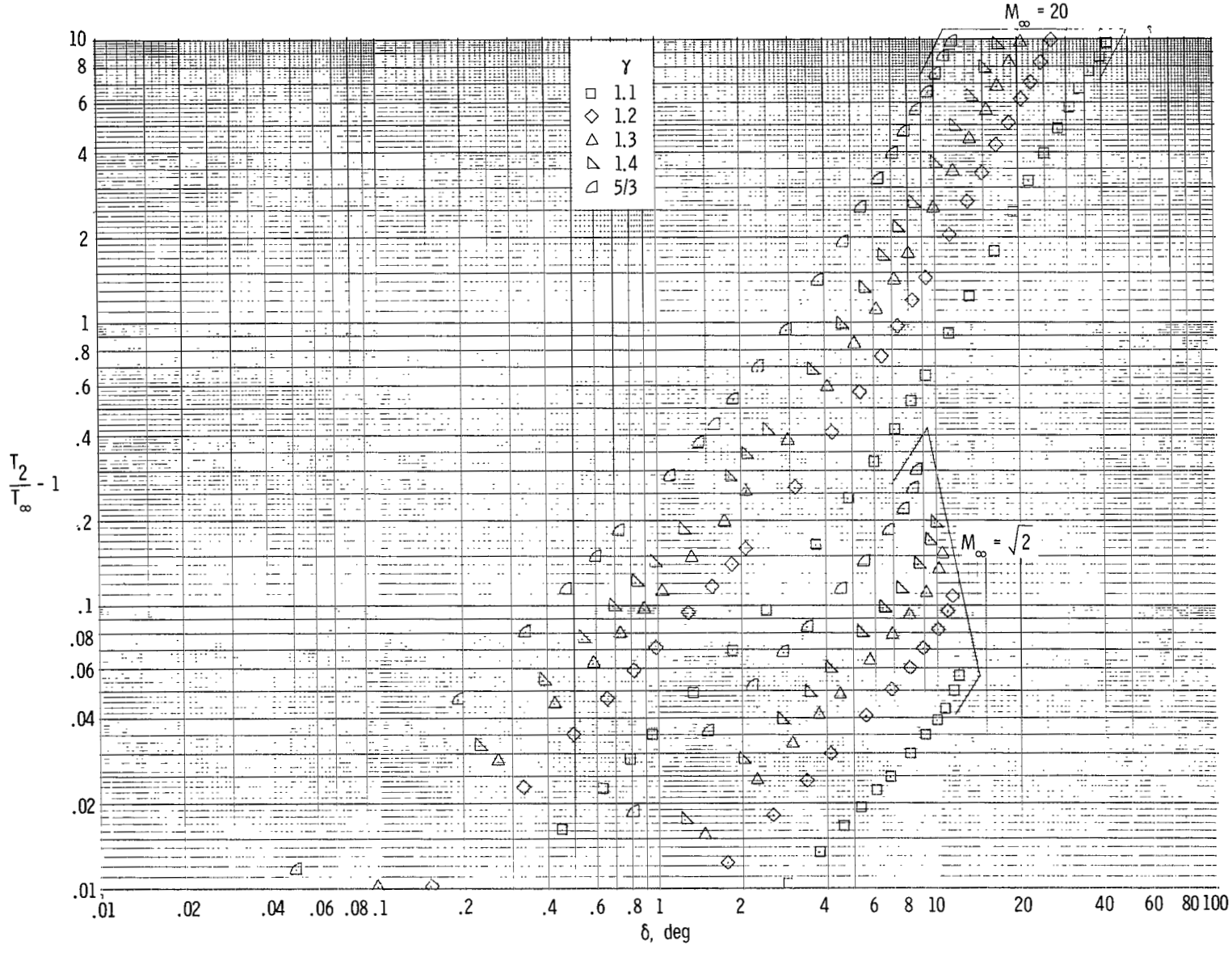

(1) $M_\infty = \sqrt{2}$ and 20; temperature difference ratio.

Figure 1.- Concluded.

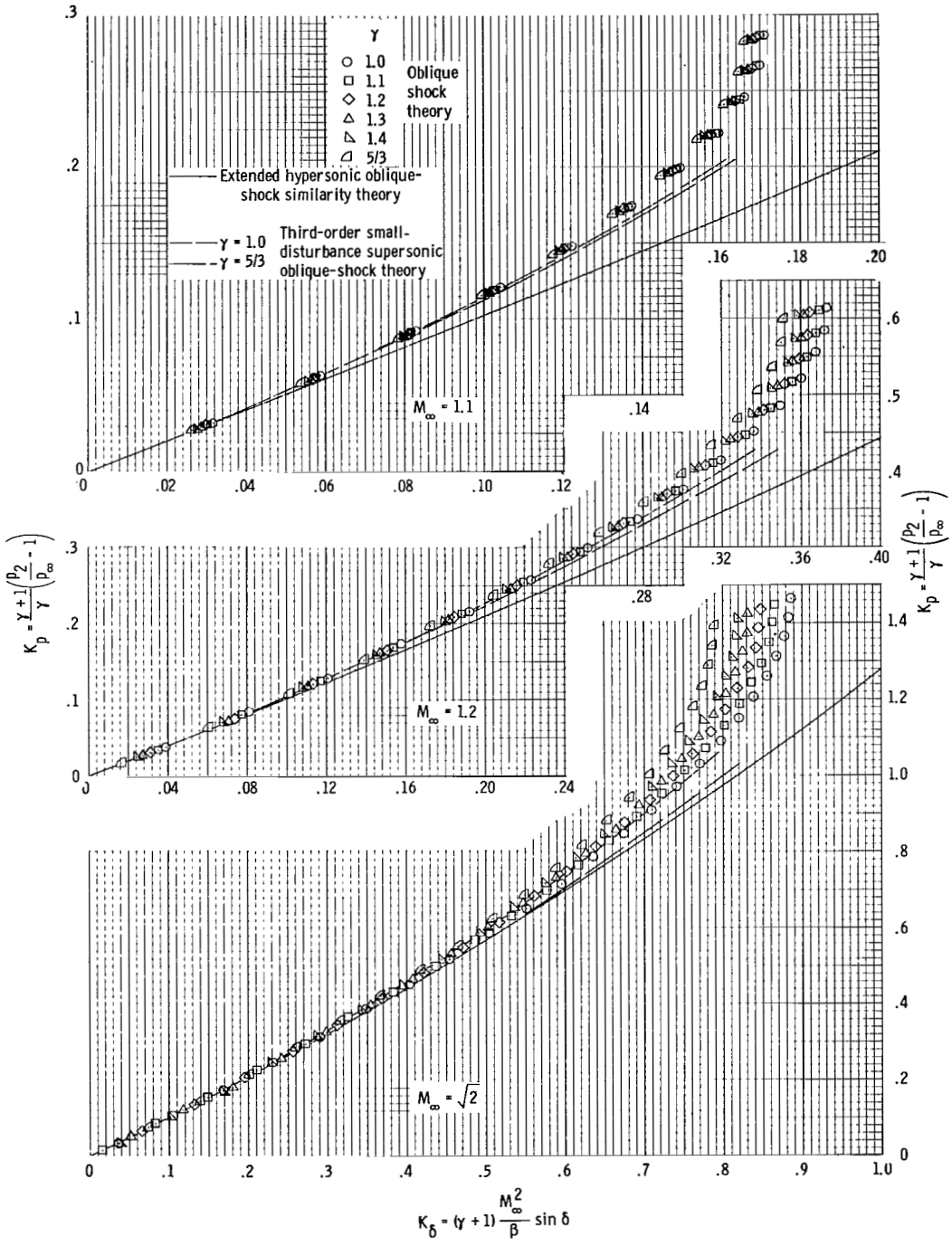

(a) Mach numbers 1.1, 1.2, and $\sqrt{2}$.

Figure 2.- Correlation of pressure ratio across oblique shock.

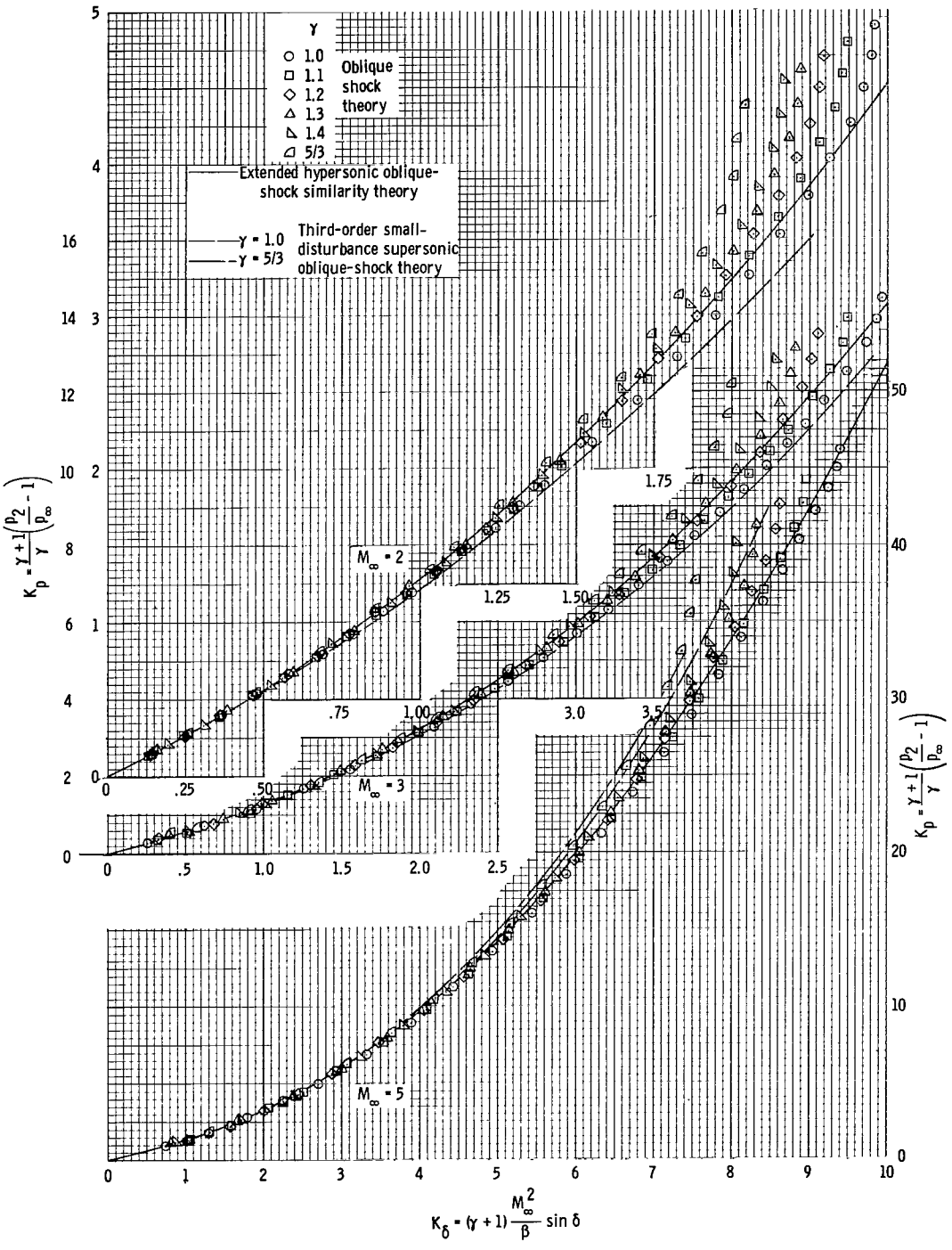

(b) Mach numbers 2, 3, and 5.

Figure 2.- Continued.

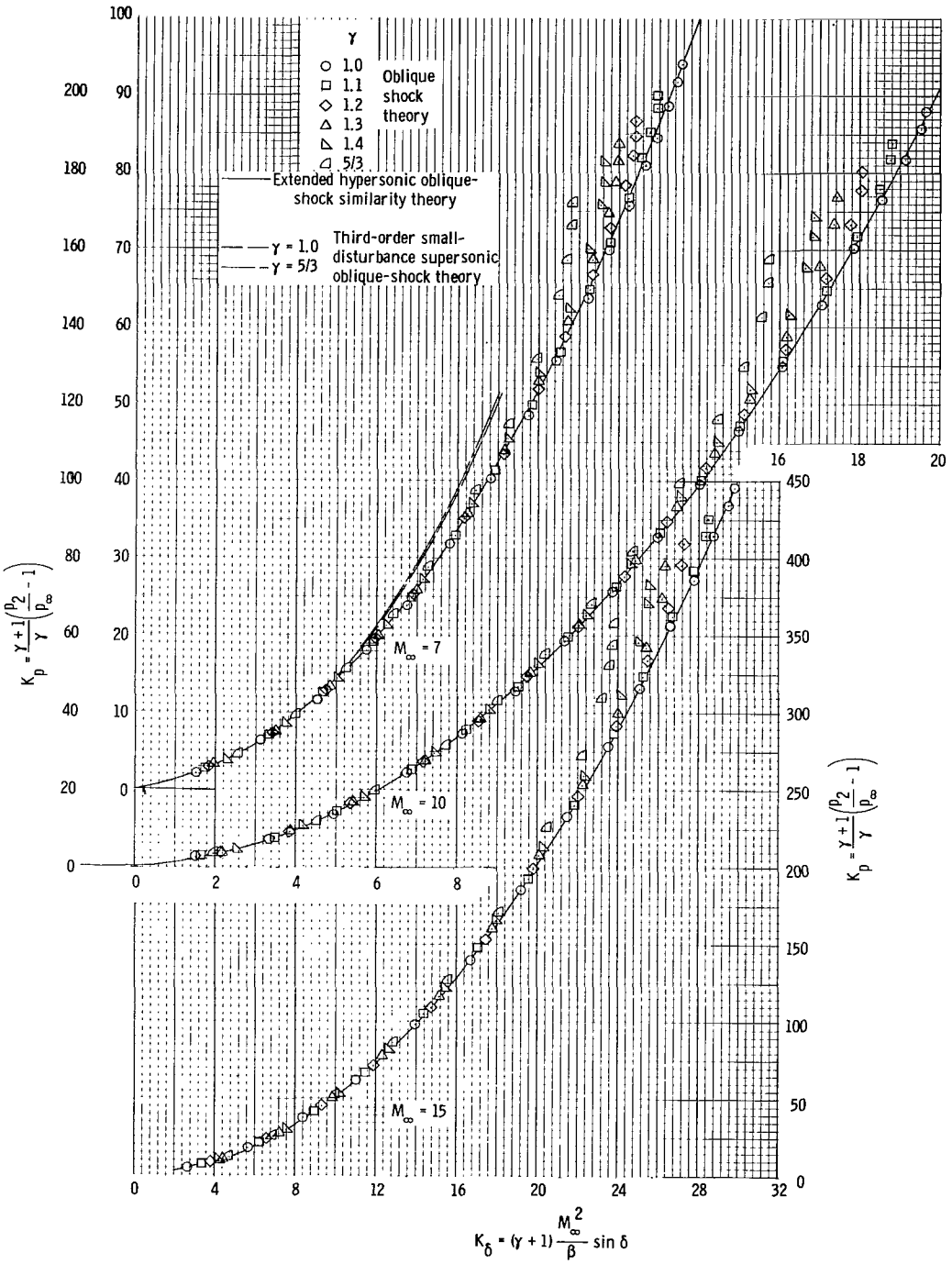

(c) Mach numbers 7, 10, and 15.

Figure 2.- Continued.

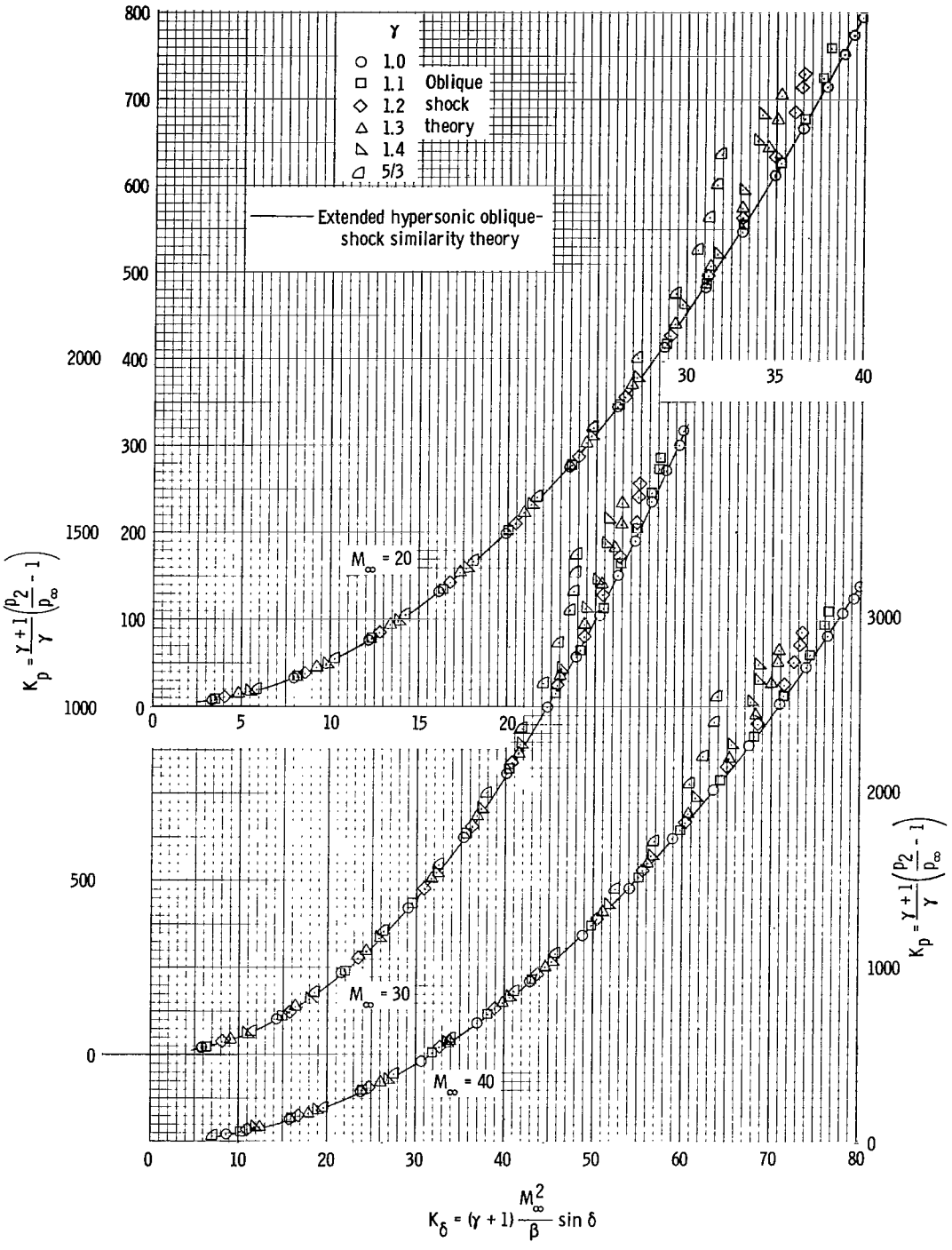

(d) Mach numbers 20, 30, and 40.

Figure 2.- Concluded.

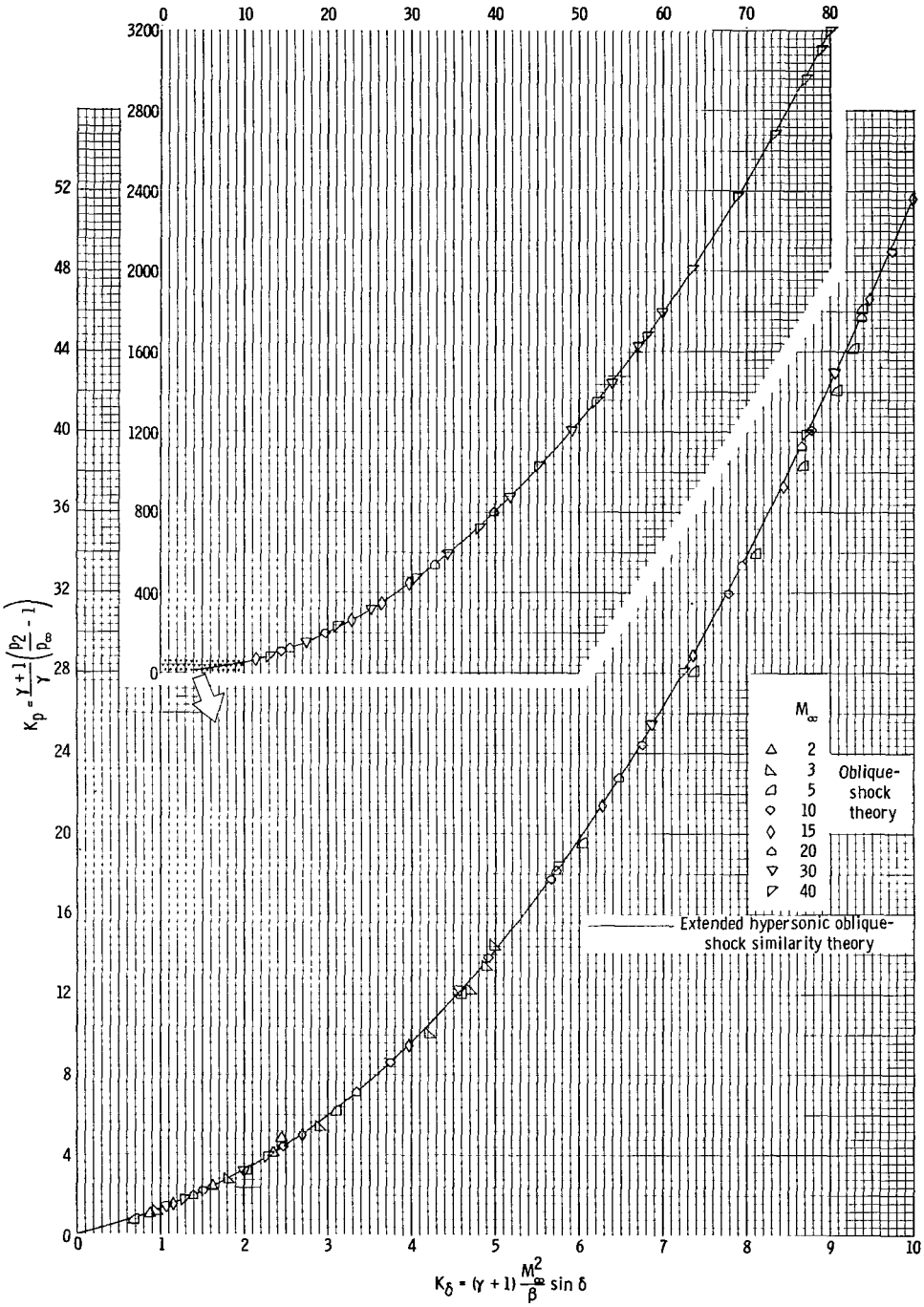

(a) $\gamma = 1$.

Figure 3.- Correlation of pressure ratio across an oblique shock at a fixed value of γ.

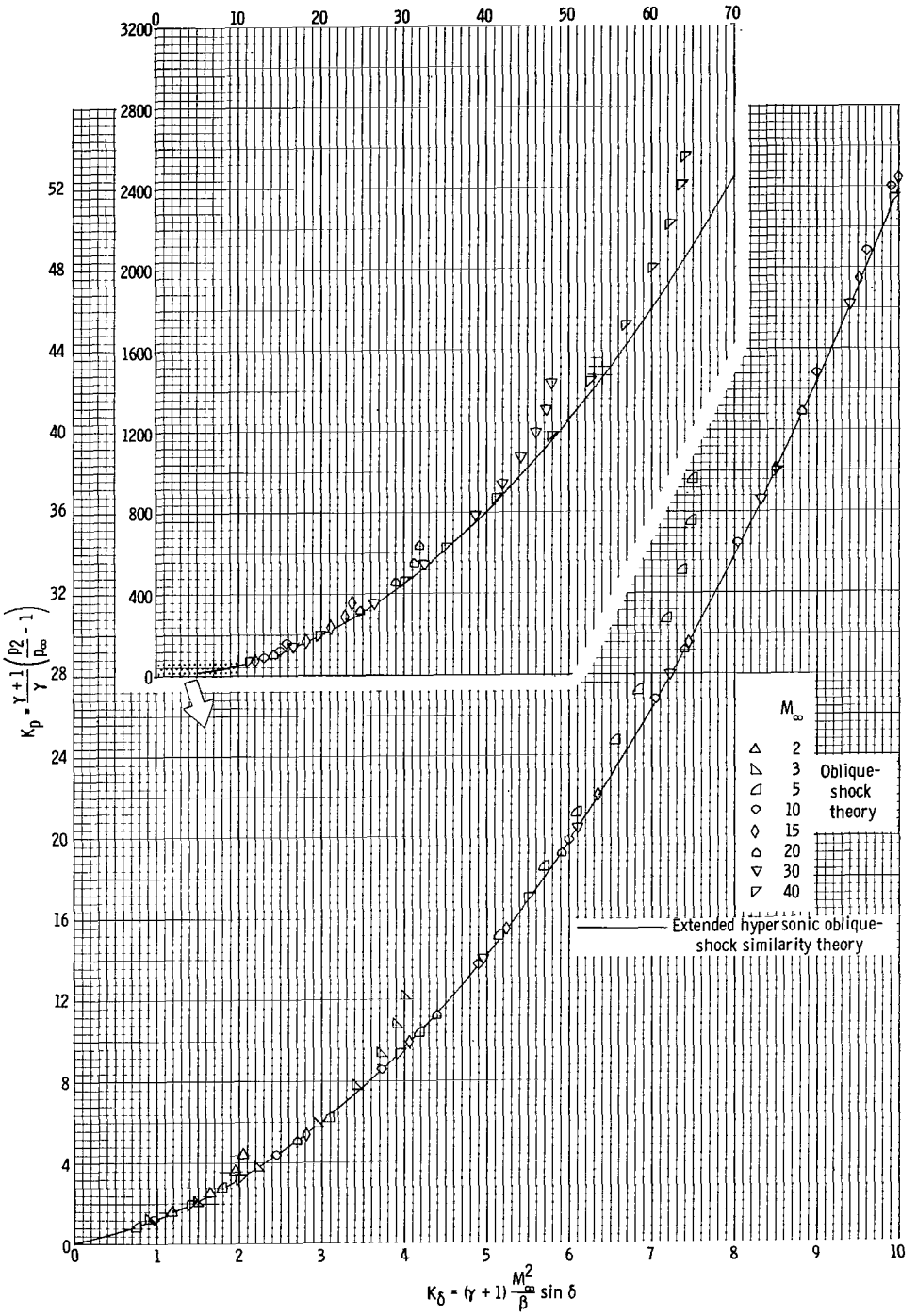

(b) $\gamma = 5/3$.

Figure 3.- Concluded.

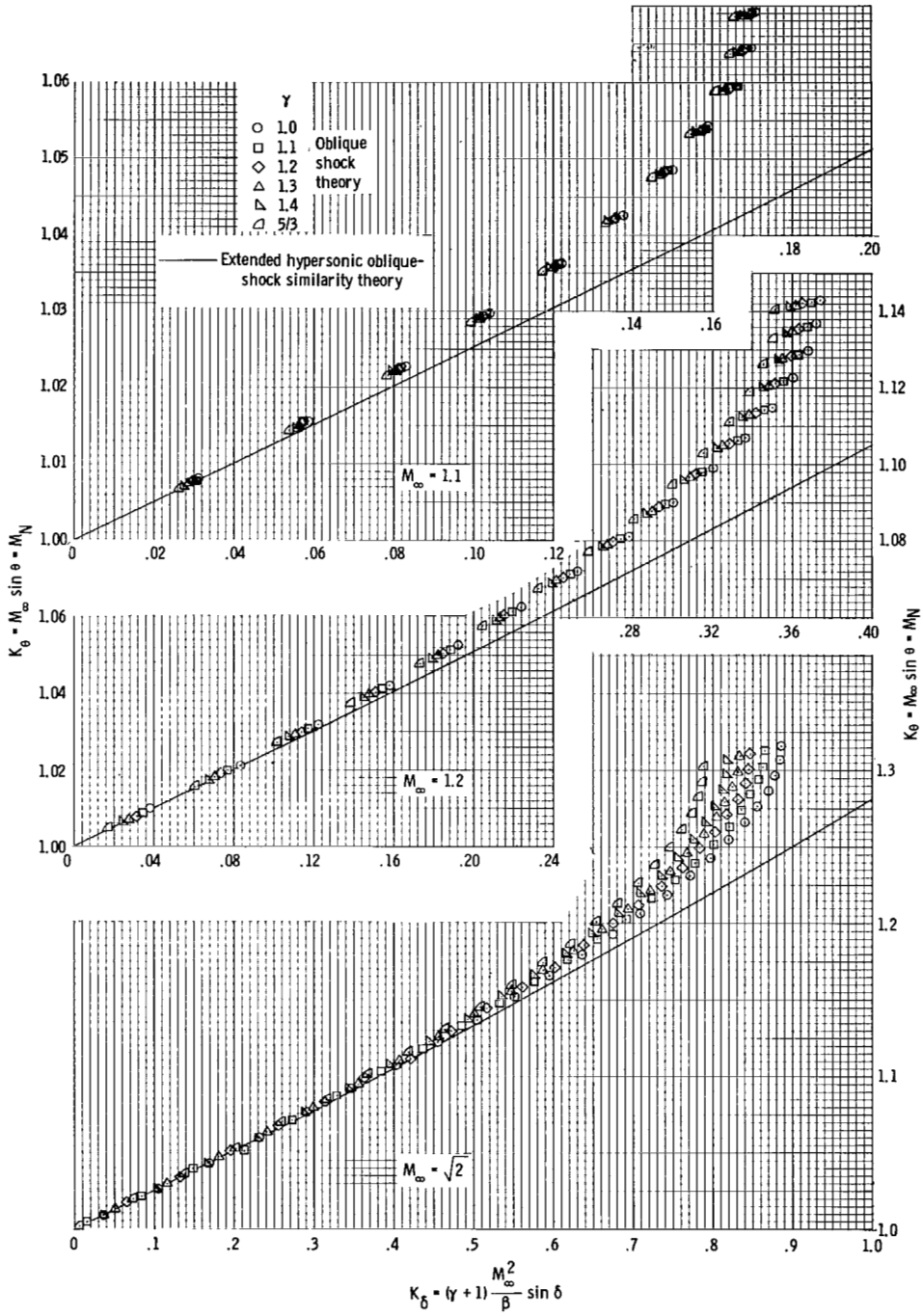

(a) Mach numbers 1.1, 1.2, and $\sqrt{2}$.

Figure 4.- Correlation of two-dimensional oblique shock angle.

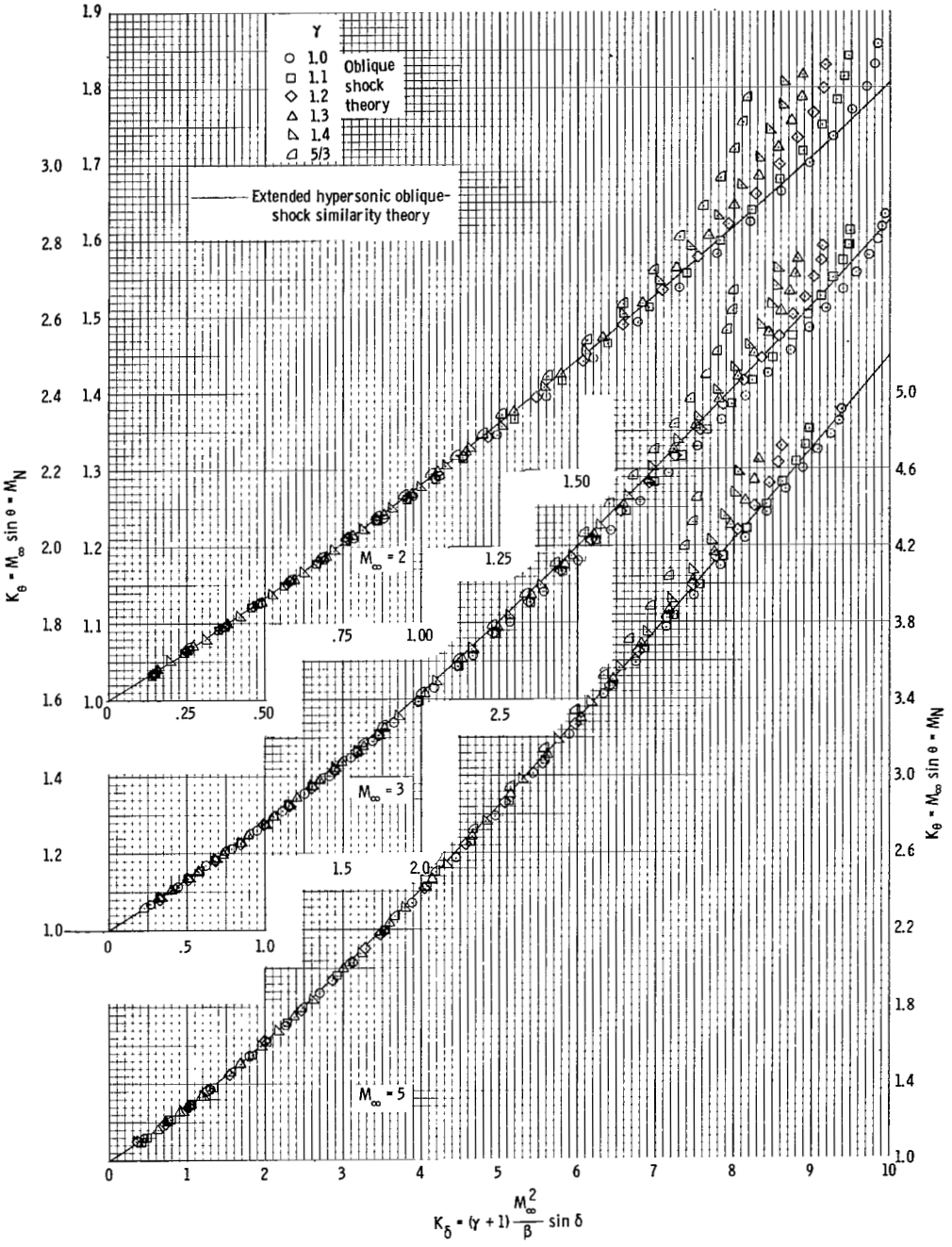

(b) Mach numbers 2, 3, and 5.

Figure 4.- Continued.

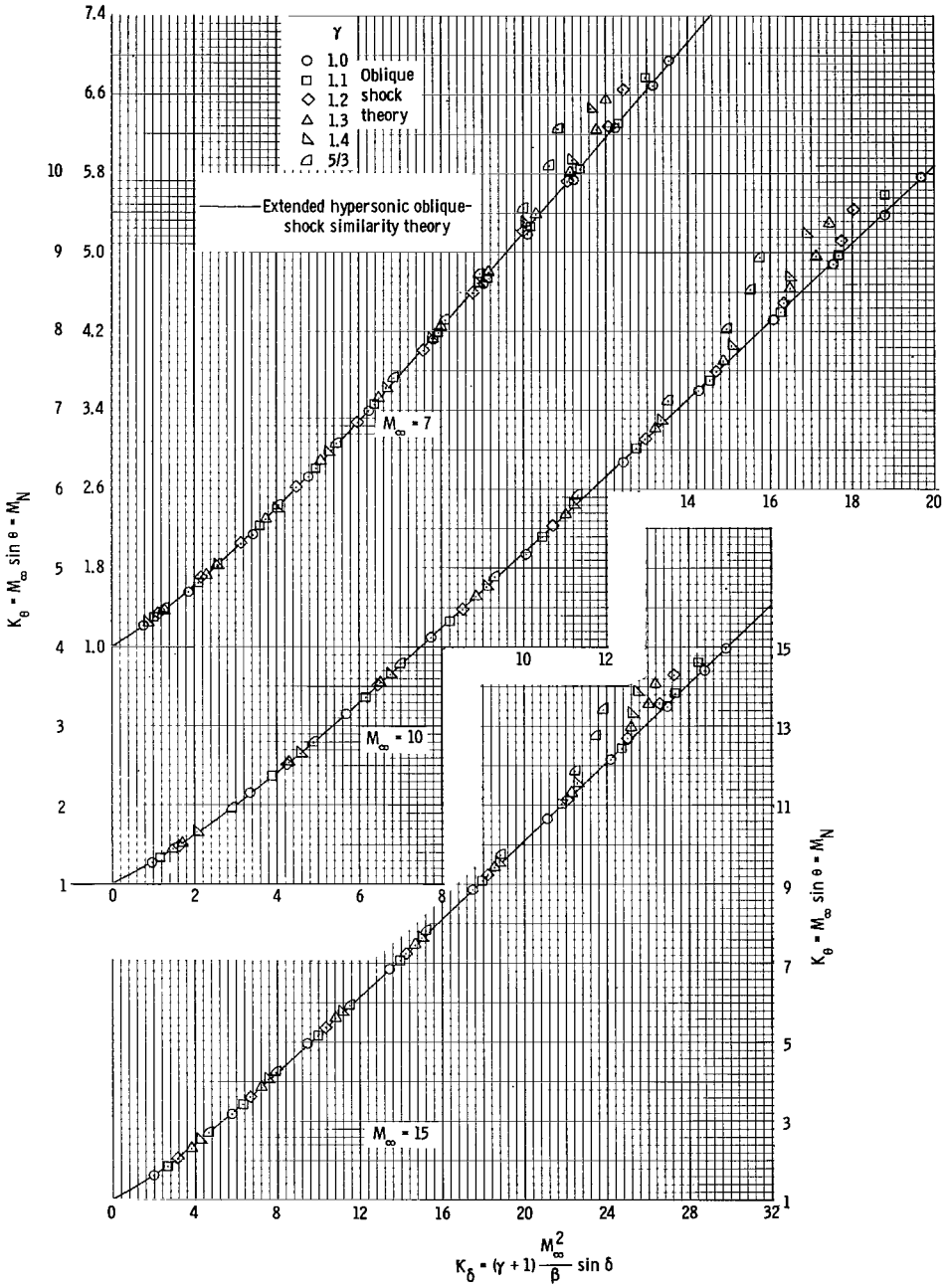

(c) Mach numbers 7, 10, and 15.

Figure 4.- Continued.

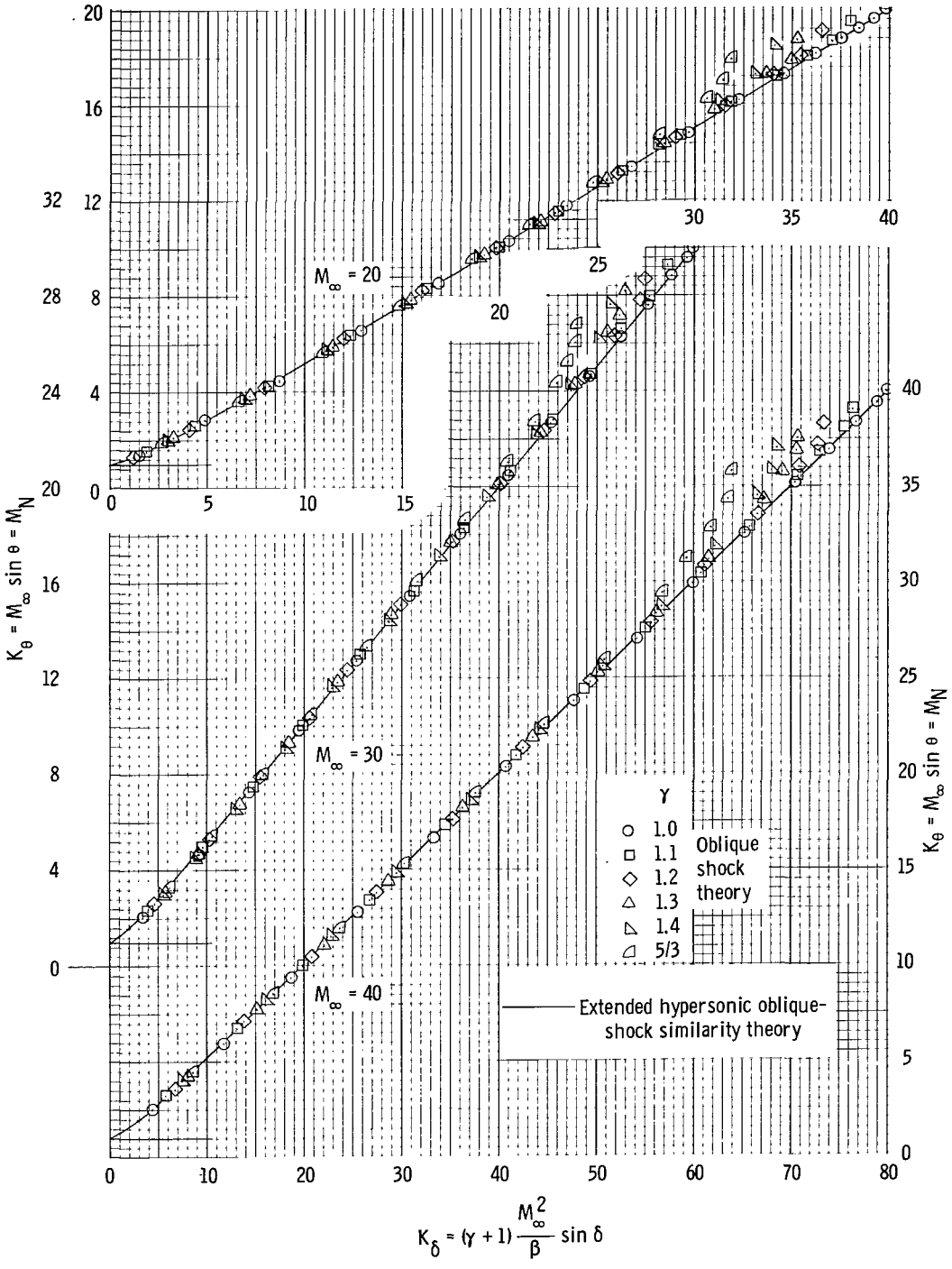

(d) Mach numbers 20, 30, and 40.

Figure 4.- Concluded.

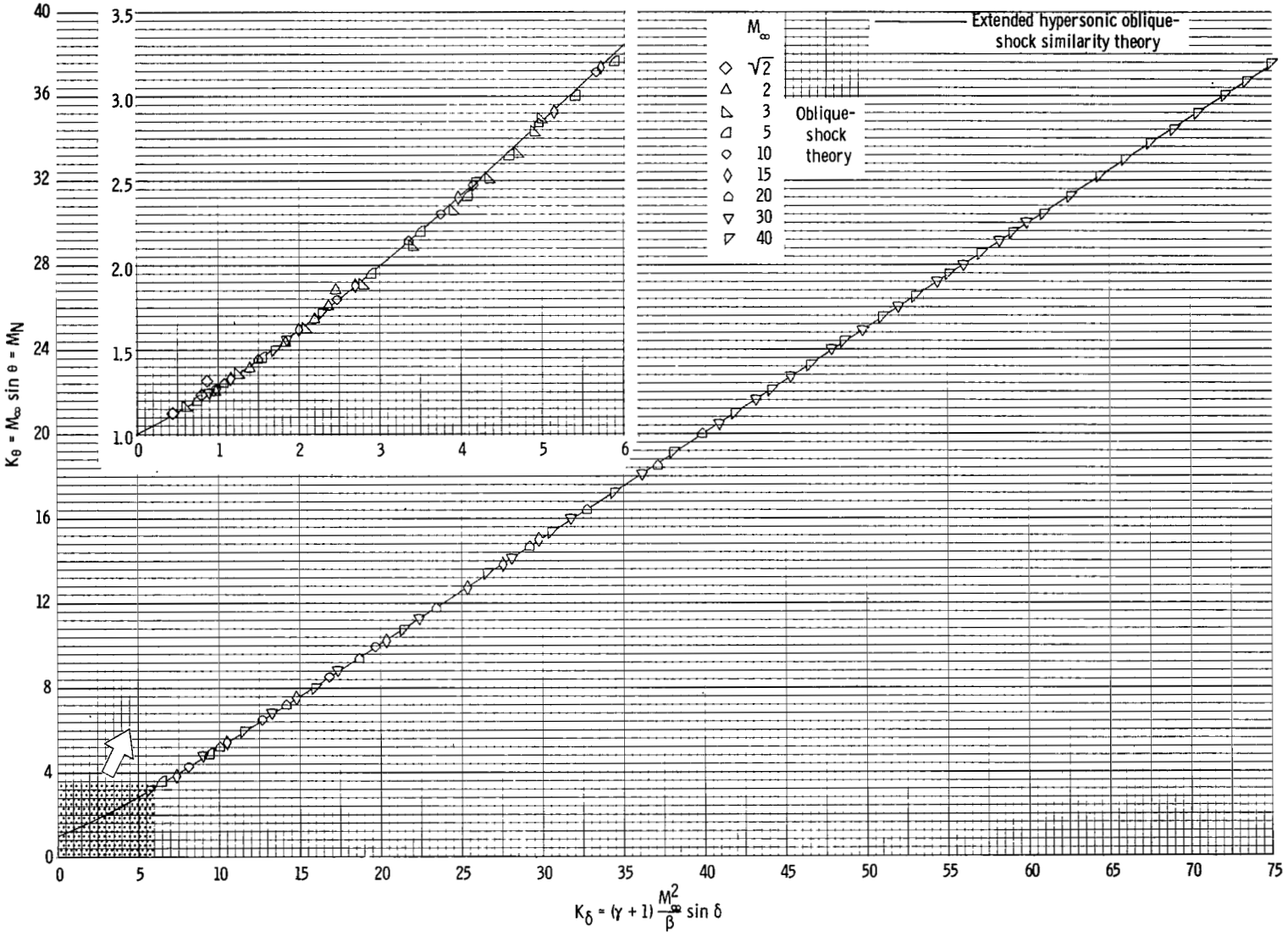

(a) $\gamma = 1$.

Figure 5.- Correlation of two-dimensional oblique shock angle at a fixed value of γ.

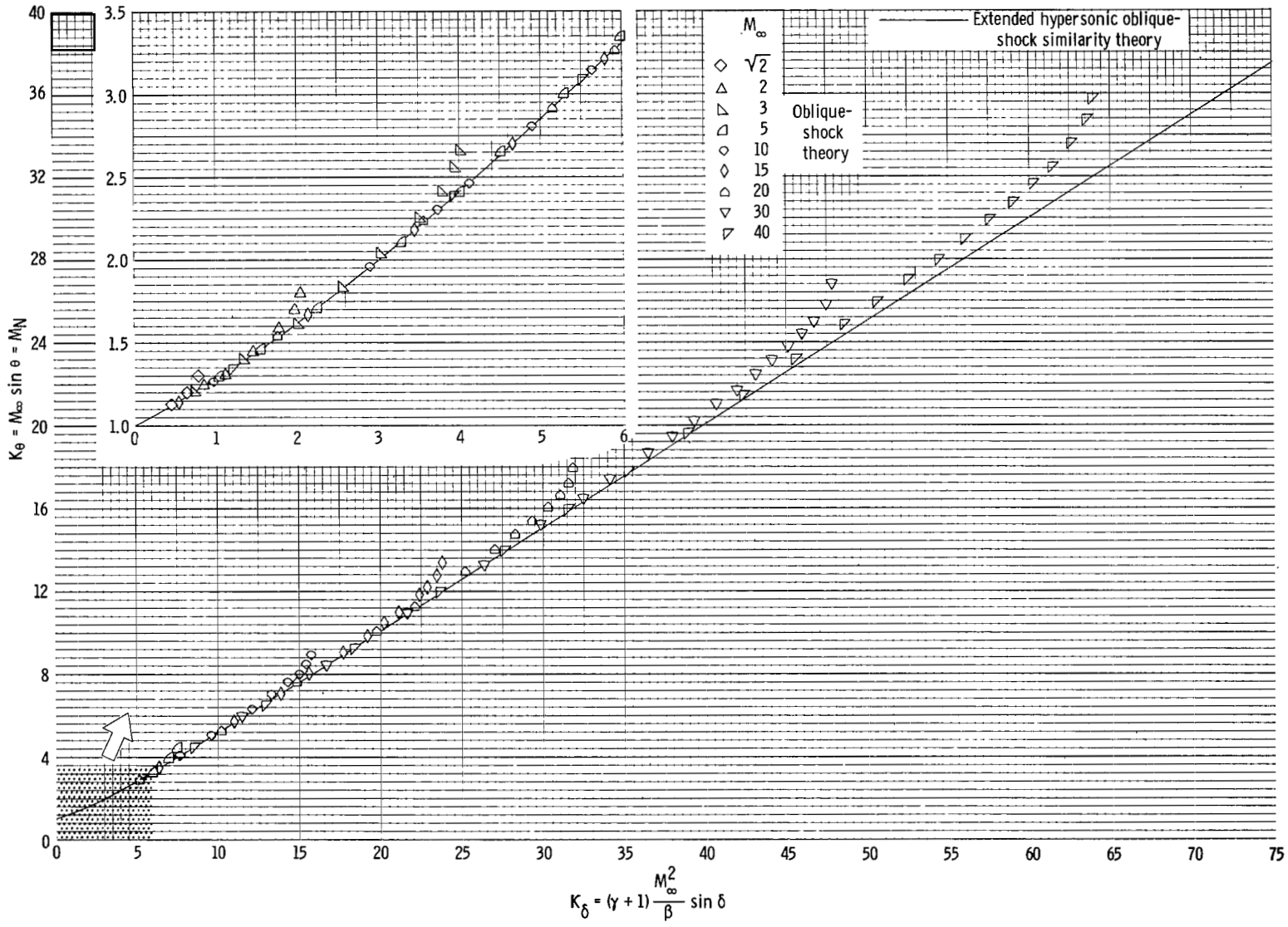

(b) $\gamma = 5/3$.

Figure 5.- Concluded.

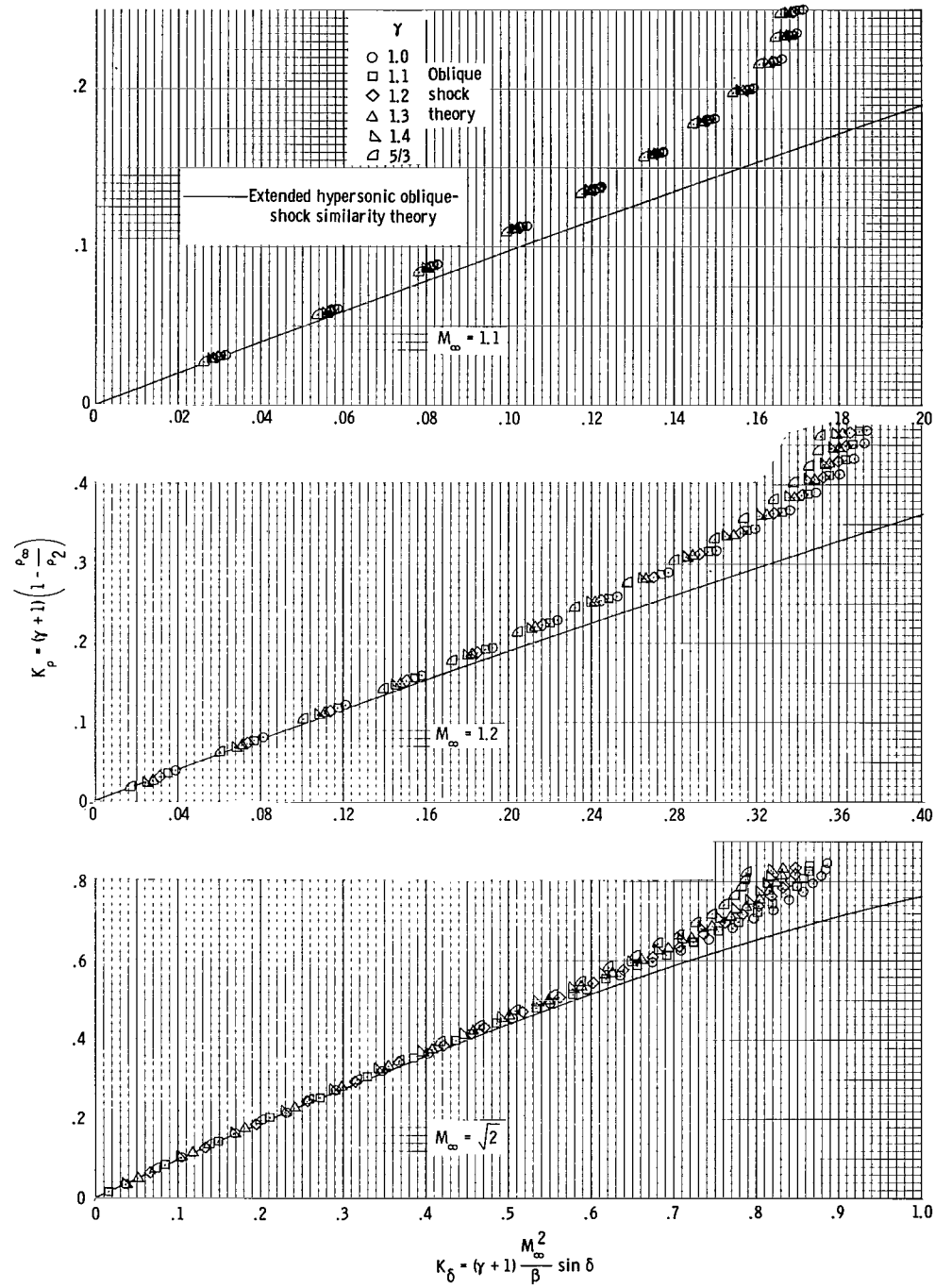

(a) Mach numbers 1.1, 1.2, and $\sqrt{2}$.

Figure 6.- Correlation of density ratio across oblique shock.

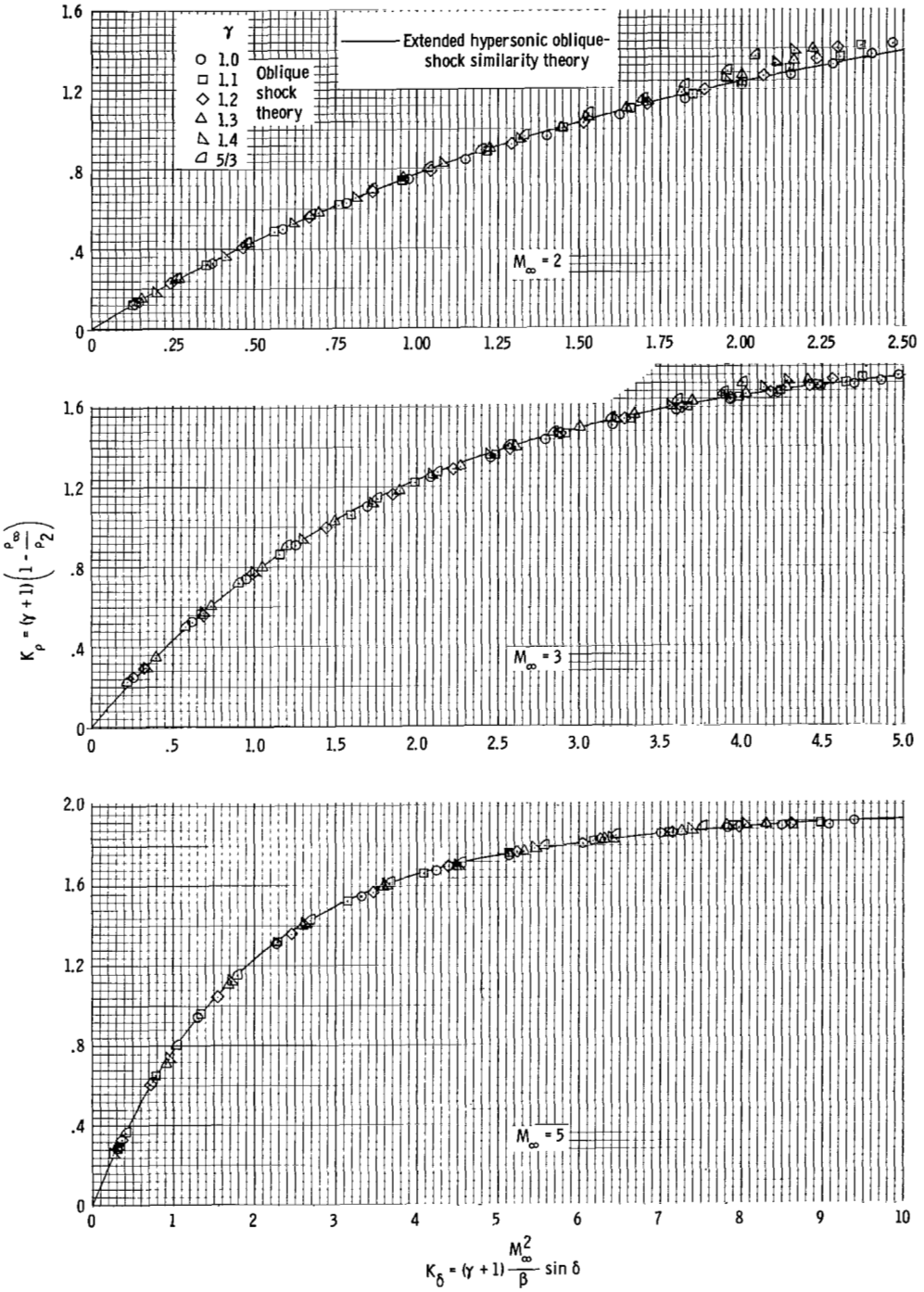

(b) Mach numbers 2, 3, and 5.

Figure 6.- Continued.

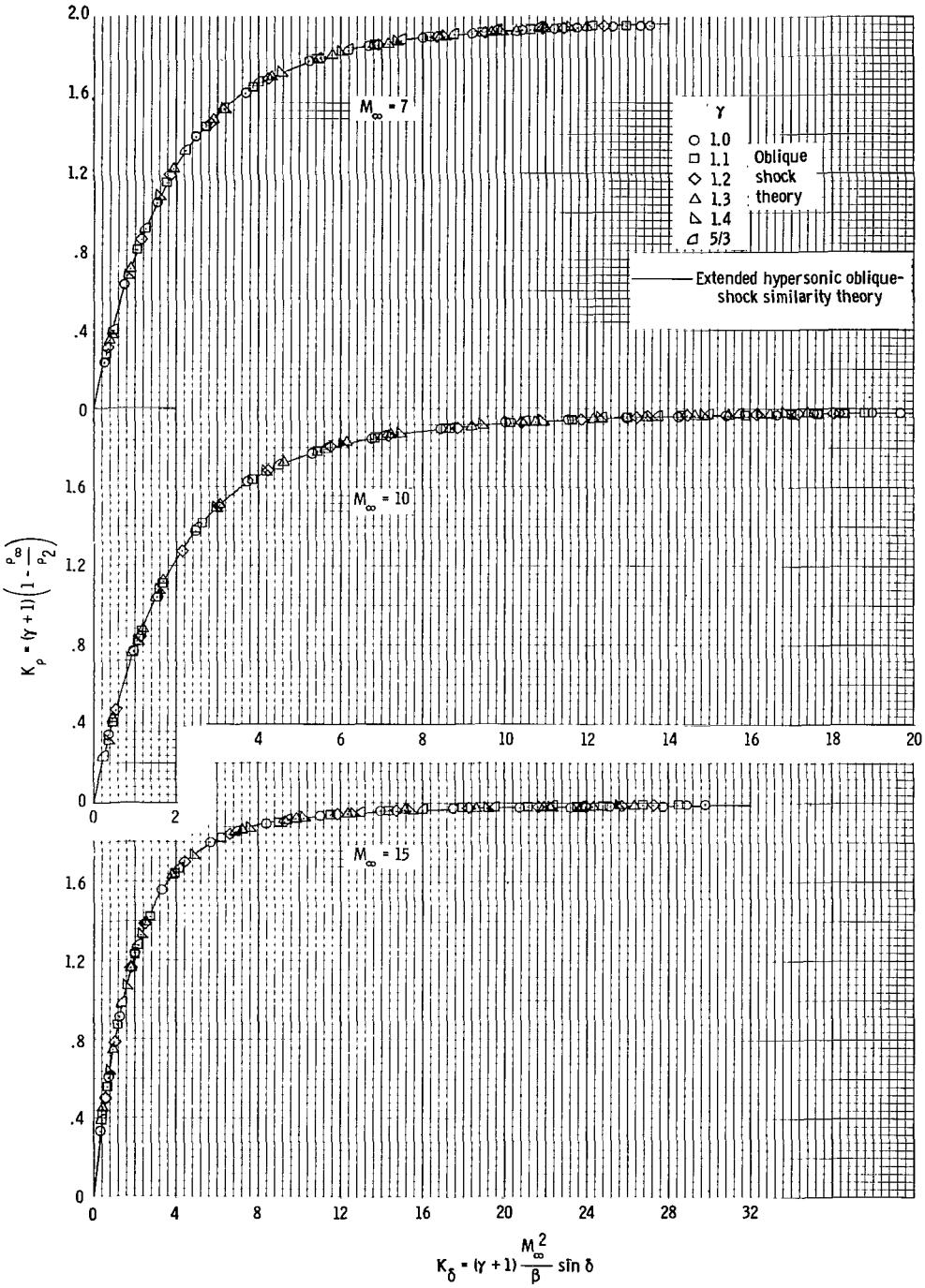

(c) Mach numbers 7, 10, and 15.

Figure 6.- Continued.

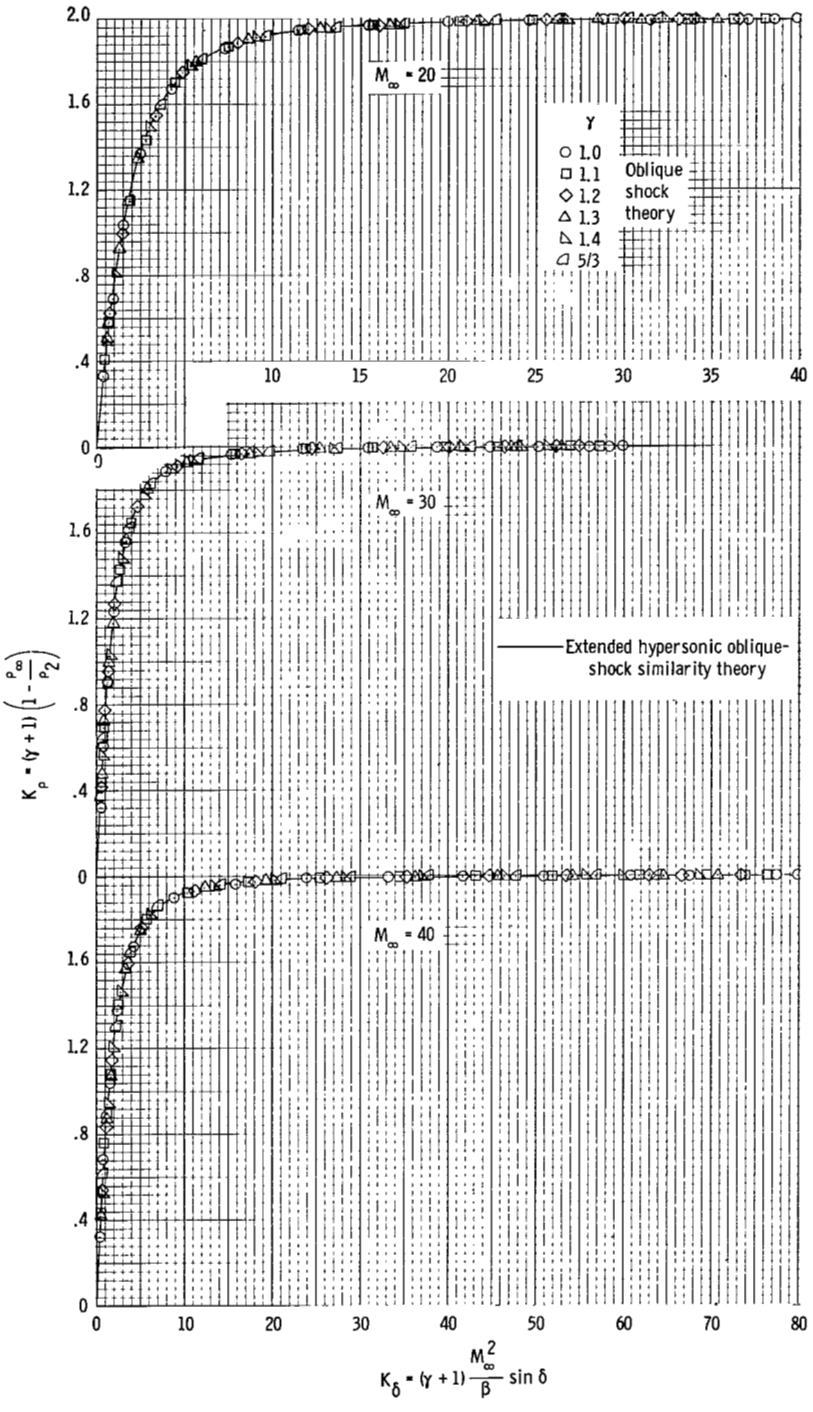

(d) Mach numbers 20, 30, and 40.

Figure 6.- Concluded.

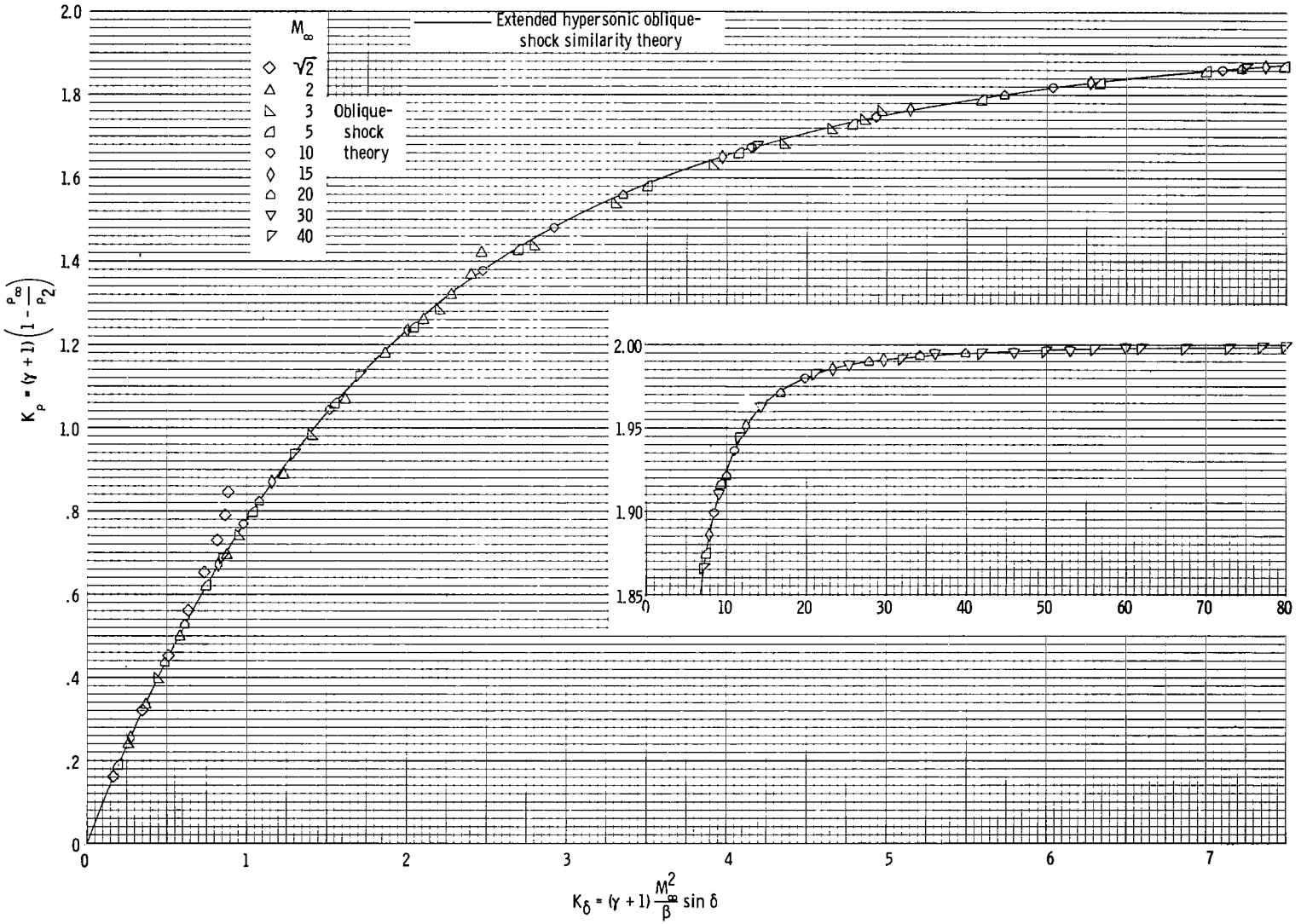

(a) $\gamma = 1$.

Figure 7.- Correlation of density ratio across an oblique shock at a fixed value of γ.

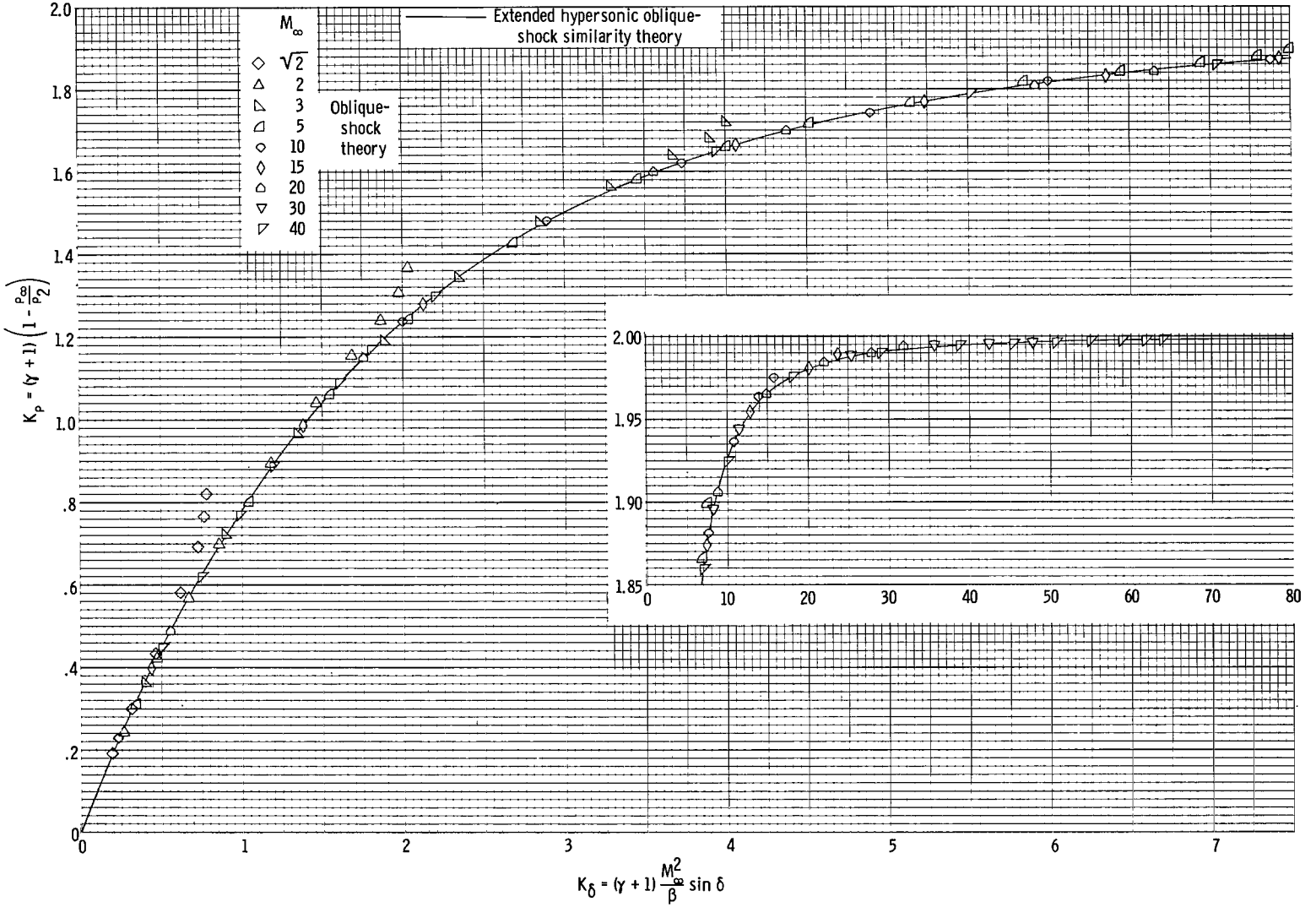

(b) $\gamma = 5/3$.

Figure 7.- Concluded.

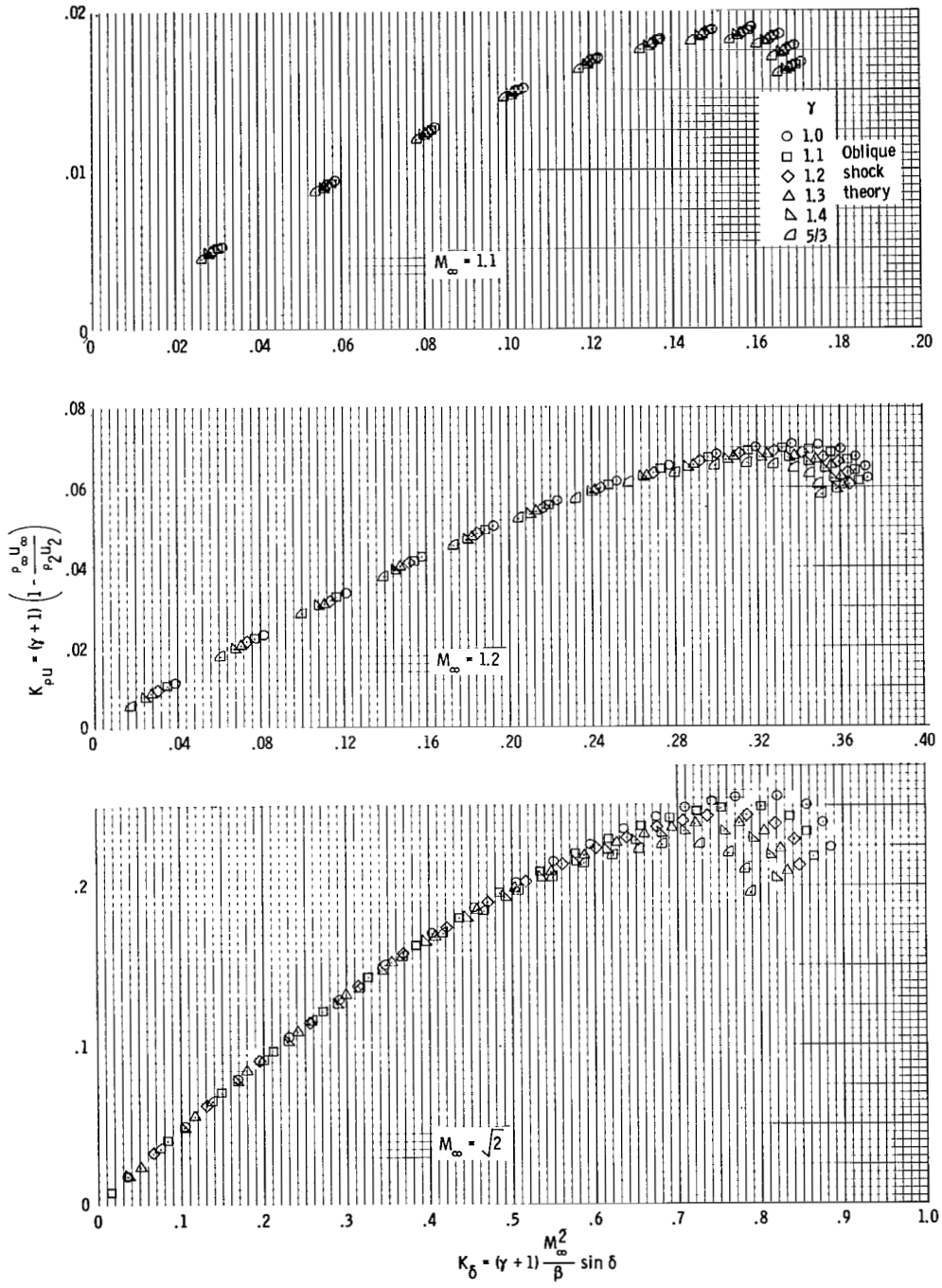

(a) Mach numbers 1.1, 1.2, and $\sqrt{2}$.

Figure 8.- Correlation of mass flow ratio across an oblique shock.

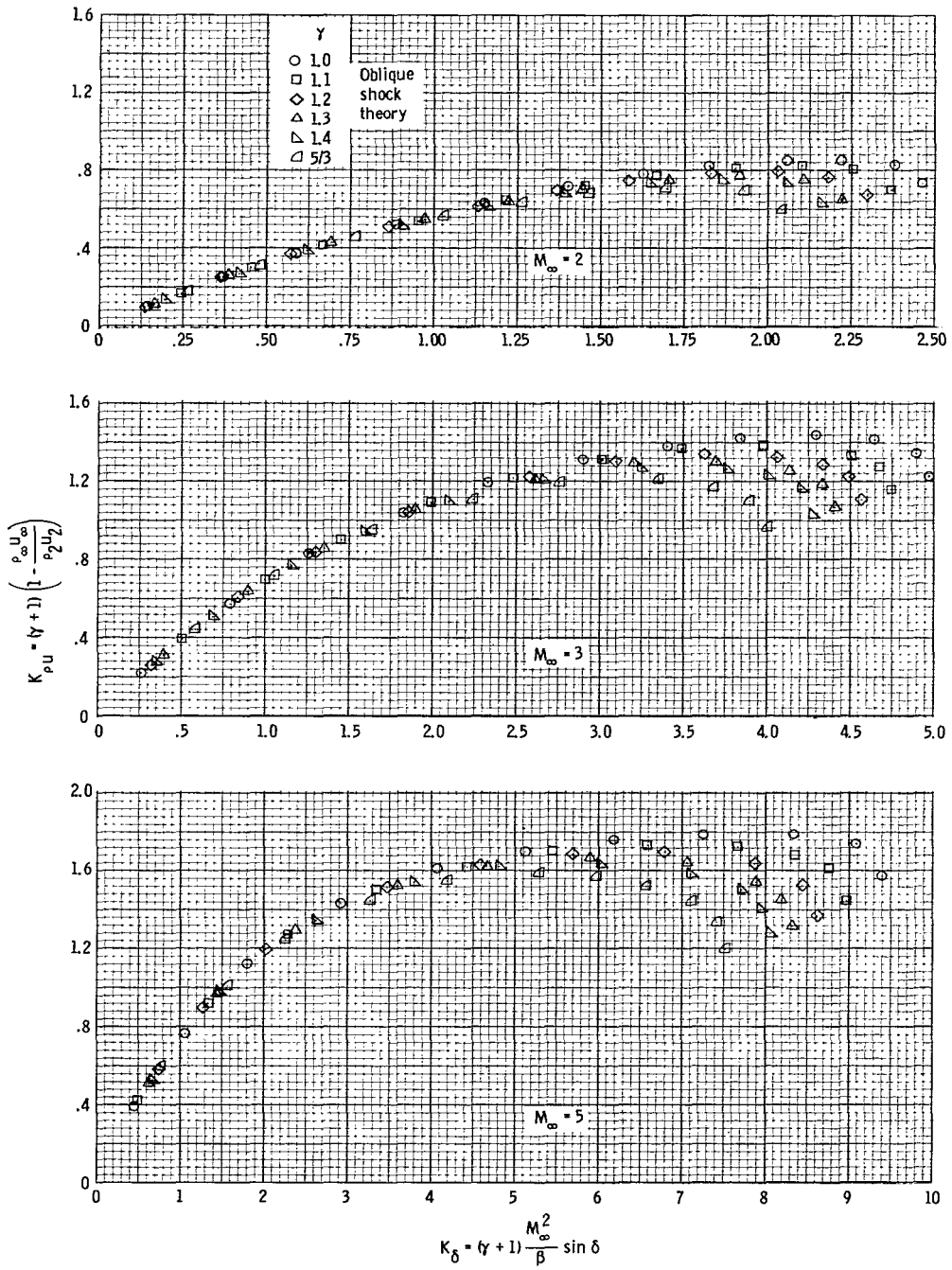

(b) Mach numbers 2, 3, and 5.

Figure 8.- Continued.

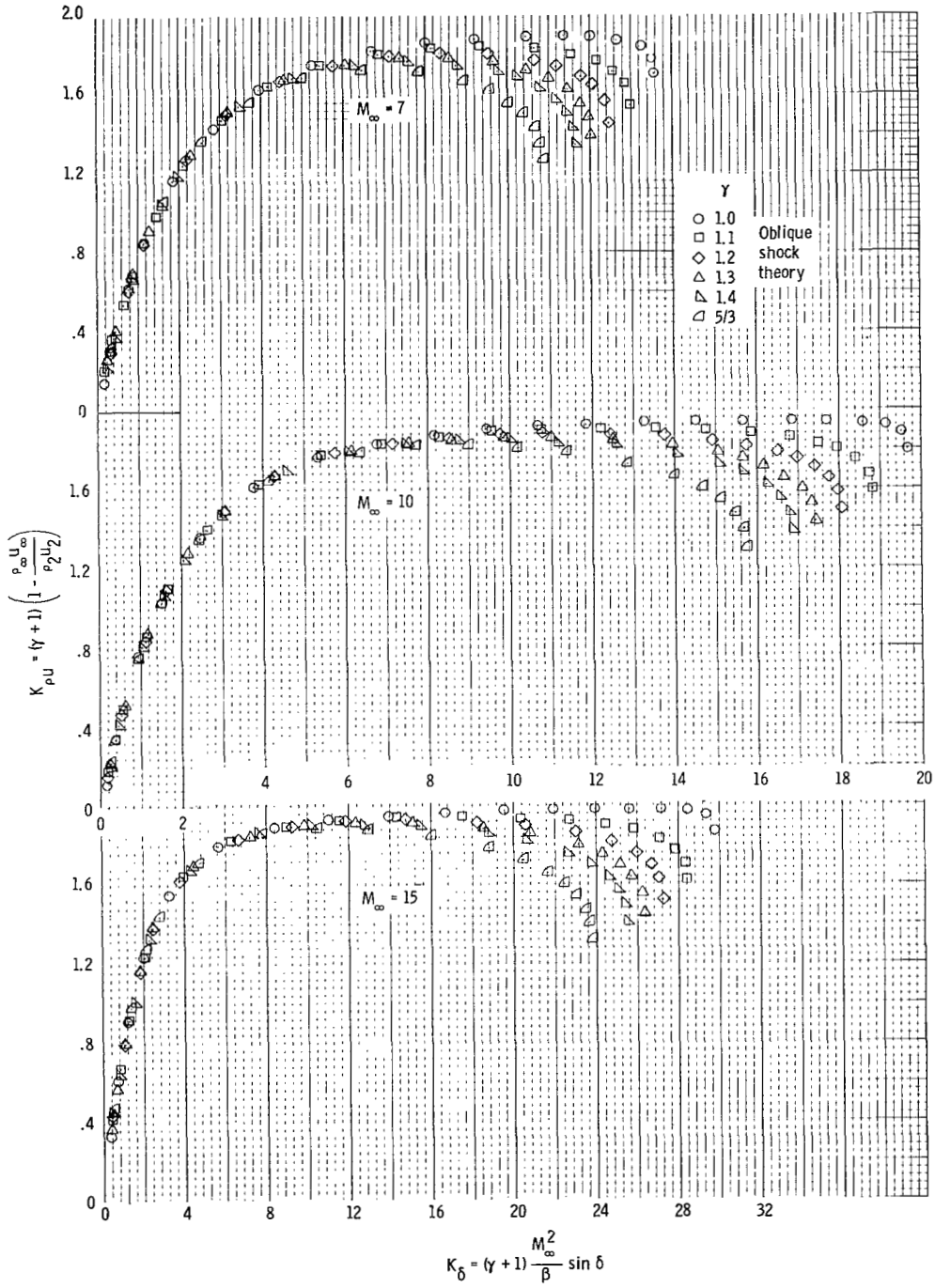

(c) Mach numbers 7, 10, and 15.

Figure 8.- Continued.

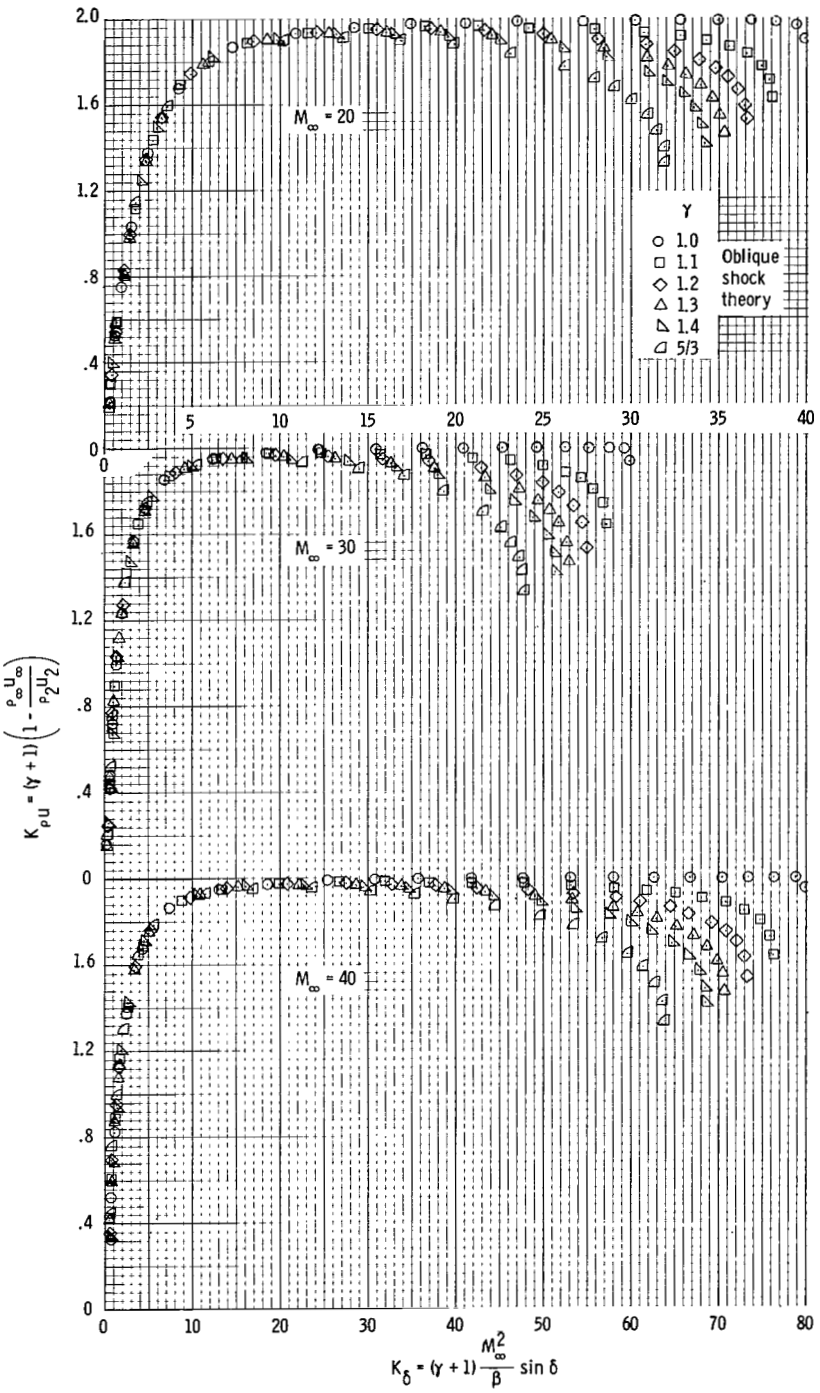

(d) Mach numbers 20, 30, and 40.

Figure 8.- Concluded.

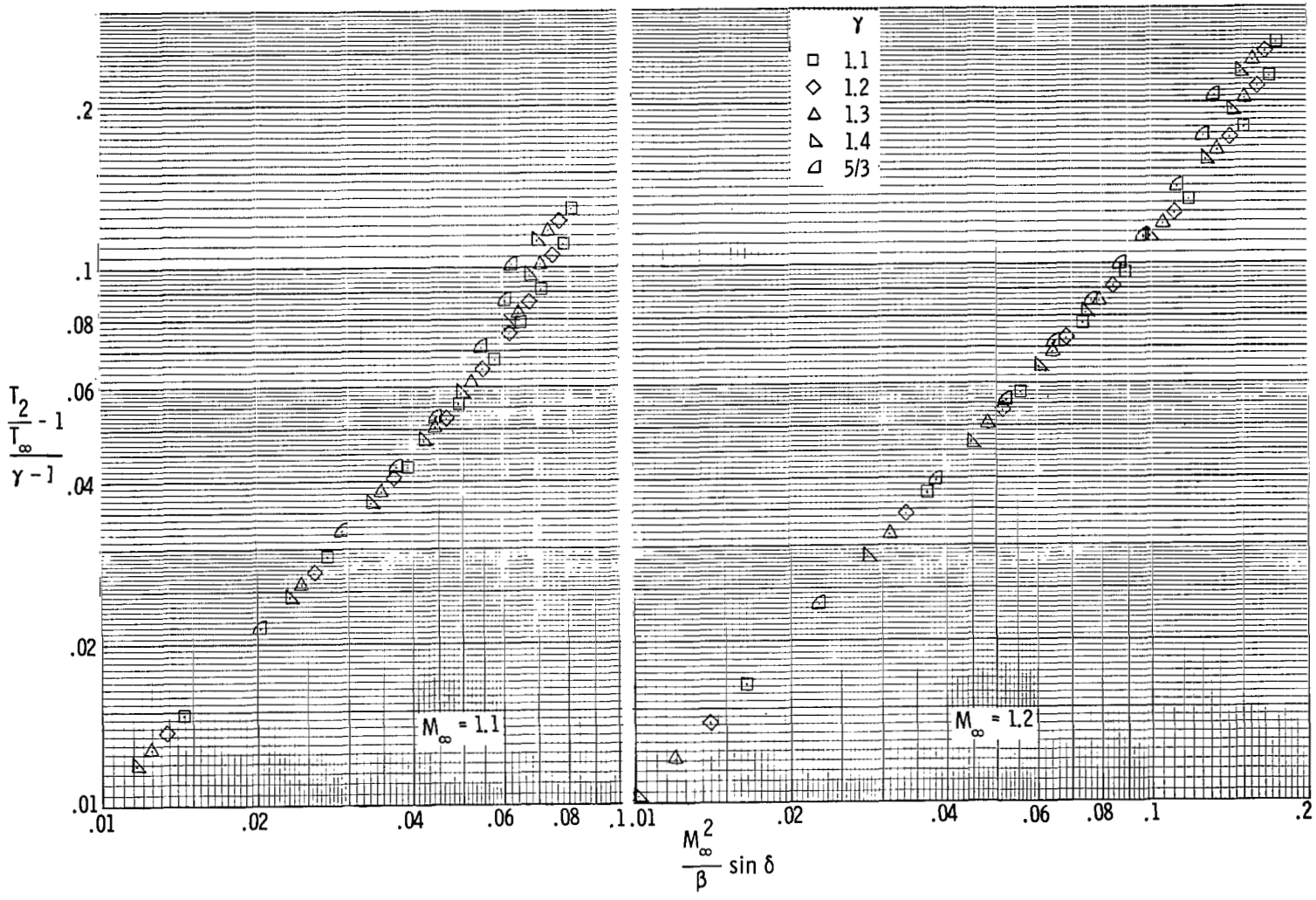

(a) Mach numbers 1.1 and 1.2.

Figure 9.- Correlation of effect of γ on temperature ratio across an oblique shock.

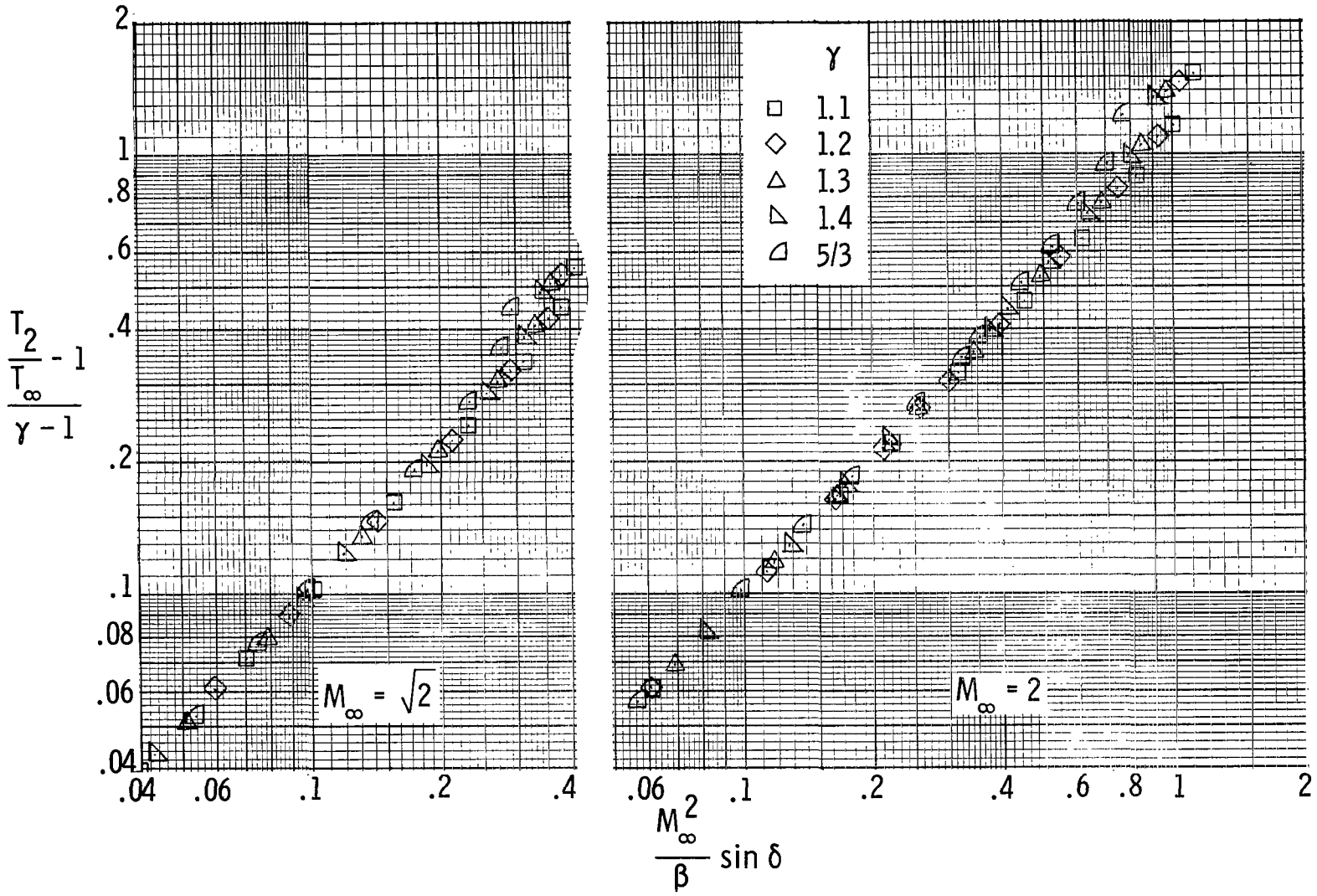

(b) Mach numbers $\sqrt{2}$ and 2.

Figure 9.- Continued.

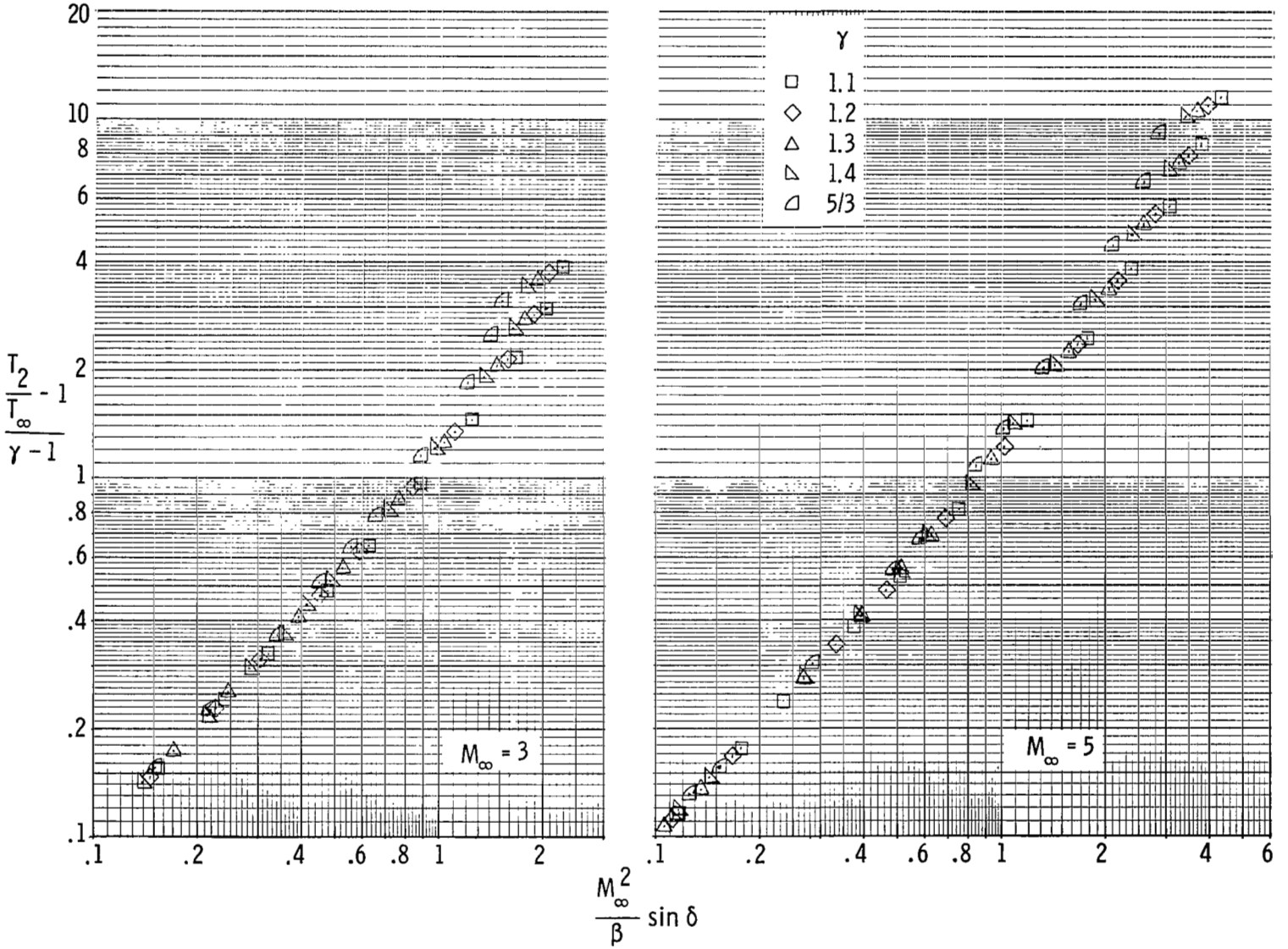

(c) Mach numbers 3 and 5.

Figure 9.- Continued.

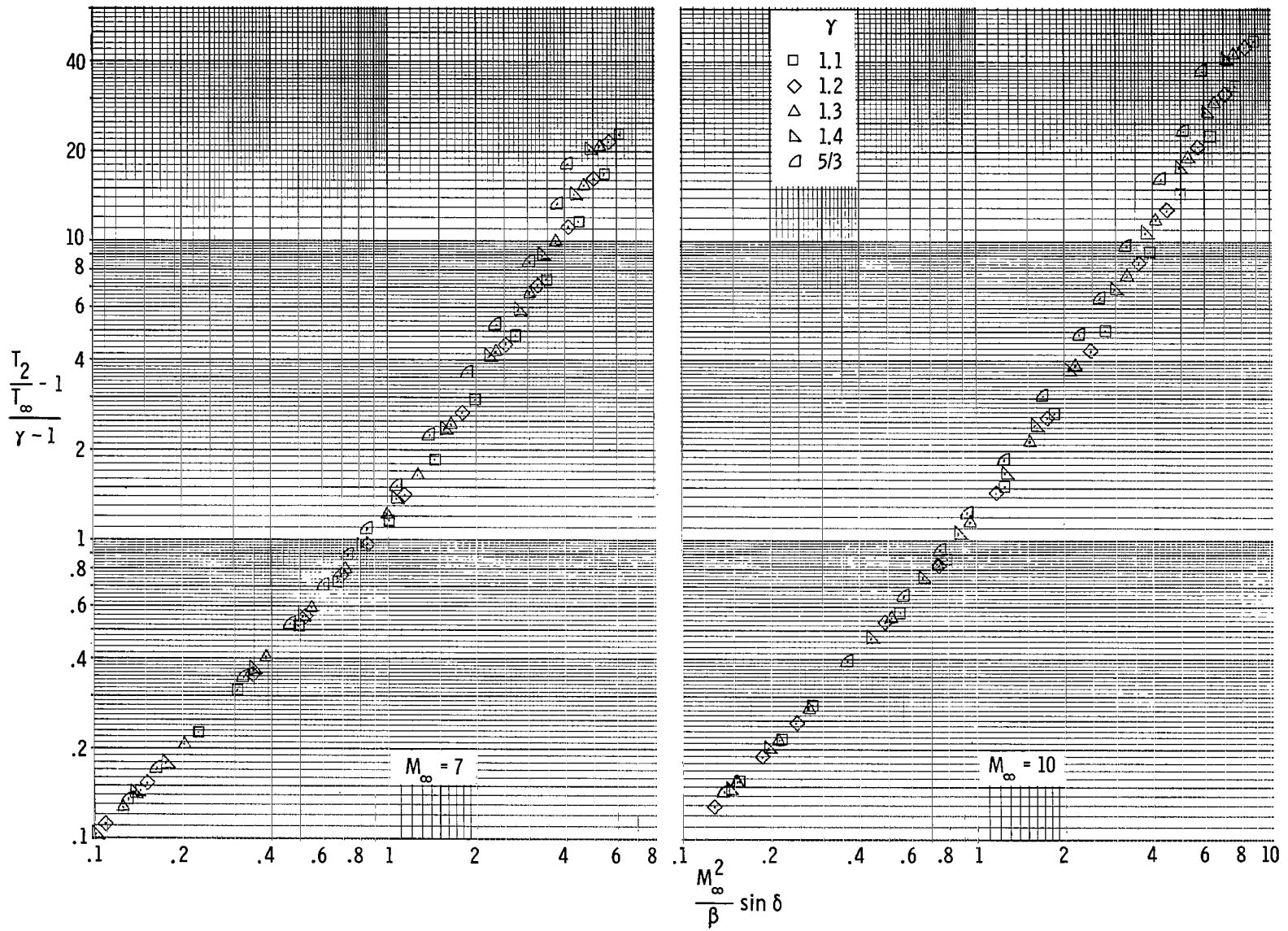

(d) Mach numbers 7 and 10.

Figure 9.- Continued.

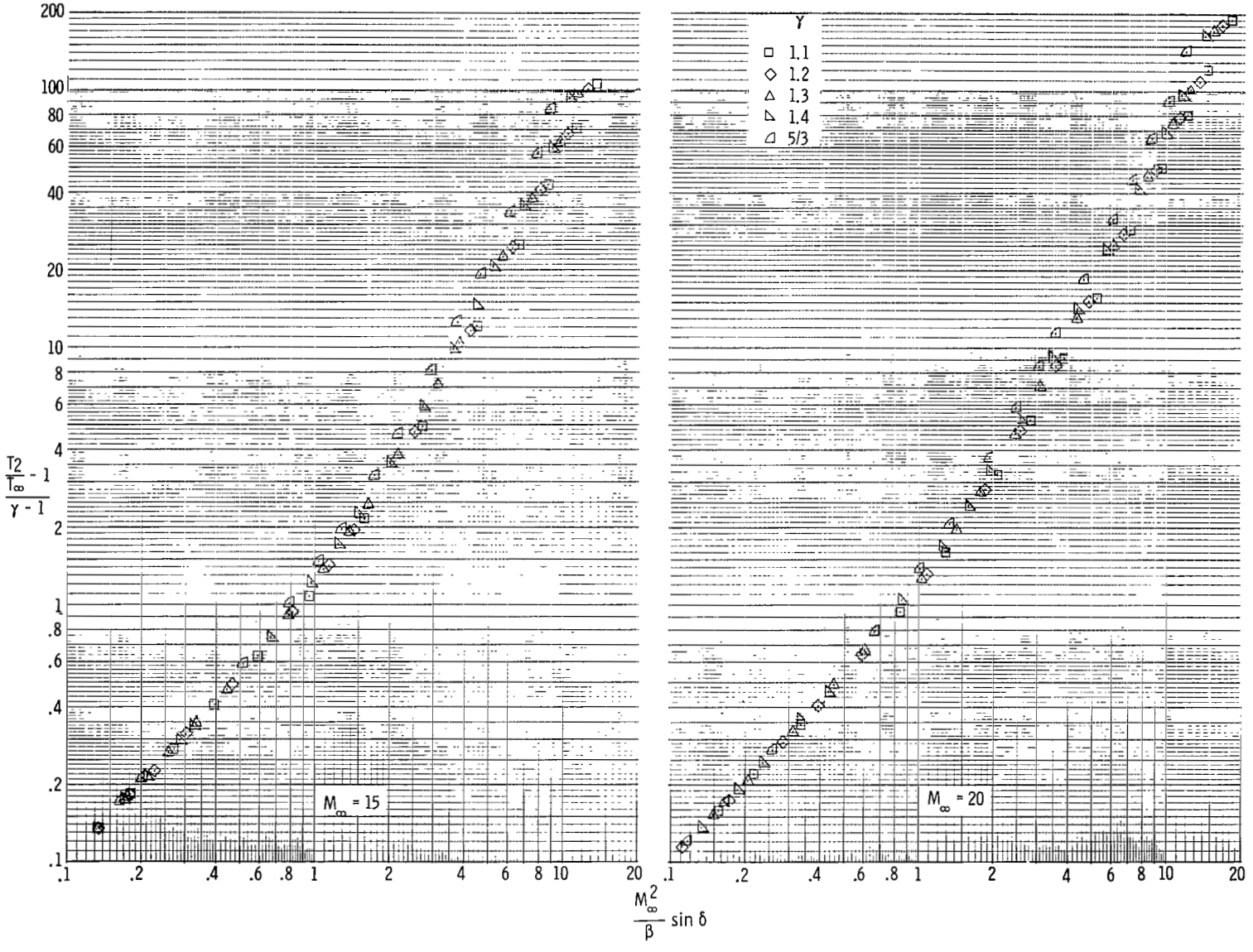

(e) Mach numbers 15 and 20.

Figure 9.- Continued.

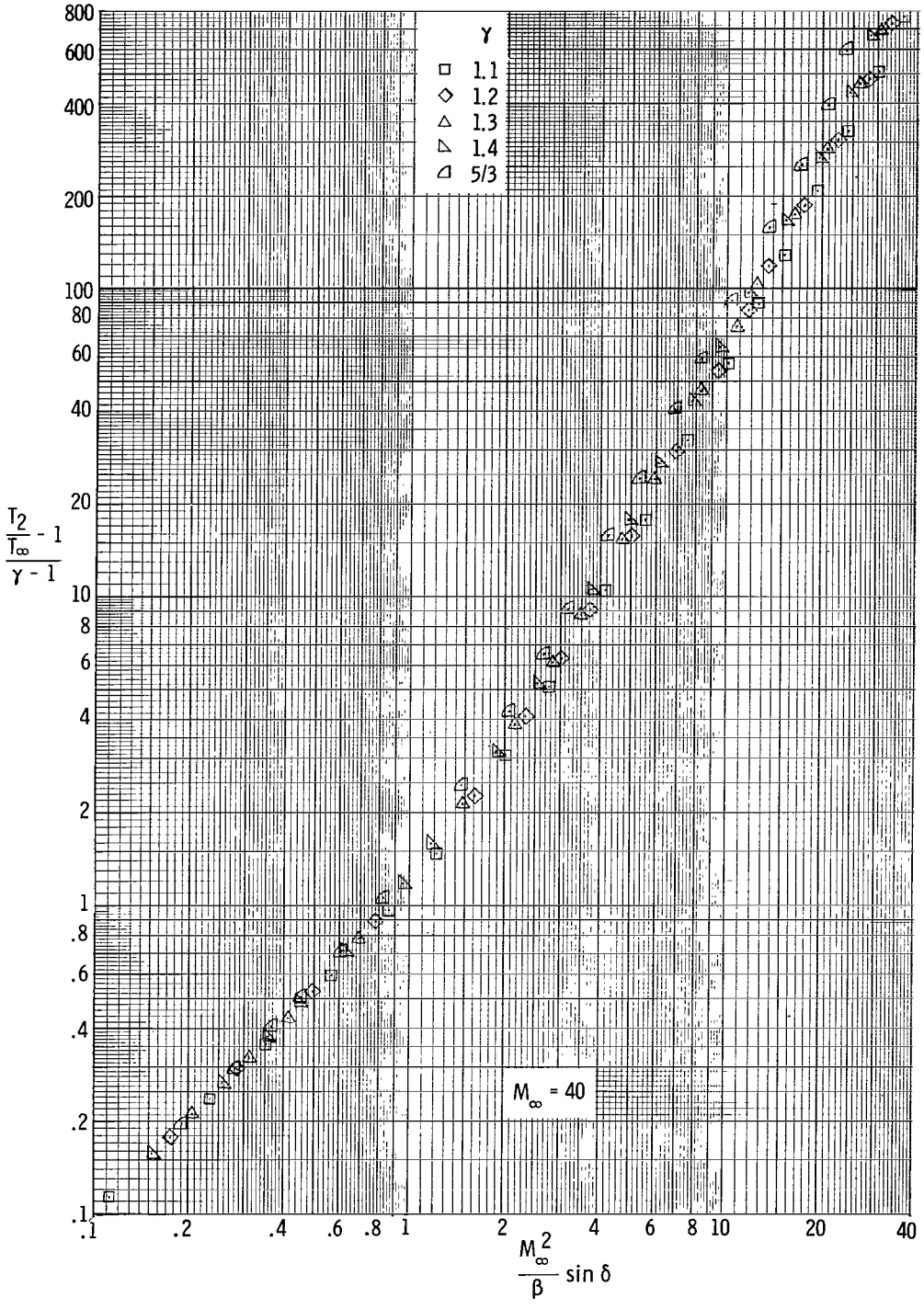

(f) Mach number 40.

Figure 9.- Concluded.

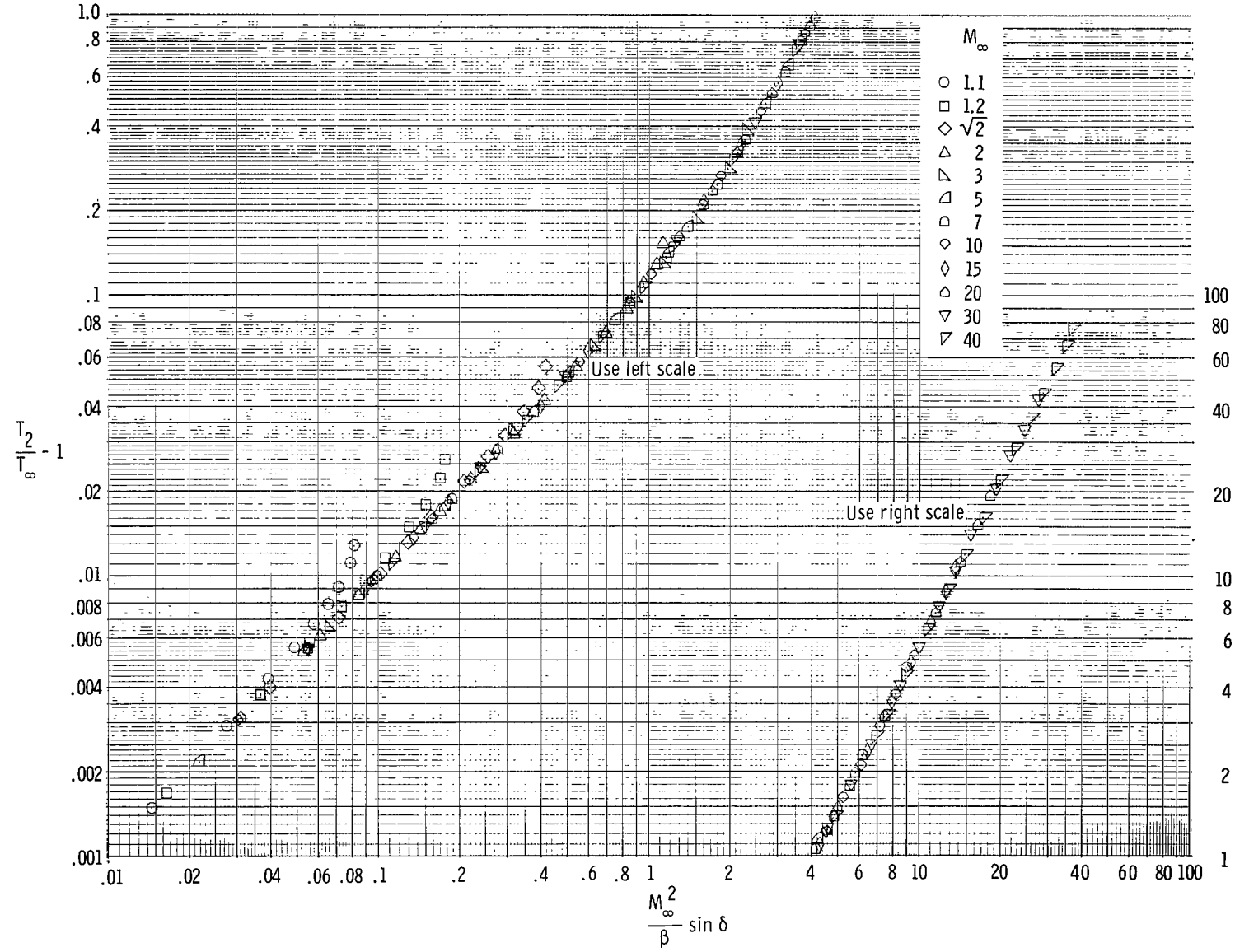

(a) $\gamma = 1.1$.

Figure 10.- Correlation of effect of Mach number on temperature ratio across an oblique shock.

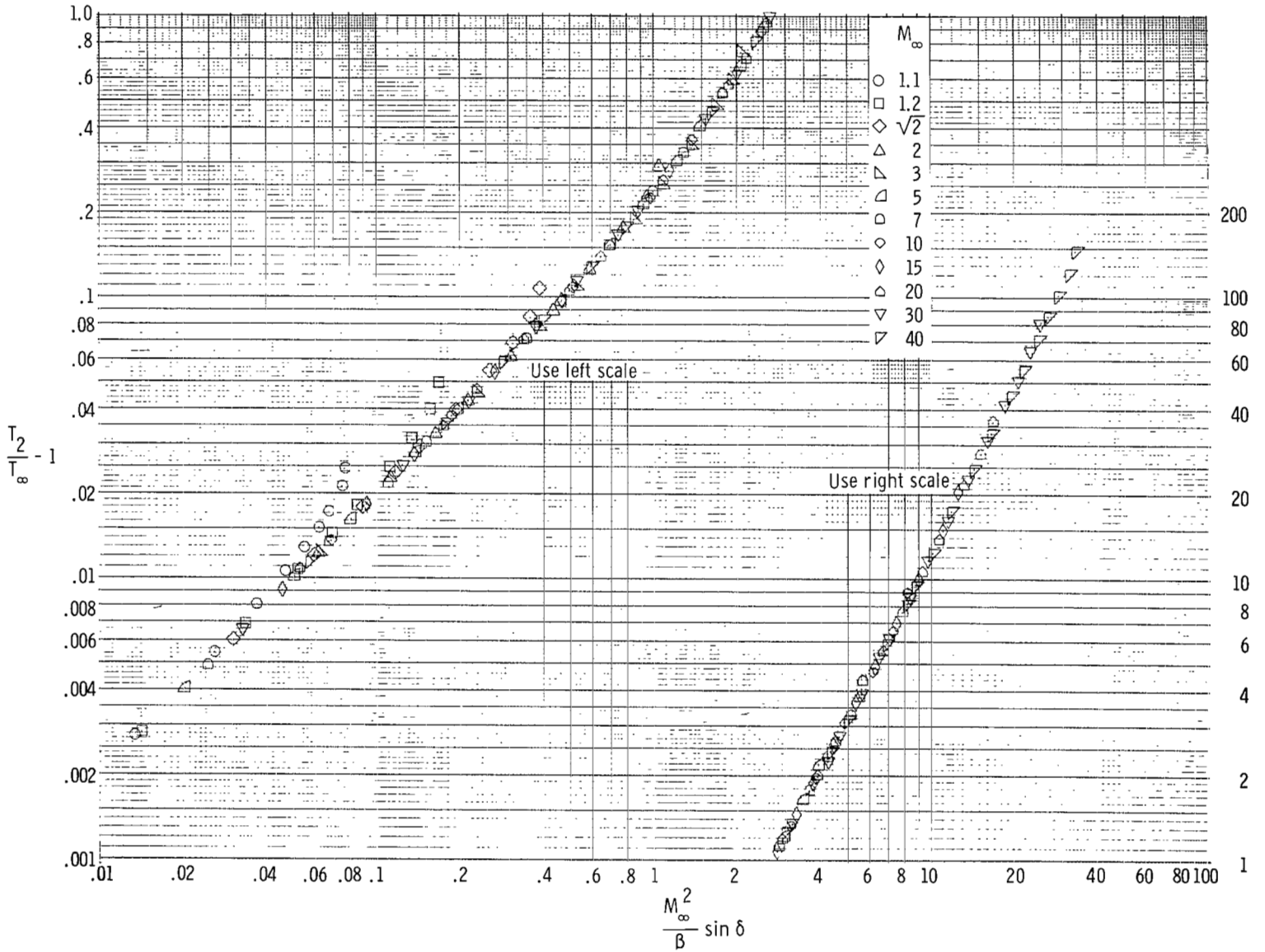

(b) $\gamma = 1.2$.

Figure 10.- Continued.

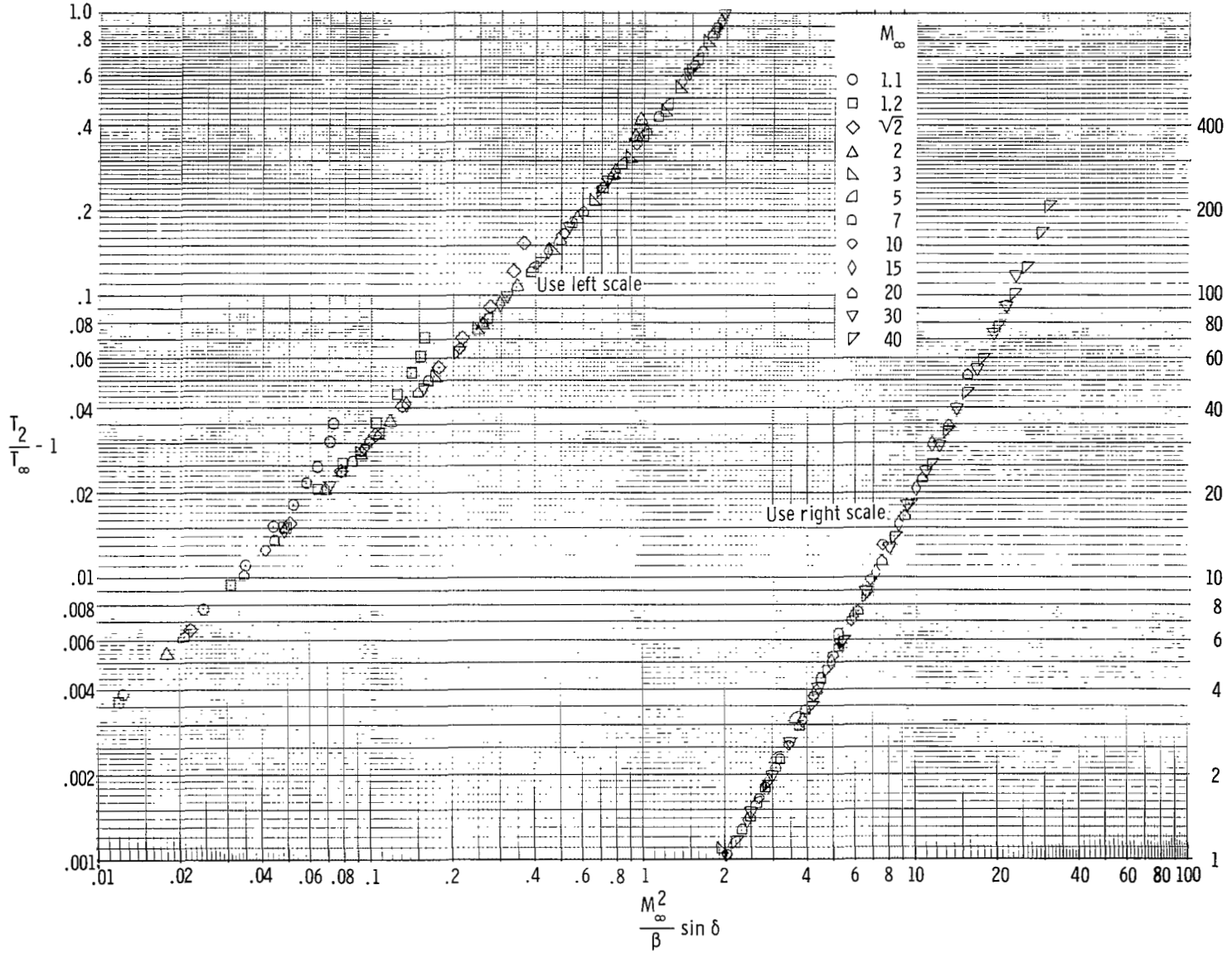

(c) $\gamma = 1.3$.

Figure 10.- Continued.

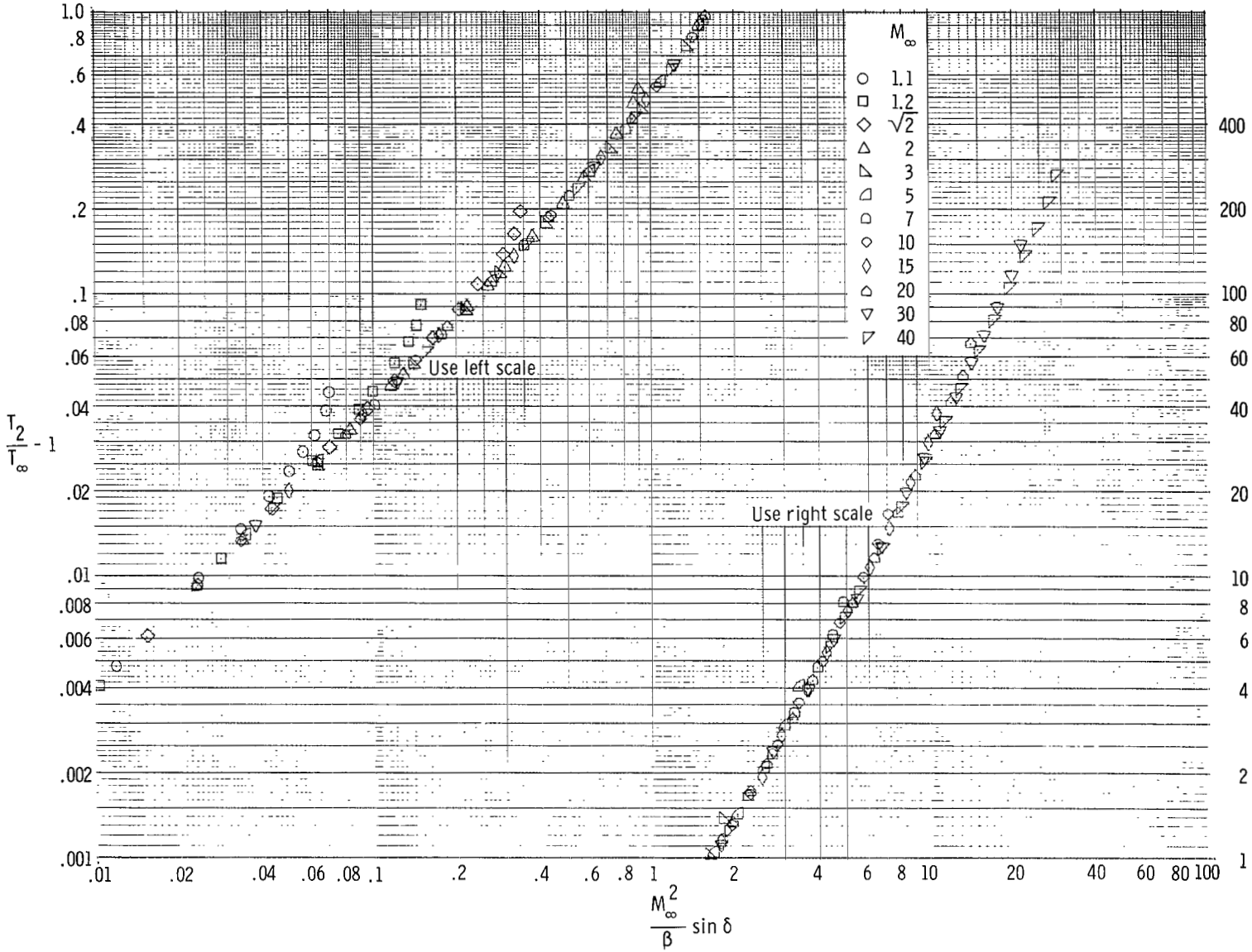

(d) $\gamma = 1.4$.

Figure 10.- Continued.

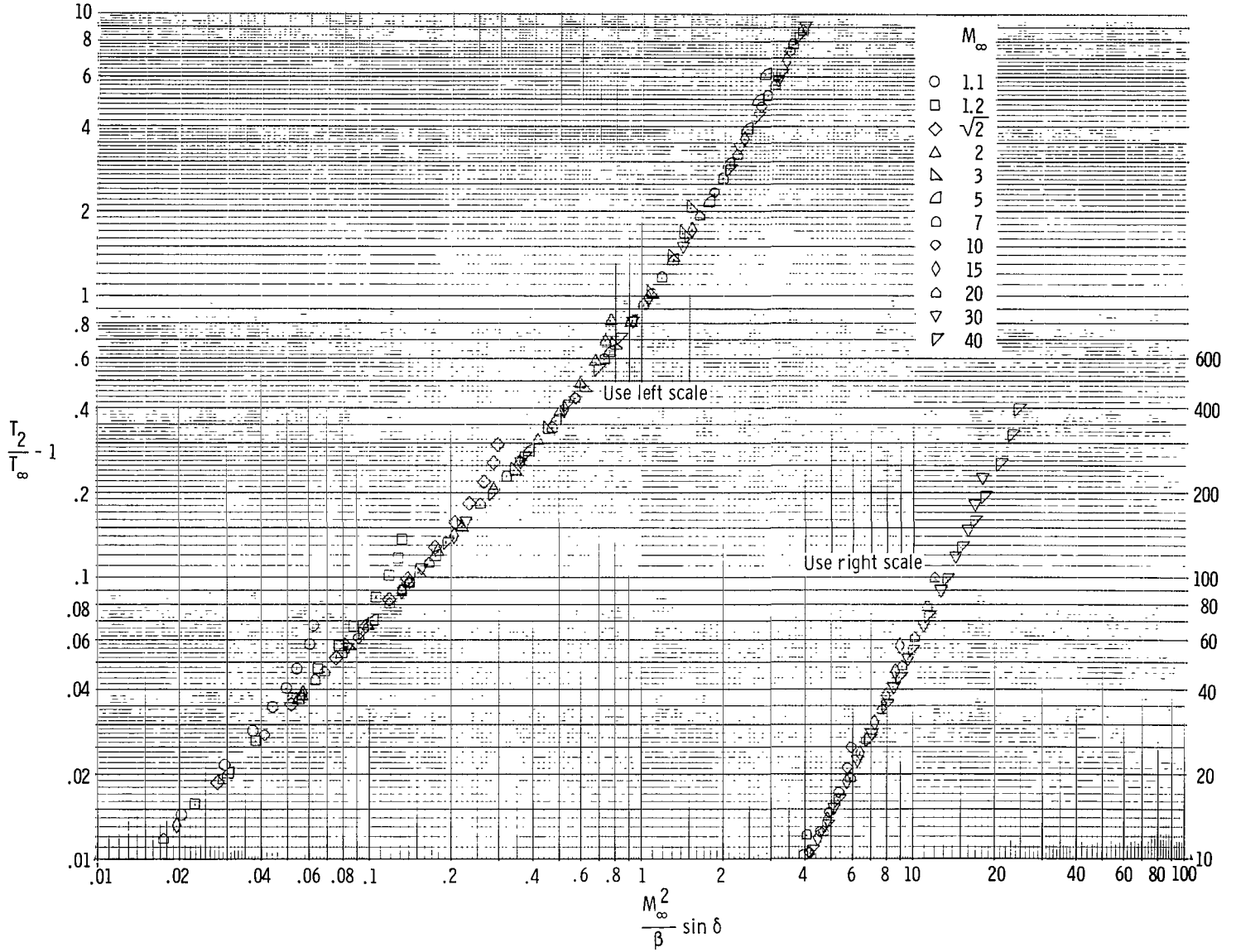

(e) $\gamma = 5/3$.

Figure 10.- Concluded.

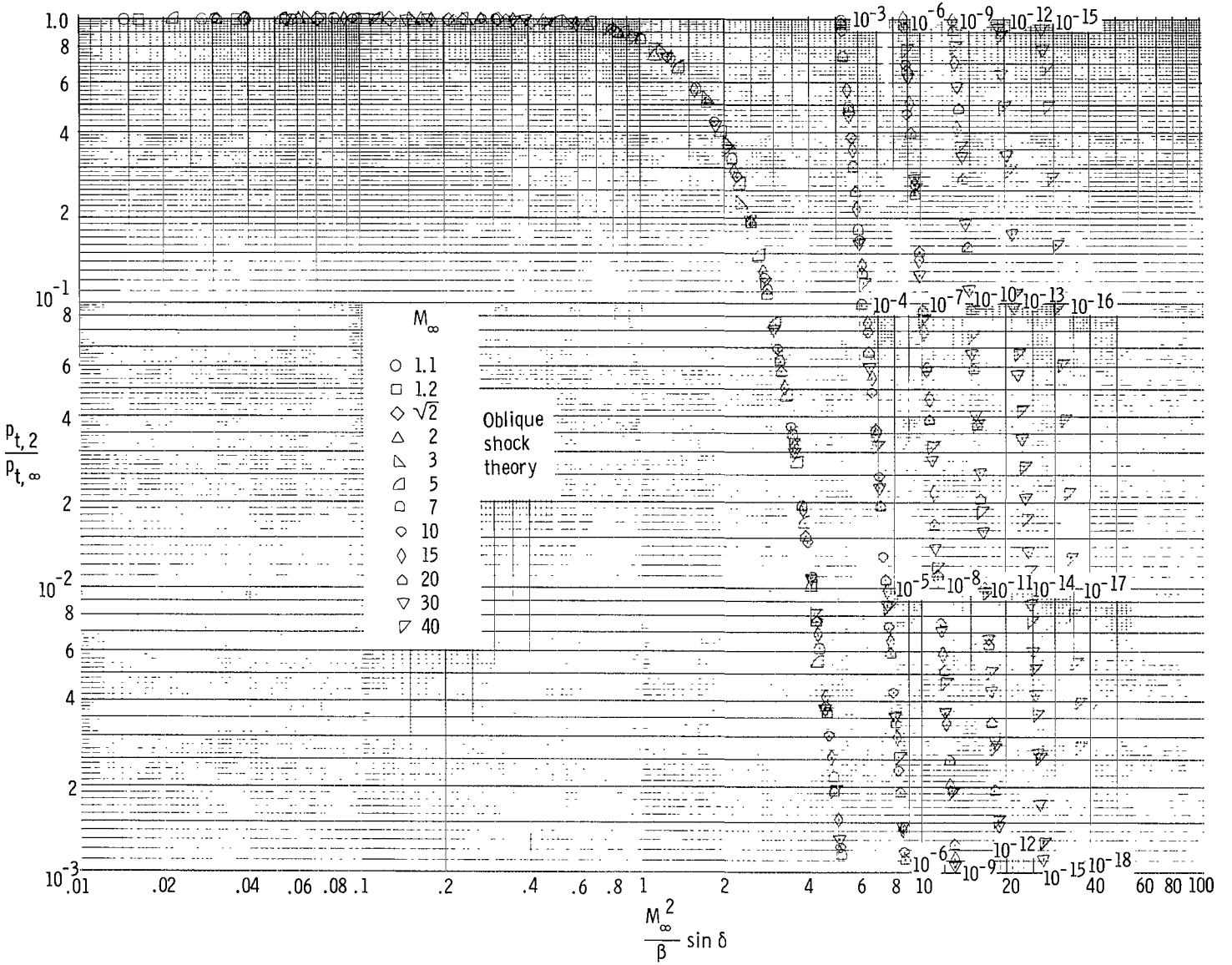

(a) $\gamma = 1.1$.

Figure 11.- Correlation of effect of Mach number on total-pressure ratio across an oblique shock.

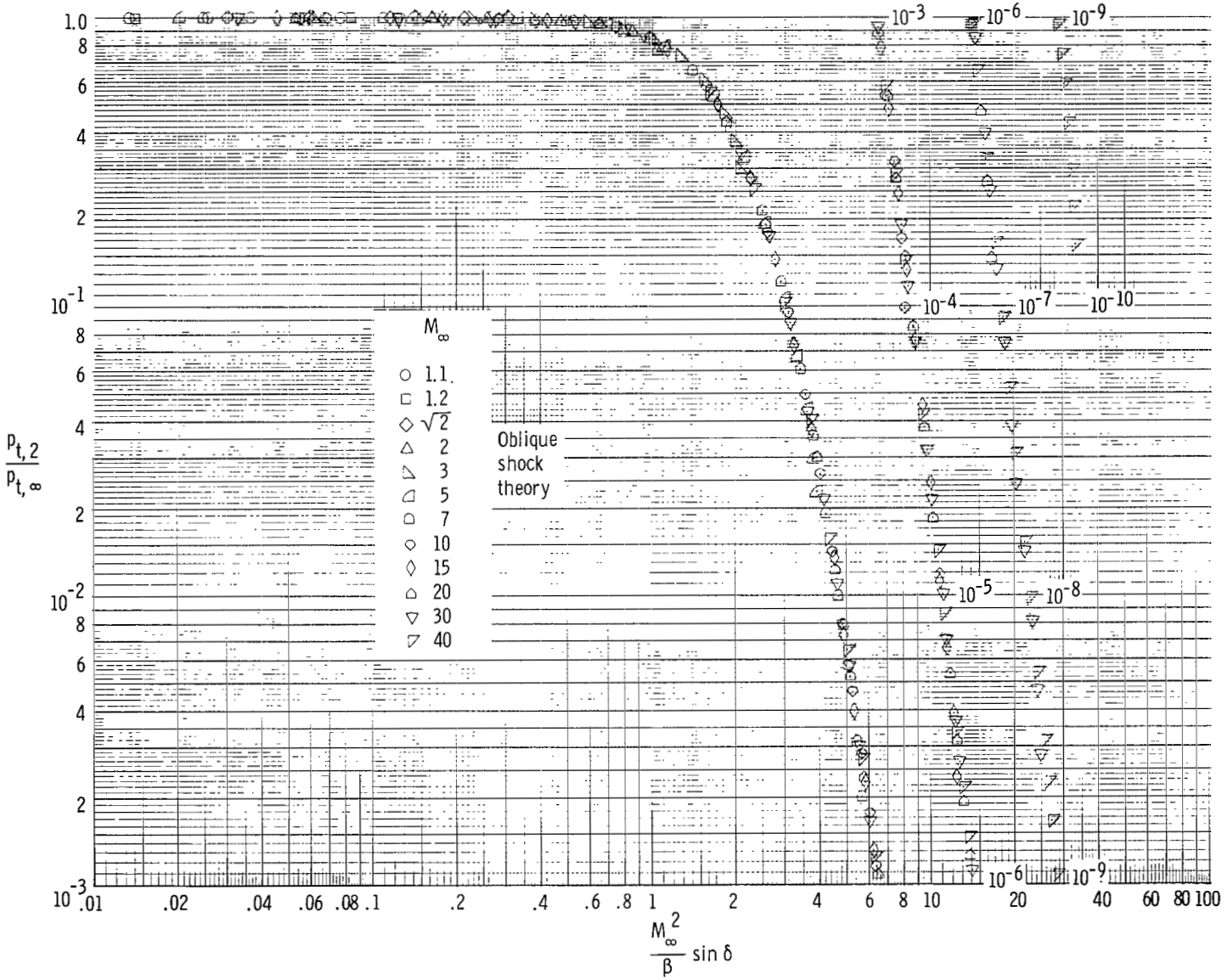

(b) $\gamma = 1.2$.

Figure 11.- Continued.

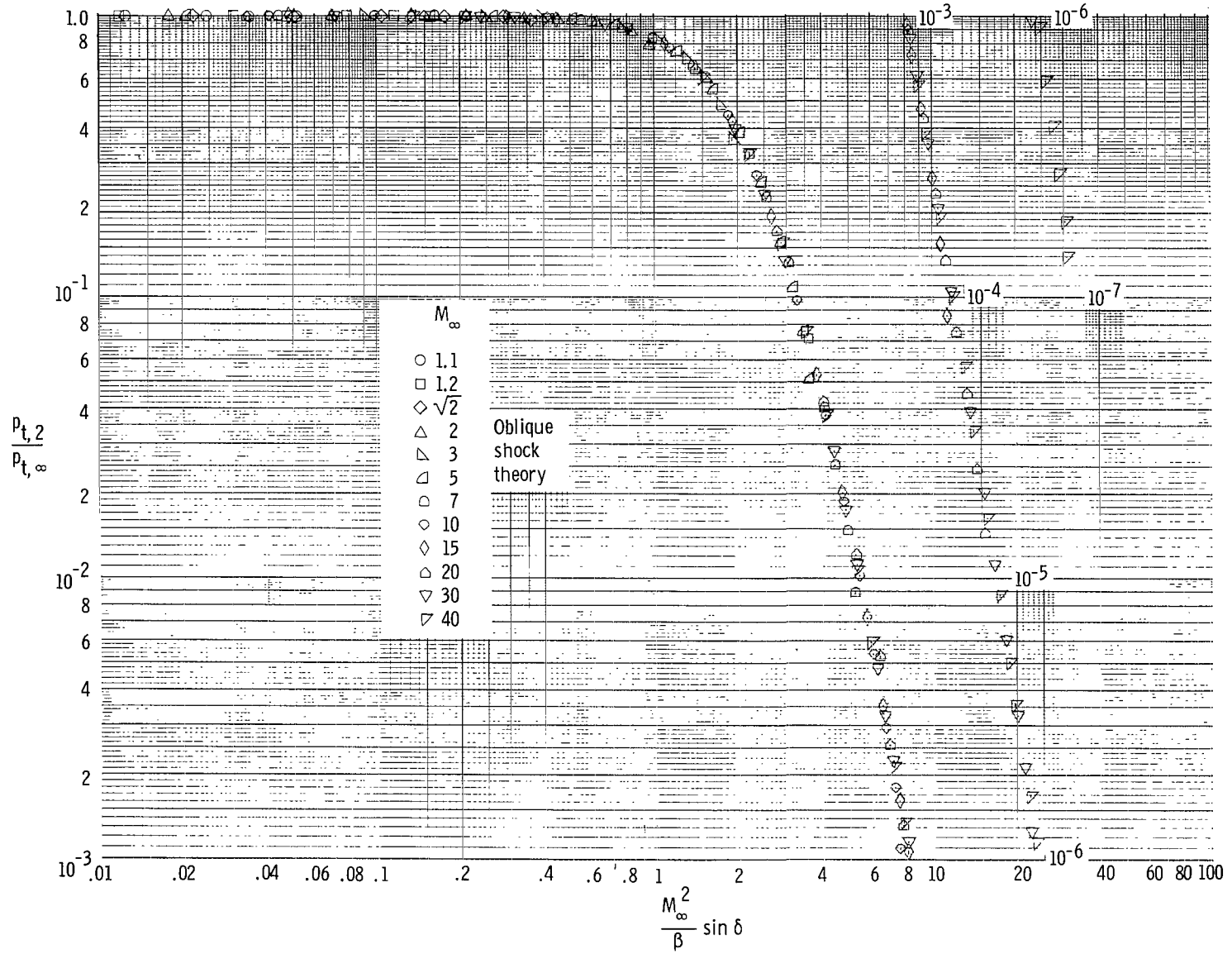

(c) $\gamma = 1.3$.

Figure 11.- Continued.

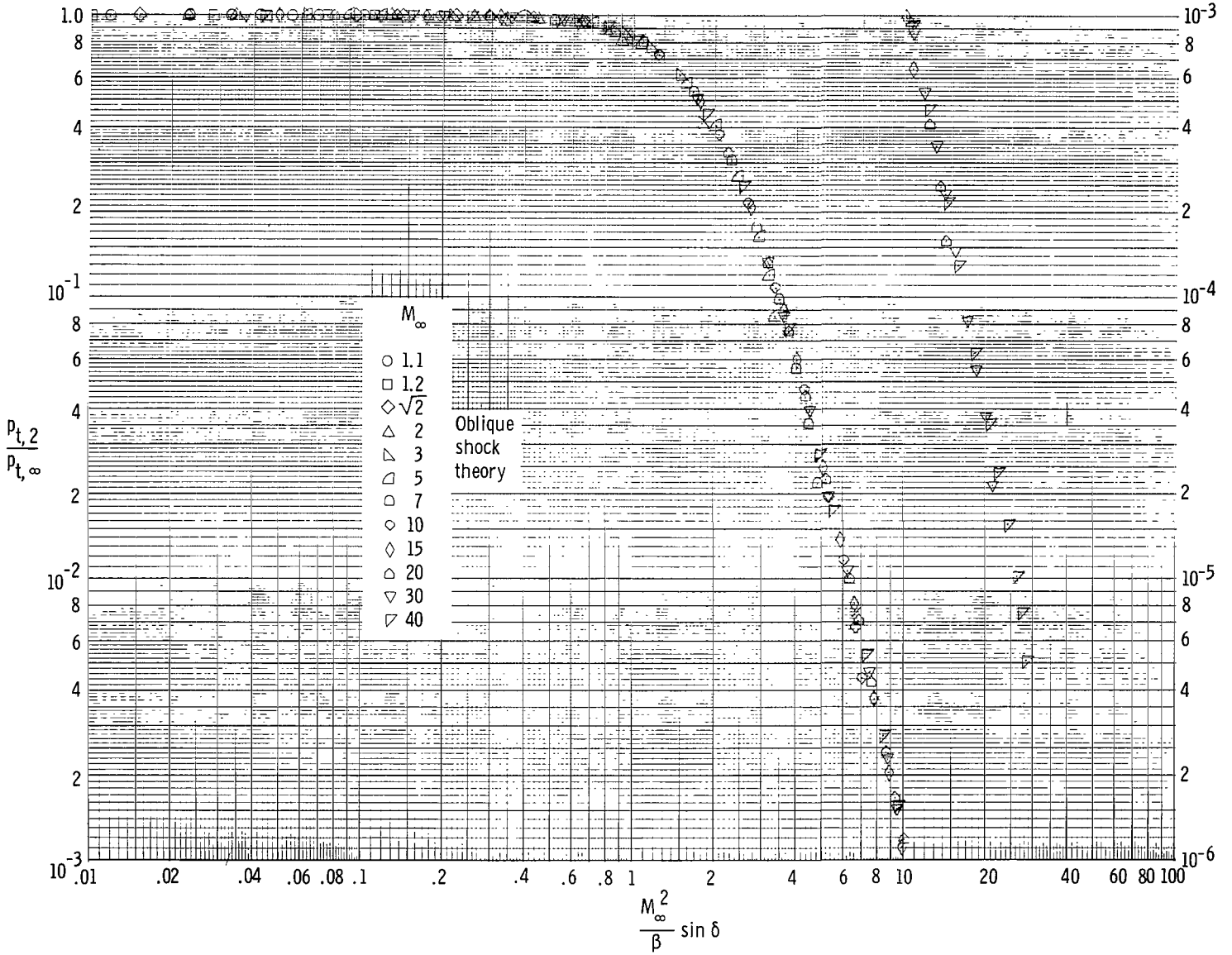

(d) $\gamma = 1.4$.

Figure 11.- Continued.

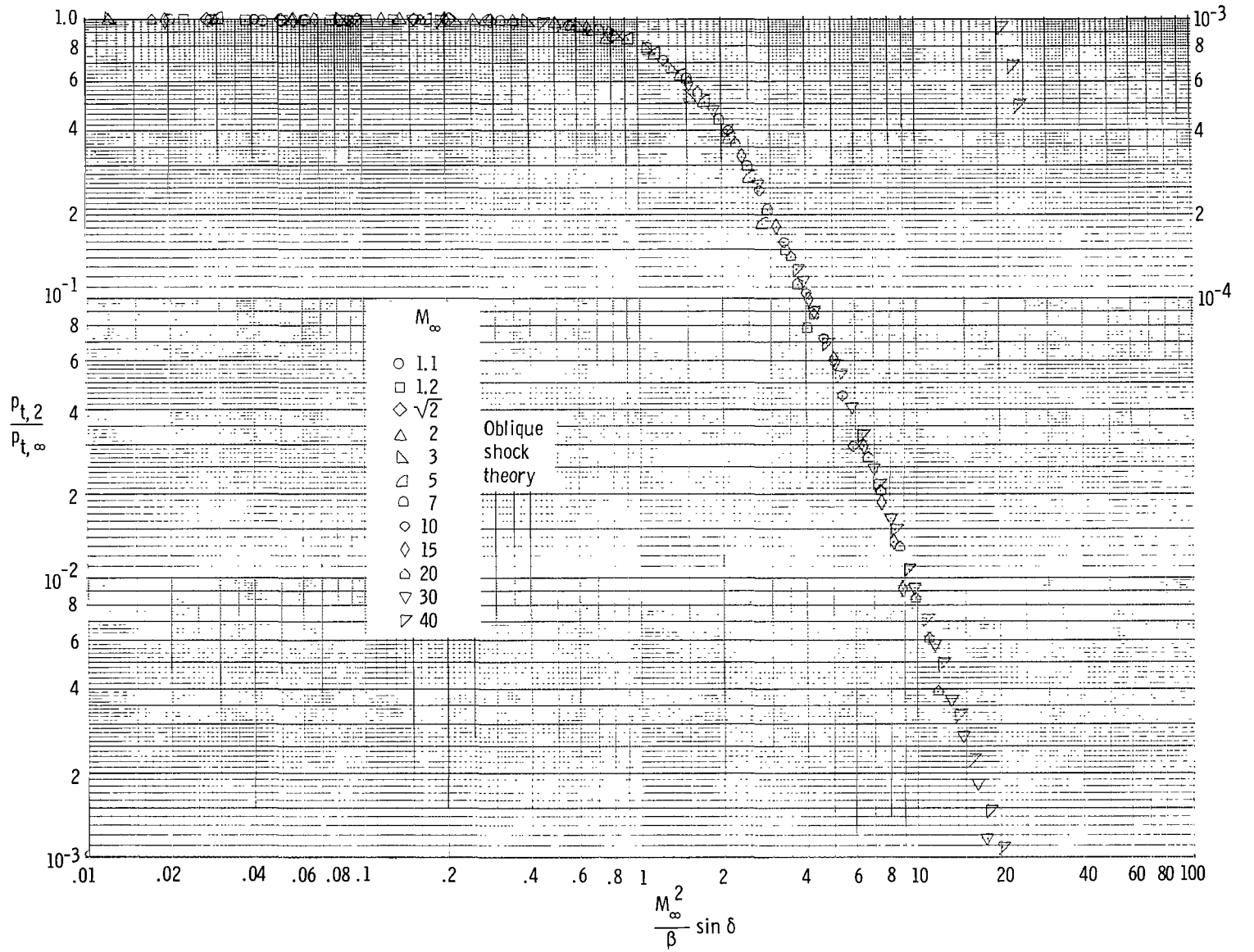

(e) $\gamma = 5/3$.

Figure 11.- Concluded.

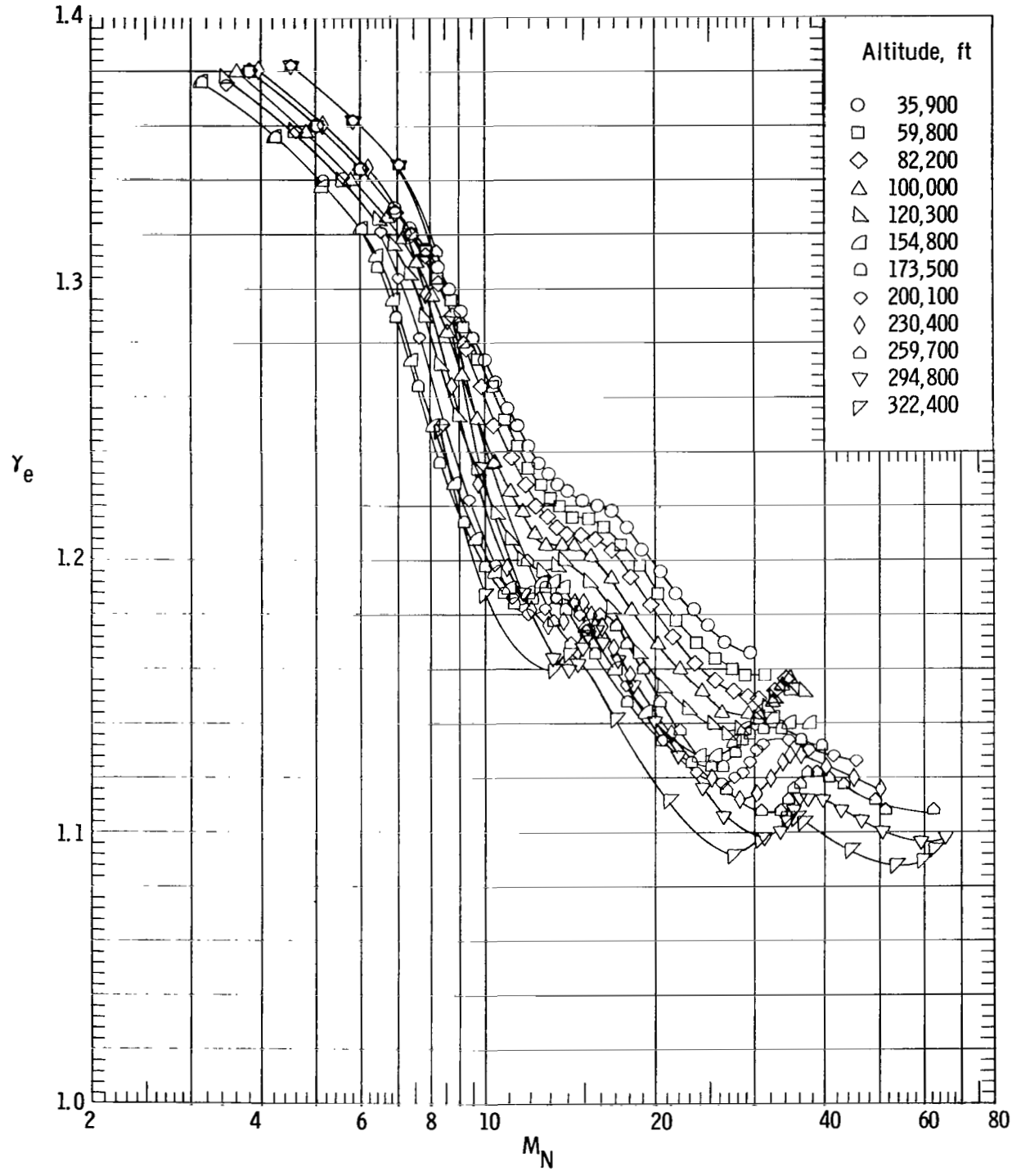

Figure 12.- The effective ratio of specific heats γ_e as a function of the Mach number normal to the shock wave M_N. The ARDC 1959 model atmosphere is used with $\gamma_\infty = 1.40$.

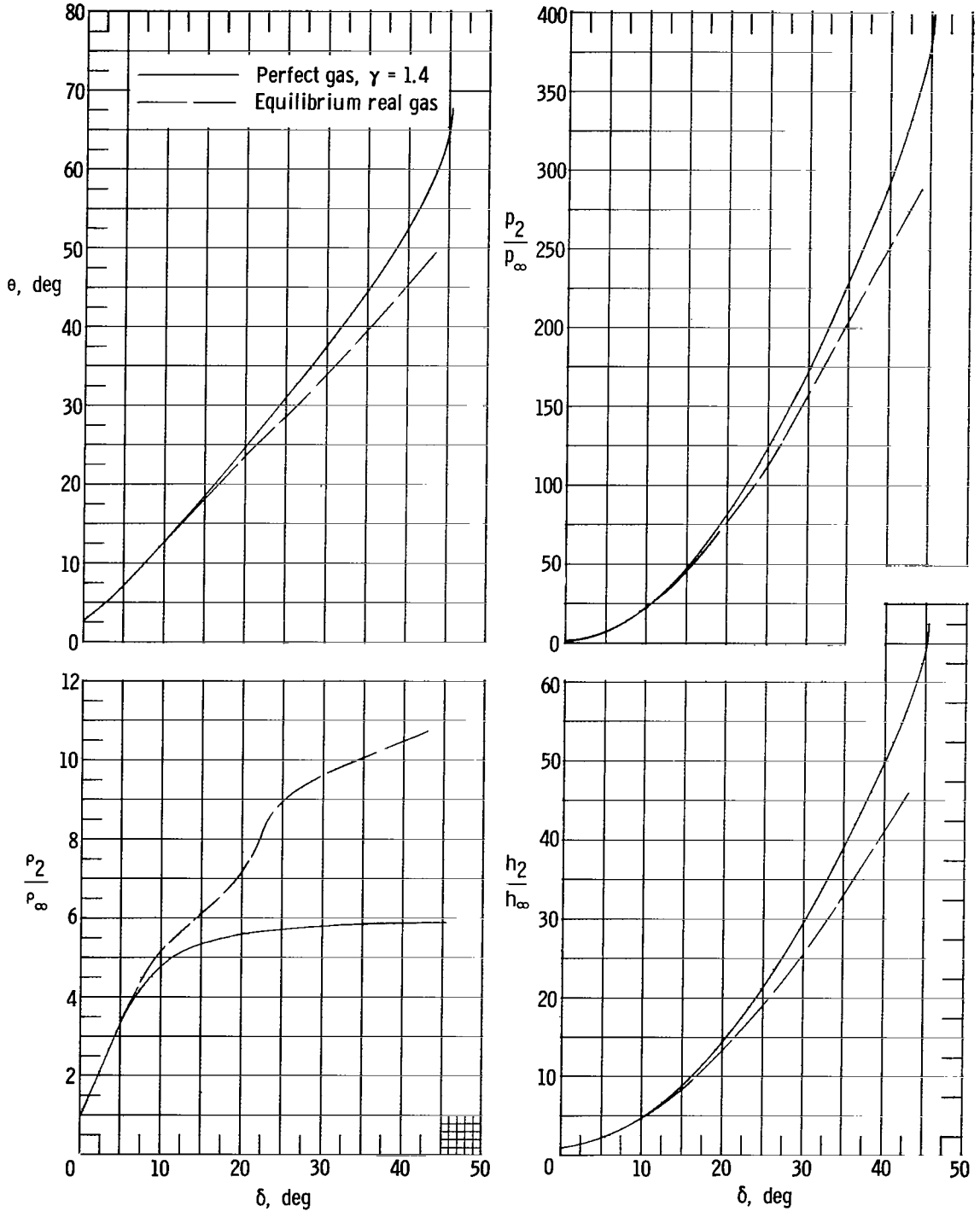

Figure 13.- Comparison of perfect gas exact oblique shock flow parameters at $M_\infty = 20$ with example of real gas flow parameters from correlation. Ambient conditions for real gas calculations: $M_\infty = 20$, $u_\infty = 20{,}950$ ft/sec, altitude = 120,300 ft.

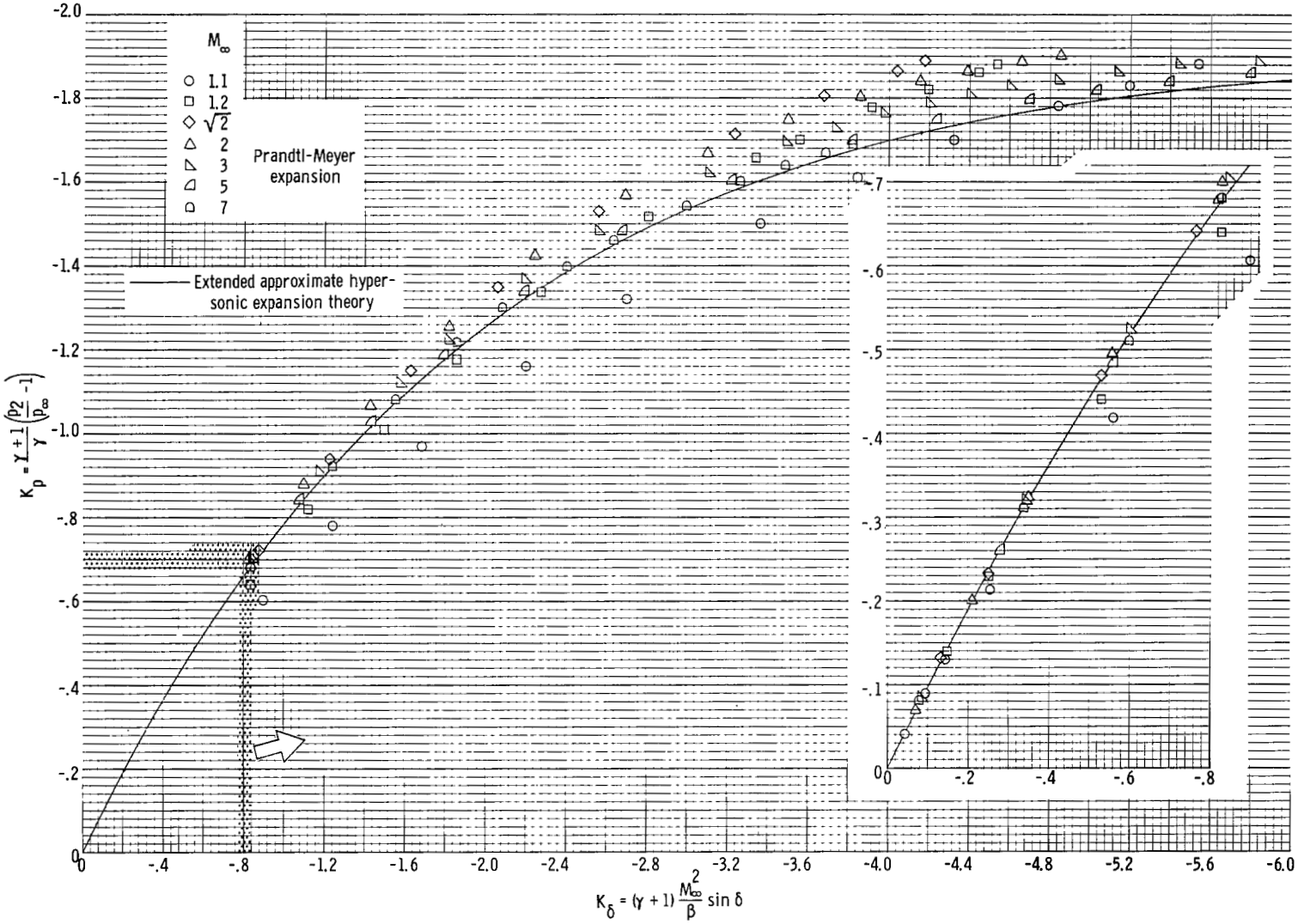

(a) $\gamma = 1.1$.

Figure 14.- Correlation of pressure ratio across sudden expansion.

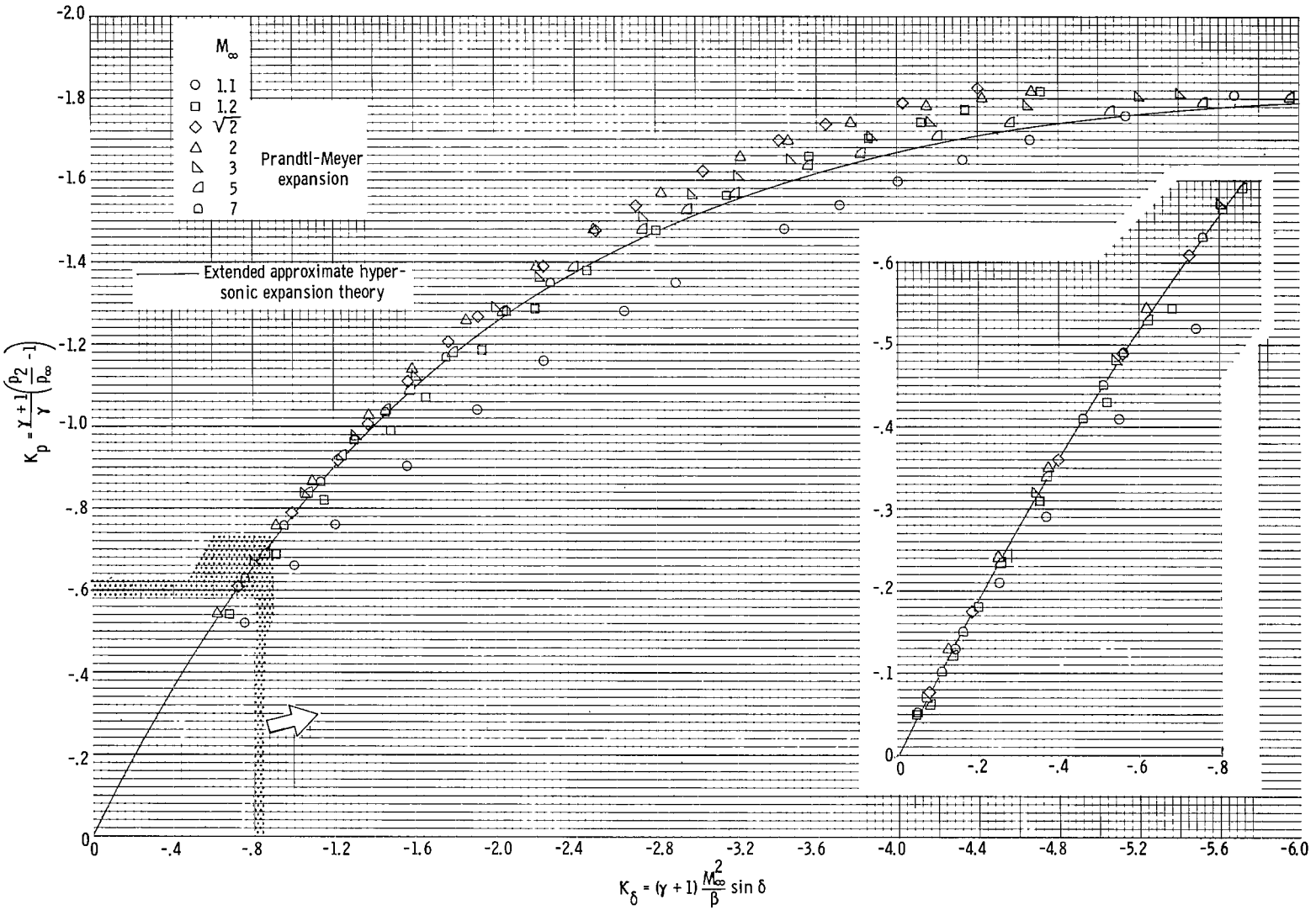

(b) $\gamma = 1.2$.

Figure 14.- Continued.

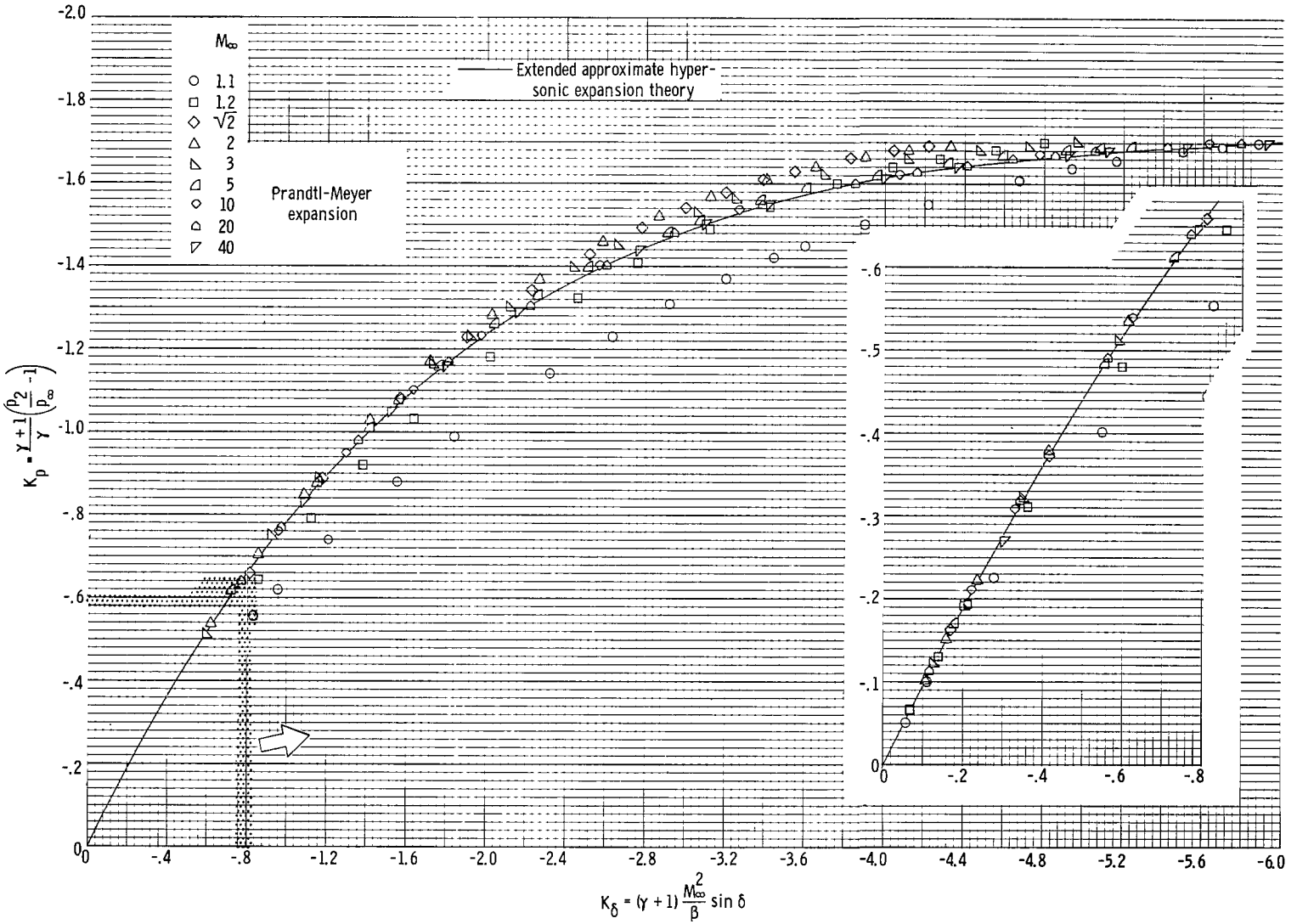

(c) $\gamma = 1.4$.

Figure 14.- Continued.

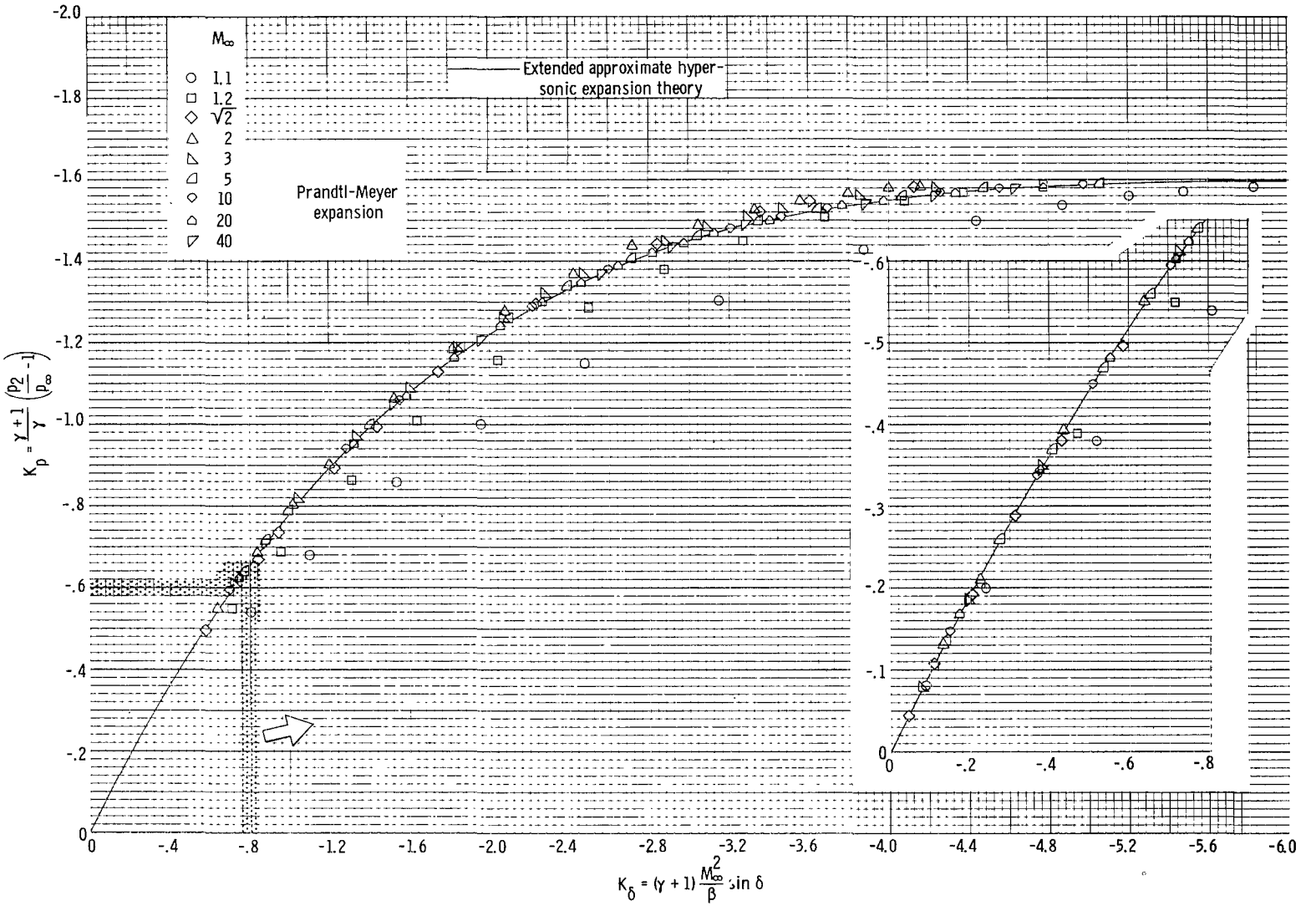

(d) $\gamma = 5/3$.

Figure 14.- Concluded.

"The National Aeronautics and Space Administration . . . shall . . . provide for the widest practical appropriate dissemination of information concerning its activities and the results thereof . . . objectives being the expansion of human knowledge of phenomena in the atmosphere and space."

—NATIONAL AERONAUTICS AND SPACE ACT OF 1958

NASA SCIENTIFIC AND TECHNICAL PUBLICATIONS

TECHNICAL REPORTS: Scientific and technical information considered important, complete, and a lasting contribution to existing knowledge.

TECHNICAL NOTES: Information less broad in scope but nevertheless of importance as a contribution to existing knowledge.

TECHNICAL MEMORANDUMS: Information receiving limited distribution because of preliminary data, security classification, or other reasons.

CONTRACTOR REPORTS: Technical information generated in connection with a NASA contract or grant and released under NASA auspices.

TECHNICAL TRANSLATIONS: Information published in a foreign language considered to merit NASA distribution in English.

TECHNICAL REPRINTS: Information derived from NASA activities and initially published in the form of journal articles or meeting papers.

SPECIAL PUBLICATIONS: Information derived from or of value to NASA activities but not necessarily reporting the results of individual NASA-programmed scientific efforts. Publications include conference proceedings, monographs, data compilations, handbooks, sourcebooks, and special bibliographies.

Details on the availability of these publications may be obtained from:

SCIENTIFIC AND TECHNICAL INFORMATION DIVISION

NATIONAL AERONAUTICS AND SPACE ADMINISTRATION

Washington, D.C. 20546